EXACT SOLUTION OF JEFFREY FLUID FLOW DUE TO STRETCHING/SHRINKING SURFACE

Thesis Submitted By

Sana Ahmed

(01-248202-009)

Supervised By

Dr. Rizwan ul Haq

A thesis submitted in fulfilment of the requirements for the award of degree of Masters of Science (Computer Science)

Department of Computer Science

BAHRIA UNIVERSITY ISLAMABAD

Session (2020-2022)

Approval of Examination

Scholar Name: Sana Ahmed

Registration Number: 71100

Enrollment: 01-248202-009

Program of Study: MS Mathematics

Thesis Tittle: Exact solution of Jeffrey fluid flow due to stretching/shrinking surface.

It is to certify that the above scholar's thesis has been completed to my satisfaction and, to my belief, its standard is appropriate for submission for examination. I have also conducted plagiarism test of this thesis using HEC prescribed software and found similarity index **10%**. That is within the permissible limit set by the HEC for the MS/M.Phil degree thesis. I have also found the thesis in a format recognized by the BU for the MS/M.Phil thesis.

Principal Supervisor Name: Dr. Rizwan ul Haq

Principal Supervisor Signature:

Date: 20-09-2022

Author's Declaration

I, **SANA AHMED** hereby state that my MS/MPhil thesis titled **"Exact solution of Jeffrey fluid flow due to stretching/shrinking surface"** is my own work and has not been submitted previously by me for taking any degree from this university Bahria University or anywhere else in the country/world. At any time if my statement is found to be incorrect even after my Graduate the university has the right to withdraw/cancel my MS/MPhil degree.

Name of student: **Sana Ahmed**

Date: September 20, 2022

Plagiarism Undertaking

I, **Sana Ahmed** solemnly declare that research work presented in the thesis titled **"Exact solution of Jeffrey fluid flow due to stretching/shrinking surface"** is solely my research work with no significant contribution from any other person. Small contribution / help wherever taken has been duly acknowledged and that complete thesis has been written by me. I understand the zero-tolerance policy of the HEC and Bahria University towards plagiarism. Therefore, I as an Author of the above titled thesis declare that no portion of my thesis has been plagiarized and any material used as reference is properly referred / cited.

I undertake that if I am found guilty of any formal plagiarism in the above titled thesis even after award of MS/MPhil degree, the university reserves the right to withdraw / revoke my MS/MPhil degree and that HEC and the University has the right to publish my name on the HEC / University website on which names of students are placed who submitted plagiarized thesis.

Name of student: **Sana Ahmed**

Date: September 20, 2022

Dedication

My Beloved Parents

I dedicate my achievement to my beloved parents. Father ASC Ch. Naseer Ahmed Tahir and Mother Abida Begum Late

My Mother gave me my drive however my Father gave me my dreams.

After passing my Mother being a single parent my Father showed a great love and sacrifice and struggle a lot to raised me to be a strong. There is no way can ever repay you but, I am always honored.

Acknowledgments

I'm thankful to ALLAH Almighty for giving me to learn and achieve seat blemishes en route to my point, His cherished Prophet Hazrat Muhammad (S.A.W), who is a super durable wellspring of direction, information, data and gift for the entire creation. His guidelines showed everybody how to live proudly, to remain with honor, and to be conscious.

My appreciation goes to my great, diligent, and incredibly energetic boss Dr. Rizwan ul Haq, who has forever been caring and strong. His important ability, remarks, ideas and guidelines are most welcome that enormously better the lucidity of this proposal. Dr. Rizwan ul Haq has my earnest appreciation. I am so thankful to work under the oversight of such an extraordinary individual.

I offer my thanks to my decent teachers who took me to the zenith of my scholarly community with their direction. Specifically, Prof. Dr. Muhammad Ramzan, Dr. Jafar Hasnain and Dr. Nazia Talat who have forever been steady in all of my course work and continued to empower me all through the meeting in Bahria University, Islamabad Campus. They are the genuine educators who have made Mathematics Department of BUIC, a genuine spot of learning.

appreciation is to my family (particularly my senior sibling Adv. Abdul Wahab Ch.) who generally the genuine mainstays of my consolation showed their affection, care and backing all through my life. Much thanks to you for invigorating me arrive at my objectives and pursue my fantasies. Not surprisingly, such countless companions and my schoolmates have helped me all through my MS that I can't show them all. Specifically, Dr. Syed Saqib Ali Shah, Dr. Tabinda sajjad, Dr. Ali Raza, Zeeshan Zahoor, and my colleagues were exceptionally remained tremendously accommodating all through the time of my MS studies.

Abstract

The present thesis determines the concept of the exact solution of Jeffrey fluid flow due to Stretching/shrinking surface. The thesis framework has been developed in the following way. In the first chapter, exhaustive literature is discussed for the exact solution of jeffrey fluid flow due to stretching/shrinking surface. The prices details about nanofluids, mass transfer, boundary layer theory, heat transfer, irreversible group and Jaffrey fluid are discussed. Basic fluid terminologies and fundamental laws are explored in the second chapter. In third chapter, an article, Entropy generation analysis for viscoelastic Magneto-Hydrodynamic flow over a stretching sheet embedded in a porous medium, is reviewed. By using appropriate tensor, develop the temperature, continuity and concentration and momentum equations. Converted governing PDEs into dimensionless non-linear ODEs by adoption of favorable similarity variables and then solved analytically. In fourth chapter, again reviewed another article of jaffrey fluid flow is numerical solution of non- Newtonian nanofluid flow over a stretching sheet which are solved numerically.it is Numerical method converted into analytical method by using new techniques. In Additional, generate new entropy generation. An analysis of conclusions are included in fifth chapter.

TABLE OF CONTENTS

Approval of Examination ii
Author's Declaration iii
Plagiarism Undertaking iv
Dedication v
Acknowledgments vi
Abstract vii
LIST OF FIGURES x
NOMENCLATURE xii
CHAPTER 1 1
INTRODUCTION AND LITERATURE REVIEW 1
CHAPTER 2 5
DEFINITIONS AND FUNDAMENTAL CONCEPTS OF FLUID 5
2.1 Fluid 5
2.2 Fluid mechanics 5
2.2.1 Fluid dynamics 5
2.2.2 Statics fluid 5
2.2.3 Fluid kinematics 5
2.3 Physical properties of fluid 6
2.3.1 Kinematic viscosity 6
2.3.2 Dynamic(absolute) viscosity 6
2.3.3 Density 6
2.4 Classification of fluid 6
2.4.1 Ideal fluid 6
2.4.2 Real fluid 6
2.4.3 Compressible fluid 7
2.4.4 Incompressible fluid 7
2.5 Two-Dimensional flow 7
2.6 Boundary layer 7

2.7 Nanofluids 7
2.8 Heat and mass transfer 7
2.9 Jaffrey fluid 7
2.10 Entropy generation 8
2.11 Hypergeometric confluent function 8
2.12 Some useful non-dimensionless number 9
2.12.1 Reynolds number 9
2.12.2 Prandtl number 9
2.12.3 Lewis number 9
2.12.4 Nusselt number 9
2.12.5 Sherwood number 9
CHAPTER 3 10
ENTROPY GENERATION ANALYSIS FOR VISCOELASTIC MAGNETO-HYDRODYNAMIC MHD FLOW OVER A STRETCHING SHEET EMBEDDED IN POROUS MEDIUM 10
3.1 Mathematical Formulation of the problem 10
3.2 Methodology 16
3.3 Results and discussion 19
CHAPTER 4 30
EXACT SOLUTION OF JEFFREY FLUID FLOW DUE TO STRETCHING/SHRINKING SURFACE 30
4.1 Mathematical modeling and exact solution 30
4.2 Methodology 34
4.3 Results and Discussion 37
CHAPTER 5 58
CONCLUSION 58
REFERENCES 60

LIST OF FIGURES

Fig. 1 Geometry of Problem 11
Fig. 2 Impact of Rc and Kp on longitudinal velocity for Mn.. 22
Fig. 3 Impact of Mn and Kp on transverse velocity for Rc. 22
Fig. 4 Impact of Rc and Kp on transverse velocity for Mn.. 23
Fig. 5 Impact of Mn and Kp on longitudinal velocity for Rc 23
Fig. 6 Impact of Pr and Kp on $\theta\eta$ for Mn., Rc, β, r 24
Fig. 7 Impact of Mn and Kp on $\theta\eta$ for Pr, Rc, β, r 24
Fig. 8 Effects of Rc and Kp on $\theta\eta$ for Pr, Mn.,β,r. 25
Fig. 9 Impact of β (source/sink) on $\theta\eta$ for Pr, Mn, Rc, r. 25
Fig. 10 Impact of r on $\theta\eta$ for Pr, Mn., β, Rc. 26
Fig. 11 Impact of Sc, Mn, Kp and r on φη. 26
Fig. 12 Impact of Pr, and Kp on Ns for s,λ1,λ2,λ3 27
Fig. 13 Impact of Mn and Kp on Ns 27
Fig. 14 Impact of Rc and Kp on Ns. 28
Fig. 15 Impact of r and Kp on Ns 28
Fig. 16 Impact of Ha and Kp on Ns. 29
Fig. 17 Impact of Re and Kp on Ns 29
Fig. 18 Geometry of Table 30
Fig. 19 Impact of $k2$ on $f'\eta$, $\theta\eta$ and φ(η). 40
Fig. 20 Impact of k1 on $f'\eta$, $\theta\eta$ and φ(η). 41
Fig. 21 Impact of Pr on $\theta\eta$ and φ(η). 41
Fig. 22 Impact of Le on $\theta\eta$ and φ(η). 42
Fig. 23 Impact of k2 on f'(η) for shrinking case. 42
Fig. 24 Impact of Pr on Ns. 43
Fig. 25 Impact of Le on Ns. 43
Fig. 26 Impact of Br on Ns. 44
Fig. 27 Impact of ϵ on Ns. 44
Fig. 28 Impact of k1 on Ns. 45
Fig. 29 Impact of $k2$ on Ns. 45
Fig. 30 Impact of Σ on Ns. 46
Fig. 31 Impact of Re on Ns. 46
Fig. 32 Variety of $-\theta'0$ w.r.t k2 and 1 . For Pr =1.0. 47
Fig. 33 Variety of $-\theta'0$ w.r.t k2 and k1. For Pr =4.0 47
Fig. 34 Variety of $-\theta'0$ w.r.t k2 and Pr. For k1=0.5,1.0 48
Fig. 35 Variety of $-\theta'0$ w.r.t k1 and 2 . For Pr =1.0. 48
Fig. 36 Variety of $-\theta'0$ w.r.t k1 and k2. For Pr =4.0. 49

Fig. 37 Variety of $-\theta'0$ w.r.t k1 and Pr. For k2=0.5. 49
Fig. 38 Variety of $-\theta'0$ w.r.t k1 and Pr. For k2=1.0. 50
Fig. 39 Variety of $-\theta'0$w.r.t k2 and k1. For Le=4.0 , Pr =1.0..... 50
Fig. 40 Variety of $-\theta'0$ w.r.t k2 and k1. For Le=4.0 , Pr =4.0..... 51
Fig. 41 Variety of -φ'(0) w.r.t and $k1$. For Le=4.0 , Pr=1.0 51
Fig. 42 Variety of -φ'(0) w.r.t $k2$ and $k1$. For Le=4.0 , Pr=4.0..... 52
Fig. 43 Variety of -φ'(0) w.r.t $k2$ and Le. For Pr=1.0 ,k1=0.5,1.0..... 52
Fig. 44 Variety of -φ'(0) w.r.t $k2$ and Pr. For Le=1.0 ,k1=0.5,1.0..... 53
Fig. 45 Variety of -φ'(0) w.r.t $k2$ and $k1$. For Le =1.0 , Pr =4.0..... 53
Fig. 46 Variety of -φ'(0) w.r.t $k1$ and k2. For Le =4.0 , Pr =4.0. 54
Fig. 47 Variety of -φ'(0) w.r.t $k1$ and $k2$. For Le =8.0 , Pr =4.0. 54
Fig. 48 Variety of -φ'(0) w.r.t $k1$ and Pr. For Le =4.0 , $k2$=0.5,1.0..... 55
Fig. 49 Variety of -φ'(0) w.r.t $k1$ and Le. For Pr =1.0 , $k2$=0.5,1.0. 55
Fig. 50 Variety of $f''0$ w.r.t $k1$ and $k2$. 56
Fig. 51 Variety of $f''0$ w.r.t $k2$ and k1..... 56
Fig. 52 Variety of dual solution skin friction $f''0$ both for (+) and for (-) function w.r.t $k1$ and $k2$. 57
Fig. 53 Variety of dual solution friction $f''0$ both for (+) and for (-) function w.r.t $k2$ and $k1$. 57

NOMENCLATURE

V	Velocity vector
A, B	Constants
K	Thermal conductivity
K'	Permeability of the medium
σ	Electrical conductivity
r	Temperature plate
s	Concentration plate
a, λ	Stretching/shrinking rate
ko	Elastic parameter
D	Molecular diffusivity
d	Characteristics length
Rc	Viscoelastic factor
Mn	Magnetic parameter
K_p	Permeability parameter
Sc	Schmidt number
Br	Brinkman number
Re, Rd	Reynold number
H_a	Hartman number
$\|M\|, \|U\|, \|W\|$	Kummer's function
Ω	Dimensionless temperature contrast
ϵ	Dimensionless parameter
Σ	Dimensionless distinction concentration
C	Fluid concentration
C_w	Wall concentration
C_∞	Ambient concentration
μ	Dynamic viscosity
ν	Kinematic viscosity
ρ	Density

θ	Temperature profile
φ	Concentration profile
f	Velocity profile
Ns	Irreversible profile
c_p	Specific heat
C_f	Skin friction
Nu_x	Nusstle number
Sh_x	Sherwood number
T	Fluid temperature
T_w	Wall temperature
T_∞	Ambient temperature
D_B	Coefficient of Brownian diffusion
α	Thermal diffusivity
u_w	Stretching/shrinking sheet velocity
x	Coordinate along the extending sheet
u, v	Velocity components
y	Distance along the Stretching sheet
$k2$	Deborah number
Pr	Prandtl number
Le	Lewis number
$k1$	Relaxation to retardation times ratio
kn	Retardation time

CHAPTER 1

INTRODUCTION AND LITERATURE REVIEW

In recent years, nanoparticles with mass and heat transfer received a significant attention from many scientists because of their regular solicitations in differential work methodology. Water, glycol, oil, and ethylene ($\boldsymbol{C_2H_4}$) are bad at transferring heat and considered bad heat conductor fluid in Newtonian/Non-Newtonian fluids. Thermal expansion inside stretched flow has a great application in many fields of science including chemical engineering, including metallurgical processes, glass fiber, polymer extrusion, and paper manufacture. The Jaffrey fluid model may explain the non-Newtonian fluids' stress relaxation feature, which the regular viscous fluid model cannot. However, Navier-e-Stokes statistics cannot accurately describe the non-Newtonian fluid flow. Also, these kinds of fluids may not be observed by one intermediate relationship between shear stress and stress rate. Therefore, no model can predict loneliness in the behavior of such kind of fluids. For the following reason, numerous models of such liquids are recommended in research. Between different non-Newtonian models of liquid, the model which is straight for the utilization of brief other options is Jeffrey model.

Exact mathematical solutions play very vital part in understanding features, methods and objects in numerous fields in science. Particularly, exact mathematical solution may work as a basis for concluding and evaluating mathematical software for solving D.E Mathematica, Maple, MATLAB, CONVODE, Python etc. Methodology used to obtain exact mathematical solution to boundary layer flow of stretching sheet is missing. Later, it was expanded by Grubka and Bobba (B.C.Sakiadis, 1961), which includes energy equation.

Nanoparticles in suspension (under 100nm) in base fluid creates fluid called Nanofluid. The Nano coating serves as a heat exchanger between solid nanoparticles and the base fluid, according to Choi's team [2]. Non-Newtonian models few objects related

to nanofluid are described by Domiarry et al. [3]. The movement of tiny particles towards reducing thermal gradient is called thermophoresis [4]. Non-Newtonian fluid are used in oil industries as stimulate reservoirs. Pearson and Tardy [5] show different degree of viscosity, Ellahi and Afzal [6] shows different degree of thixotropy and Ellahi [7] shows different degree of elasticity depending on their shears.

The boundary layer is very thin layer of a viscous liquid moving closest to the apparent. Sakiadis [8] discovers the awareness of boundary layer flow along a surface which is moving.

Good amount of studies are conducted on exponentially stretching sheet for nanofluid. Makinde and Aziz [9] investigated a technical issue with the advent of a convection surface configuration. The flow of nanofluid with boundary layer across an increasingly stretched surface has been discovered by Lee and Nadeem [10].

Gupta and Dandapat [11] and Rollins and Vajravelu [12] have many studies on cases of heat transfer, Andersson [13] has investigated viscoelastic fluid flow on stretching surface under the effect of magnetic field which is uniformly distributed over the surface. Consequently, many authors have made number of research on effects of transfering heat on viscoelastic fluid under a diverse physical conditions including [14–16]. A uniform solution for the heat transfer over the stretching surface and the flow of the viscoelastic boundary layer is established by Sanjayanand and Khan [17]. In recent times, research has been made about heat transfer and flow of viscoelastic fluids over stretching surface taking constant temperature and also constant temperature of sheet by Cortell [18]. A study conducted by Abel et al [19] on the viscoelastic flow of boundary layer and the transfer of heat to the stretching region where there is viscous dispersion and non-unifrom heat source taking into account the set temperature and the fixed temperature variations.

Narrative exploration shows that interest in researching non-Newtonian fluid flow conduct in various utilizations developed in last ten years [21-24]. The peristaltic flow of Jeffrey fluid at unequal network with lengthy frequency and presumption of a smaller Reynolds number is examined by Kothandapani and Srinivas [25]. Jeffrey fluid is a comparatively easy to understand and simple model that took attention among specialists. Some of the most recent papers on the Jeffrey fluid are from Hayat et al. [26], Mustafa and Hayat [27], Das [28], and Qasim [29] Main purpose of these studies is stretching

sheet of Jeffrey fluid model of nanofluid. The Jeffery fluids models impressed several scholars because it is a superior physiological fluid model. The effect of speed variabilities and transfer of heat in magneto-hydrodynamic flow of non-Newtonian nanofluid on a flexible sheet with heat source analyzed by Bhargava and Goyal [31]. They found accurate solutions as power series technique utilizing Kummer's intersecting hyper-mathematical capacities and analyzed the impacts of arising boundaries on speed, temperature, and fixation profiles. Pop and Turkyilmazoglu [30] evaluated the flow and intensity move of a Jeffrey fluid with a parallel outside flow close the stagnation point on a stretching or shrinking sheet. Show them that creation of any scientific arrangements relies seriously upon the boundary that actions the pace of outside flow to the stretching/shrinking surface. Numerous scientists have concentrated on the generation of entropy in fluid flow and heat transfer over space. The utilization of the second law of thermodynamics to viscoelastic magneto hydrodynamic (MHD) flow over a stretching surface presented by Aiboud and Saouli [32]. By logicss, they found profiles of speed and temperature utilizing Kummer works and gathered the irreversible number. Makinde [33] broke down the innate irreversibility in the flow of the hydromagnetic limit of a variable consistency fluid over an endlessly level plate affected by warm radiation and Newtonian intensity. Involving a neighborhood system for consistency and shooting quadrature, he got by number the speed, the temperature and the creation amount of entropy. Dehsara et al [34]. The age of entropy broke down mathematical flow of (MHD) blended convection over a stretching slanted straightforward plate implanted in a permeable medium because of sun based radiation. Freshly, Nemat Dalir et al [35] investigated entropy for heat transfer of a Jeffrey nanofluid and magneto-hydrodynamic flow over a stretching surface. [36] Also worked on exact solution of jaffrey fluifd flow.

My review work is reviewed the exact solution of research paper. Initially, I reviewed S. Baag et al [37] non-newtonian viscoelastic fluid (Walter B') research paper of exact solution and I also reviewed another paper of Jaffrey fluid flow model which are solved numerically then I convert numerical solution into analytical solution and additional I also generate entropy generation.

The reason for the ongoing review is to scientifically explore the exact solution of Jaffrey fluid flow because of stretching/shrinking surface. To the best of the creators' information, no paper in the writing has up until this point off studied on exact solution of Jeffrey nanofluid, entropy generation over a stretching sheet. Appropriate

transformation changes have been taken advantage of for the benefit of the decrease of administering fractional differential conditions into customary differential conditions. The attained explanation is examined with the help of charts of dimensionless velocity, nanoparticles portion volume, temperature, and number of irreversible generations.

CHAPTER 2

DEFINITIONS AND FUNDAMENTAL CONCEPTS OF FLUID

In this part, we will discuss certain several elementary concepts, explanation and few laws associated with fluid movement, heat, and mass transfer.

2.1 Fluid

If an unrelated or shear pressure is applied to a substance, and it ceaselessly deform(flow). All stress are fluids. Part of mechanics that arrangements with liquid behavior at rest and motion. very still and movement

2.2 Fluid mechanics

The part of science that arrangements with the movement of fluids, gases and plasma and their communication with strong bodies. It is subdivided into three parts. fluid dynamics, static fluid, and kinematics.

2.2.1 Fluid dynamics

Liquid elements are the investigation of the impact of powers on smooth movement and at some point, liquid at rest.

2.2.2 Statics fluid

It manages the investigation of effects of force when liquid is very still.

2.2.3 Fluid kinematics

The part of liquid mechanics that arrangements with the investigation of liquid when it is moving without integrating the impact of forces.

2.3 Physical properties of fluid

2.3.1 Kinematic viscosity

Kinematics viscosity is a measure of rate at which momentum is transferred through a fluid. It is denoted by $\boldsymbol{\nu}$. Mathematically,

$$\nu = \frac{\mu}{\rho} = \frac{\text{dynamic viscosity}}{density}.$$

2.3.2 Dynamic(absolute) viscosity

Dynamic viscosity is identified fractional connection of shear stress to deformation rate.

That is denoted by μ. Mathematically,

$$\mu = \tau \left(\frac{du}{dy}\right)^{-1}.$$

2.3.3 Density

The thickness of a liquid's particle characterized as the proportion of its mass to its volume, and it is represented as ρ. Mathematically,

$$\rho = \frac{m}{v}.$$

2.4 Classification of fluid

2.4.1 Ideal fluid

Ideal fluid (inviscid fluid) is defined as the fluid whose viscosity is zero.

2.4.2 Real fluid

Real fluid (viscous fluid) is defined as the fluid whose viscosity is not zero.

Viscous fluid is of two types i.e.

(a) Newtonian Fluid

Fluids for which deformation rate does not obeys the following defined relation are classified as Newtonian fluids.

$$\tau \propto \mu \frac{du}{dy},$$

(b) Non-Newtonian Fluid

Fluids for which deformation rate obeys the following defined relation are classified as non Newtonian fluids.

$$\tau \propto \mu \left(\frac{du}{dy}\right)^{n-1}, \quad n \neq 2.$$

2.4.3 Compressible fluid

Density of each fluid particles are not constant and varies with space and time. All gases are to be compressible

2.4.4 Incompressible fluid

Density of each fluid particles is relatively constant and varies with space and time. All gases are compressible. All liquids are to be incompressible.

2.5 Two-Dimensional flow

The size is basically the space coordinates and especially the movement of the liquid is considered so that it has three sides but for ease of calculation, it is considered two sides so that it can be easily dealt with. 2-D flow means flow to the plane coordinates.

2.6 Boundary layer

A slim layer adjacent to the strong surface where effects of viscosity are prominent is called boundary layer.

2.7 Nanofluids

The liquid in which nano-sized particles with diameter of 1-100nm is called nanofluid. Nanofluids have a strong ability to improve the thermal conductivity of basic fluid, Nanoparticles have greater potential to improve heat transfer.

2.8 Heat and mass transfer

Heat transfer remains a kinetic procedure in which energy is transferred from one particle to another with the flow of particles. Mass transfer, instead, is the movement of mass from one place to another such as absorption, evaporation, and so on.

2.9 Jaffrey fluid

The Jeffrey fluid model can be defined as the stress relaxation stuff of non-Newtonian fluids, which the normal viscous fluid model cannot define. Examples: Paints, rubber, mud etc.

2.10 Entropy generation

In the thermodynamic system, the generation of entropy is how much entropy, which is normally produced during irreversible cycles utilizing warm course through heat obstruction, fluid movement through a stream struggle, diffusion, Joule warming, contact during strong surfaces, fluid thickness inside framework and so on.

2.11 Hypergeometric confluent function

A blended hypergeometric capability is an answer for an intersecting hypergeometric equation, which is a savage type of a hypergeometric differential condition in which two-three ordinary singularities consolidate to deliver an unpredictable peculiarity.

2.11.1 Kummer's function

In 1837 a researcher named Kummer introduced Kummer's (intersecting hypergeometric) work $M(F, E, s)$, is an answer for Kummer's differential condition. Which is otherwise called intersecting hypergeometric capacity of principal kind.

Kummer's condition can be composed as:

$$s\frac{d^2w}{ds^2} + (E - s)\frac{dw}{ds} - Fw = 0,$$

with a customary particular point at $s = 0$, and an unpredictable particular point at $s = \infty$. It consumes two (regularly) directly free arrangements $M(F, E, s)$ and $U(F, E, s)$. M Kummer's capacity of the principal kind is given by:

$$M(F, E, s) = \sum_{n=0}^{\infty} \frac{F^n s^n}{E^n n!} = |W|(F; E; s),$$

Where:

$$F^0 = 1,$$

$$F^n = F\ (F + 1)\ (F + 2)\ \ldots\ (F + n - 1),$$

is the increasing factorial.

2.12 Some useful non-dimensionless number

2.12.1 Reynolds number

Reynold number is basically non-dimensionless ratio of the inertia and viscous force of the fluid. Mathematically:

$$Re = \frac{\alpha x^2}{\nu}.$$

2.12.2 Prandtl number

It is change in kinematics viscosity ν w.r.t thermal diffusivity α. It is non-dimensional number. Mathematically,

$$Pr = \frac{\nu}{\alpha}.$$

2.12.3 Lewis number

It is dimensionless number which is the change in thermal diffusivity α w.r.t the coefficient of Brownian diffusion D_B.

$$Le = \frac{\nu}{D_B}.$$

2.12.4 Nusselt number

A non-dimensionless number which is the relation between the convective and the conductive heat transfer on the boundary is termed as local Nusselt number. This can be measured by flexibility, and it provides the ratio of heat transfer from the surface to liquid.

2.12.5 Sherwood number

Dimensionless relation in the convective mass transfer and the mass transport diffusion's rate is Sherwood number.

2.12.6 Skin friction coefficient

Skin-friction coefficient Cf is flawless quality distinct from the shear stress on the wall.

$$Cf = \frac{\tau_w}{\rho}.$$

Where ρ is the density and longitudinal speed at the edge of the limit layer.

CHAPTER 3

ENTROPY GENERATION ANALYSIS FOR VISCOELASTIC MAGNETO-HYDRODYNAMIC MHD FLOW OVER A STRETCHING SHEET EMBEDDED IN POROUS MEDIUM

Motivation behind composing this section is to explore the stream of viscoelastic MHD to investigate boundary layer, entropy production, heat and mass transfer over an expandable sheet embedded in a porous medium. The momentum, energy, concentration equations are defined in mathematical formulation and subsequently released. Boundary conditions are also stated. Later, we converted the governed nonlinear PDEs into dimensionless nonlinear ODEs in order to find a solution to a closed form of momentum, energy and concentration equations. The existence of certain other parameters on energy, momentum and equations of concentration can also be perceived. The solution of dimensionless ODEs including B. Cs will therefore be analytically solved by using Kummer's function.

3.1 Mathematical Formulation of the problem

Consider 2-D steady laminar fluid flow which is incompressible over a viscoelastic electrically conductivity affected through a stretching external fixed in a permeable medium where there is a uniform transverse field magnetic to Cartesian coordinates $(\boldsymbol{x}, \boldsymbol{y})$. Where $\boldsymbol{x}$-axis is reserved beside the pate in the direction of fluid flow and $\boldsymbol{y}$-axis stands normal towards plate, is measured (see Fig. 1). The governing equation of boundary layer of steady 2-D viscoelastic fluid flow over a Walters B' model by small reduction period. Governing equations associated with this problem are:

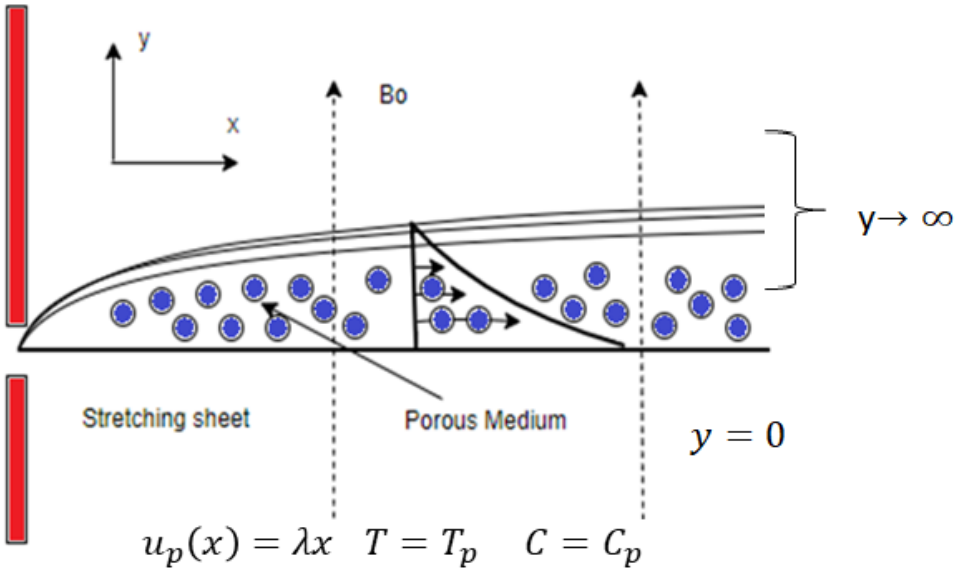

Fig. 1 Geometry of Problem

$$\nabla \cdot V = 0, \tag{3.1}$$

$$\rho\left(\frac{dV}{dt}\right) = \text{div}\,(\tilde{\tau}) - \sigma B_o^2 V - \frac{\nu}{k_p'} V, \tag{3.2}$$

$$\rho C_p \left[\frac{\partial T}{\partial t} + V.(\nabla T)\right] = K\nabla.(\nabla T) - div\,(q)\,, \tag{3.3}$$

$$\frac{\partial C}{\partial t} + V.(\nabla C) = -\frac{1}{\rho}\nabla.(\rho D \nabla C), \tag{3.4}$$

Where, $\tilde{\tau}$ is equal to:

$$\tilde{\tau} = -\bar{p}I + S, \tag{3.5}$$

S is equals to:

$$S = \mu(b_1) - \frac{k_o}{\rho}(b_2), \tag{3.6}$$

$$b_1 = (\nabla V) + (\nabla V)^T, \tag{3.7}$$

$$b_2 = \frac{db_1}{dt} = \left(\frac{\partial}{\partial t} + u\frac{\partial}{\partial x} + v\frac{\partial}{\partial y} + w\frac{\partial}{\partial z}\right) b_1, \tag{3.8}$$

Where μ is the viscosity and S is Rivlin-Ericksen tensor.

Velocity field of the form are respectively given as

$$V = [u(x,y), v(x,y), 0]. \tag{3.9}$$

Now, using velocity field from equation (3.9) in equation (3.1) and (3.2) , continuity equation holds and by neglecting body force nonlinear PDEs of momentum in component form yields

$$\rho\left(\frac{dV}{dt}\right)_x = \frac{\partial\tilde{\tau}_{xx}}{\partial x} + \frac{\partial\tilde{\tau}_{xy}}{\partial y} + \frac{\partial\tilde{\tau}_{xz}}{\partial z}, \tag{3.10}$$

$$\rho\left(\frac{dV}{dt}\right)_y = \frac{\partial\tilde{\tau}_{yx}}{\partial x} + \frac{\partial\tilde{\tau}_{yy}}{\partial y} + \frac{\partial\tilde{\tau}_{yz}}{\partial z}, \tag{3.11}$$

$$\rho\left(\frac{dV}{dt}\right)_z = \frac{\partial\tilde{\tau}_{zx}}{\partial x} + \frac{\partial\tilde{\tau}_{zy}}{\partial y} + \frac{\partial\tilde{\tau}_{zz}}{\partial z}. \tag{3.12}$$

Using equation (3.9) in equation(3.7), we get

$$b_1 = \begin{bmatrix} 2\,u_x & u_y + v_x & 0 \\ u_y + v_x & 2v_y & 0 \\ 0 & 0 & 0 \end{bmatrix}, \tag{3.13}$$

Where $u_x = \frac{\partial u}{\partial x}$, $v_x = \frac{\partial v}{\partial x}$, $w_x = \frac{\partial w}{\partial x}$ and $u_y = \frac{\partial u_y}{\partial y}$, $v_y = \frac{\partial v}{\partial y}$, $w_y = \frac{\partial w}{\partial y}$.

By using equations (3.13) in (3.8), we get

$$b_2 = \begin{bmatrix} 2uu_{xx} + 2vu_{xy} & uu_{xy} + uv_{xx} + vu_{yy} + vv_{xy} & 0 \\ uu_{xy} + uv_{xx} + vu_{yy} + vv_{xy} & 2uv_{xy} + 2vv_{yy} & 0 \\ 0 & 0 & 0 \end{bmatrix}, \tag{3.14}$$

Substituting equation (3.13) and equation (3.14) into equation(3.6), we get

$$S = \begin{bmatrix} 2\mu u_x - \frac{k_o}{\rho}\left(2uu_{xx} + 2vu_{xy}\right) & \mu\left(u_y + v_x\right) - \frac{k_o}{\rho}\left(uu_{xy} + uv_{xx} + vu_{yy} + vv_{xy}\right) & 0 \\ \mu\left(u_y + v_x\right) - \frac{k_o}{\rho}\left(uu_{xy} + uv_{xx} + vu_{yy} + vv_{xy}\right) & 2\mu v_y - \frac{k_o}{\rho}\left(2uv_{xy} + 2vv_{yy}\right) & 0 \\ 0 & 0 & 0 \end{bmatrix}, \tag{3.15}$$

Again, substituting equation (3.15) into equation(3.5), then we have a matrix whose component form can be expressed as:

$$\tilde{\tau}_{xx} = -p + 2\mu u_x - \frac{k_o}{\rho}\left(2uu_{xx} + 2vu_{xy}\right), \tag{3.16}$$

$$\tilde{\tau}_{xy} = \tilde{\tau}_{yx} = -p + \mu\left(u_y + v_x\right) - \frac{k_o}{\rho}\left(uu_{xy} + uv_{xx} + vu_{yy} + vv_{xy}\right), \tag{3.17}$$

$$\tilde{\tau}_{yy} = -p + 2\mu v_y - \frac{k_o}{\rho}\left(2vv_{yy} + 2uv_{xy}\right), \tag{3.18}$$

$$\tilde{\tau}_{zz} = -p, \tag{3.19}$$

$$\tilde{\tau}_{xz} = \tilde{\tau}_{zx} = \tilde{\tau}_{yz} = \tilde{\tau}_{zy} = 0. \tag{3.20}$$

Substituting equations(3.16) , (3.17) and (3.20) into equation(3.10), we get

$$uu_x + vu_y = -\frac{1}{\rho}\left(\frac{\partial p}{\partial x}\right) + \nu\left(u_{xx} + u_{yy}\right) - \frac{k_o}{\rho}\left(uu_{xxx} + 2u_x u_{xx} + vu_{xx}u_y\right)$$

$$-\frac{k_o}{\rho}\left(2v_x u_{xy} + u_y v_{xx} + u_y u_{xy} + uu_x u_{yy} + v_y v_{xy} + v_y u_{yy} + vu_{yyy}\right). \tag{3.21}$$

And Substituting equations(3.17) , (3.18) and (3.20) into equation(3.11), we get

$$uu_x + vu_y = -\frac{1}{\rho}\left(\frac{\partial p}{\partial y}\right) + \nu\left(v_{xx} + u_{yx} + 2v_{yy}\right) - \frac{k_o}{\rho}\left(u_x v_{xx} + u_x u_{xy} + uv_{xxx}\right)$$

$$-\frac{k_o}{\rho}\left(uu_{xxy} + v_x u_{yy} + v_x v_{xy} + vu_{xyy} + vv_{xxy} + 2u_y v_{xx} + 2uv_{xyy} + 2v_y\, v_{yy} \quad + \right.$$

$$\left. 2vv_{yyy}\right). \tag{3.22}$$

Substituting equations(3.19) , (3.20) and (3.20) into equation(3.12), we get

$$0 = -\frac{\partial p}{\partial z}. \tag{3.23}$$

Following are boundary layer estimates

$$\tilde{x} = \frac{x}{L}, \tilde{y} = \frac{y}{\delta}, \tilde{u} = \frac{u}{U}, \tilde{v} = \frac{v}{U}\frac{L}{\delta}, \tilde{p} = \frac{p}{\rho U^2}, \tilde{t} = t\frac{U}{L}, \tag{3.24}$$

Finally Substituting equation(3.24) into equation(3.21) and also by dropping the primes, we get

$$u\frac{\partial u}{\partial x} + v\frac{\partial u}{\partial y} = \nu\frac{\partial^2 u}{\partial y^2} - \frac{k_o}{\rho}\left(\frac{\partial}{\partial x}\left(u\frac{\partial^2 u}{\partial y^2}\right) + v\frac{\partial^3 u}{\partial y^3} - \frac{\partial u}{\partial y}\frac{\partial^2 u}{\partial xy}\right) - \sigma B_o^2 V - \frac{\nu}{k_p'}V, \tag{3.25}$$

By using boundary layer approximation equation(3.22)is neglected. In equation(3.3) q represents the heat flux of the nanofluid which is the summation of diffusion and conduction heat flux.

$$q_c^* = -k\nabla T + \boldsymbol{J} \times \boldsymbol{B}, \tag{3.26}$$

Where

$$\nabla \mathrm{T} = [Tx, Ty, 0]. \tag{3.27}$$

Now, using equation(3.3) and simplifying

$$\rho C_p \left[\frac{\partial T}{\partial t} + V.(\nabla T)\right] = K\nabla.(\nabla T) - div\,(q)\,,$$

Then,

$$\rho C_p \left[u\frac{\partial T}{\partial x} + v\frac{\partial T}{\partial y}\right] = K\frac{\partial^2 T}{\partial y^2} + q(T - T_\infty). \tag{3.28}$$

Now using equation(3.4) and simplifying

$$\frac{\partial C}{\partial t} + V.(\nabla C) = -\frac{1}{\rho}\nabla.(\rho D\nabla C)\,,$$

Then,

$$u\frac{\partial C}{\partial x} + v\frac{\partial C}{\partial y} = D\frac{\partial^2 C}{\partial y^2}. \tag{3.29}$$

The boundary conditions of equation(3.25), (3.28)and(3.29) are:

$$\left.\begin{aligned} &u = \lambda x = u_p, T = T_p(x) = A\left(\frac{x}{l}\right)^r + T_\infty, v = 0\,, && \\ &C = C_p(x) = B\left(\frac{x}{l}\right)^s + C_\infty, && at\ y = 0, \\ &u \to 0, T \to T_\infty, C \to C_\infty\,, \frac{\partial u}{\partial y} \to 0, && as\ y \to \infty. \end{aligned}\right\} \tag{3.30}$$

Converting the governed PDEs (3.25), (3.28)and(3.29) into dimensionless non-linear ODEs, following similarity variables are used to transform the system of equation:

$$\eta = y\sqrt{\frac{\lambda}{\nu}},\ \varphi(\eta) = \frac{C - C_\infty}{C_p - C_\infty},\ \ \theta(\eta) = \frac{T - T_\infty}{T_p - T_\infty},\ \ \Psi(x, y) = \sqrt{\lambda\nu}xf(\eta). \tag{3.31}$$

Dimensionless stream function

$$u = \frac{\partial}{\partial x}\psi(x, y),\ v = -\frac{\partial}{\partial y}\psi(x, y). \tag{3.32}$$

Converting ψ into u and v, we get

$$u = x\lambda f'(\eta),\ v = -\sqrt{\lambda\nu}f(\eta). \tag{3.33}$$

Using equation (3.31) in equations (3.25), (3.28) and (3.29) and continuity equation satisfies

$$f''' - f'^2 + ff'' - Rc\{2f'f''' - f''^2 - ff''''\} - \left(Mn + \frac{1}{K_p}\right)f' = 0, \tag{3.34}$$

$$\theta'' + Prf\theta' + Pr(\beta - rf')\theta = 0, \tag{3.35}$$

$$\varphi'' + Scf\varphi' - Scf'\varphi = 0. \tag{3.36}$$

With Reduce associated boundary conditions are:

$$\left.\begin{array}{l} f(0) = 0,\ f'(0) = 1,\ f''(\infty) = f'(\infty) = 0, \\ \theta(0) = 1,\ \theta(\infty) = 0, \\ \varphi(0) = 1,\ \varphi(\infty) = 0. \end{array}\right\} \tag{3.37}$$

Where Rc is viscoelastic parameter, Mn is magnetic parameter, K_p is impermeability parameter, Pr is Prandtl number.

$$Rc = \frac{k_0\lambda}{\mu}, \quad Mn = \frac{\sigma B_0^2}{\rho\lambda}, \quad K_p = \frac{K_p'}{\rho\lambda}, \quad Pr = \frac{\mu C_p}{K}, \quad \beta = \frac{q}{\rho C_p}, \quad Sc = \frac{\nu}{D}.$$

Local Skin friction coefficient is written as:

$$C_f = \frac{\tau_w}{\mu\lambda x\sqrt{\frac{\lambda}{\nu}}} = \alpha. \tag{3.38}$$

Where τ_w is the wall shearing sheet.

Dimensionless physical quantities

$$Re_x^{1/2}\, C_f = (1 - Rc)f''(0), \quad Re_x^{-1/2}\, Nu_x = -\theta'(0), \quad Re_x^{-1/2}\, Sh_x = -\varphi'(0).$$

Where C_f, Nu_x and Sh_x is dimensionless skin friction, Nusselt number and Sherwood number.

Entropy generation analysis

$$E_{Gen} = \frac{k}{T_\infty^2}\left(\left(\frac{\partial T}{\partial x}\right)^2 + \left(\frac{\partial T}{\partial y}\right)^2\right) + \frac{D}{C_\infty}\left(\left(\frac{\partial C}{\partial x}\right)^2 + \left(\frac{\partial C}{\partial y}\right)^2\right) + \frac{D}{T_\infty}\left(\frac{\partial T}{\partial x}\frac{\partial C}{\partial x} + \frac{\partial T}{\partial y}\frac{\partial C}{\partial y}\right) + \frac{\mu}{T_\infty}\left(\frac{\partial u}{\partial y}\right)^2 + \frac{\sigma B_0^2}{T_\infty}u^2 + \frac{\mu}{T_\infty K_p^*}u^2. \tag{3.39}$$

Where E_{Gen} is the nearby volumetric pace of irreversible generation within the sight of attractive field.

$$(E_{Gen})_0 = \frac{k(\Delta T)^2}{d^2 T_\infty^2}. \tag{3.40}$$

Where $(E_{Gen})_0$ is the typical irreversible generation rate.

Accordingly, the dimensionless entropy age number is characterized as the proportion of nearby volumetric entropy age rate to the trademark entropy rate:

$$Ns = \frac{E_{Gen}}{(E_{Gen})_0}. \tag{3.41}$$

Using equations (3.39) and (3.40) in equation (3.41). Then, we get the dimensionless entropy generation numbers is

$$Ns = \frac{r^2}{X^2}\theta^2(\eta) + Re\theta'^2(\eta) + Re\,\frac{Br}{\Omega}f''^2(\eta) + \frac{Br\left(H_a^2 + {}^1/_{D_a}\right)}{\Omega}f'^2(\eta) + \frac{s^2}{X^2}\lambda_1\varphi^2(\eta) + Re\,\lambda_2\varphi'^2(\eta) + \lambda_3\left(\frac{rs}{X^2}\theta(\eta)\varphi(\eta) + Re\theta'(\eta)\varphi'(\eta)\right), \tag{3.42}$$

Where Re is defined as,

$$Re = \frac{u_d d}{\nu}.$$

Br is defined as,

$$Br = \frac{\mu u_p^2}{k\Delta T}.$$

Dimensionless temperature contrast (Ω) is defined as,

$$\Omega = \frac{\Delta T}{T_\infty}.$$

Hartman number (H_a) is defined as:

$$H_a = B_o d\sqrt{\frac{\sigma}{\mu}},\ \frac{1}{D_a} = \frac{d^2}{K_p^*},\ X = \frac{x}{d},\ \lambda_1 = \frac{DT_\infty}{kC_\infty}\left(\frac{\Delta T}{\Delta C}\right)^2,\ \lambda_2 = \frac{DT_\infty^2}{kC_\infty}\left(\frac{\Delta T}{\Delta C}\right)^2,\ \lambda_3 = \frac{DT_\infty}{k}\left(\frac{\Delta T}{\Delta C}\right),\ u_d = \lambda d,\ u_p = \lambda x.$$

3.2 Methodology

To establish the solution of the transformed dimensionless nonlinear ODEs, assume the solution of equation (3.33) satisfying boundary conditions as

$$f(\eta) = \frac{1}{\alpha} - \frac{e^{-\alpha\eta}}{\alpha}. \tag{3.43}$$

Using equation (3.42) in equation (3.33), it yields

$$f(\eta) = \frac{1}{\alpha} - \frac{e^{-\alpha\eta}}{\alpha}. \tag{3.44}$$

Solving the above equation for the value of α, we get

$$\alpha = \sqrt{\frac{1+Mn+1/K_p}{1-R_c}}. \tag{3.45}$$

Equation (3.45) shows solution of the given problem. From equation (3.33) and (3.43), we obtain

$$u = x\lambda e^{-\alpha\eta},\ v = -\sqrt{\lambda\nu}\left(\frac{1}{\alpha} - \frac{e^{-\alpha\eta}}{\alpha}\right). \tag{3.46}$$

In order to get the arrangement of the energy condition in the structure of non-dimensional nonlinear ODE, we consider a new variable ξ as follows:

$$\xi = \frac{Pr}{\alpha^2} e^{-\alpha\eta}. \tag{3.47}$$

To apply this variable in equation (3.35), we convert the differentiation w.r.t η by using chain rule for first and second order ODEs, that is

$$\frac{d}{d\eta} = \frac{d}{d\xi} * \frac{d\xi}{d\eta} \quad and \quad \frac{d^2}{d\xi^2}\left(\frac{d\xi}{d\eta}\right)^2 + \frac{d}{d\xi} * \frac{d^2\xi}{d\eta^2}. \tag{3.48}$$

After applying the above chain rule on equation (3.35), we obtain

$$\xi\frac{d^2\theta}{d\xi^2} + \left(1 - \frac{Pr}{\alpha^2} + \xi\right)\frac{d\theta}{d\xi} - \left(r - \frac{Pr\beta}{\alpha^2\xi}\right)\theta(\xi), \tag{3.49}$$

and the reduced boundary conditions are

$$\theta\left(\xi = \frac{Pr}{\alpha^2}\right) = 1\ ,\ \theta\ (\xi = 0) = 0\ . \tag{3.50}$$

Eq. (3.49) is similar to Kummer's D.E that's give Kummer confluent hypergeometric function $|M|$, $|M|$(WhittakerM).

$$\theta(\xi) = -\frac{\left(|W|\left(A,B,\frac{1}{10000000}\right)\xi^C e^{-\frac{1}{2}\xi}|M|(A,B,\xi)\right)}{\left(\left(\frac{Pr}{\alpha^2}\right)^{\frac{1}{2}\frac{-\alpha^2+Pr}{\alpha^2}} e^{-\frac{1Pr}{2\alpha^2}}\left(\begin{pmatrix}|M|\left(A,B,\frac{1}{10000000}\right)\\ |W|\left(A,B,\frac{Pr}{\alpha^2}\right)\end{pmatrix} - \begin{pmatrix}|W|\left(A,B,\frac{1}{10000000}\right)\\ |M|\left(A,B,\frac{Pr}{\alpha^2}\right)\end{pmatrix}\right)\right)} + \frac{\left(|M|\left(A,B,\frac{1}{10000000}\right)\xi^C e^{-\frac{1}{2}\xi}|W|(A,B,\xi)\right)}{\left(\left(\frac{Pr}{\alpha^2}\right)^C e^{-\frac{1Pr}{2\alpha^2}}\left(\begin{pmatrix}|M|\left(A,B,\frac{1}{10000000}\right)\\ |W|\left(A,B,\frac{Pr}{\alpha^2}\right)\end{pmatrix} - \begin{pmatrix}|W|\left(A,B,\frac{1}{10000000}\right)\\ |M|\left(A,B,\frac{Pr}{\alpha^2}\right)\end{pmatrix}\right)\right)}, \tag{3.51}$$

Where $A = \frac{1}{2}\frac{-2r\alpha^2-\alpha^2+Pr}{\alpha^2}, B = \frac{1}{2}\frac{\sqrt{Pr}\sqrt{-4\alpha^2\beta+Pr}}{\alpha^2}, C = \frac{1}{2}\frac{-\alpha^2+Pr}{\alpha^2}$.

The solution of Eq. (3.44) in terms of η it gives

$$\theta(\eta) = -\frac{\left(|W|\left(A,B,\frac{1}{10000000}\right)\left(\frac{Pr}{\alpha^2}e^{-\alpha\eta}\right)^C e^{-\frac{1}{2}\left(\frac{Pr}{\alpha^2}e^{-\alpha\eta}\right)}|M|\left(A,B,\left(\frac{Pr}{\alpha^2}e^{-\alpha\eta}\right)\right)\right)}{\left(\left(\frac{Pr}{\alpha^2}\right)^{\frac{1}{2}\frac{-\alpha^2+Pr}{\alpha^2}} e^{-\frac{1Pr}{2\alpha^2}}\begin{pmatrix}\begin{pmatrix}|M|\left(A,B,\frac{1}{10000000}\right)\\ |W|\left(A,B,\frac{Pr}{\alpha^2}\right)\end{pmatrix}-\\ \begin{pmatrix}|W|\left(A,B,\frac{1}{10000000}\right)\\ |M|\left(A,B,\frac{Pr}{\alpha^2}\right)\end{pmatrix}\end{pmatrix}\right)} +$$

$$\frac{\left(|M|\left(A,B,\frac{1}{10000000}\right)\left(\frac{Pr}{\alpha^2}e^{-\alpha\eta}\right)^C e^{-\frac{1}{2}\xi}|W|\left(A,B,\left(\frac{Pr}{\alpha^2}e^{-\alpha\eta}\right)\right)\right)}{\left(\left(\frac{Pr}{\alpha^2}\right)^C e^{-\frac{1Pr}{2\alpha^2}}\begin{pmatrix}\begin{pmatrix}|M|\left(A,B,\frac{1}{10000000}\right)\\ |W|\left(A,B,\frac{Pr}{\alpha^2}\right)\end{pmatrix}-\\ \begin{pmatrix}|W|\left(A,B,\frac{1}{10000000}\right)\\ |M|\left(A,B,\frac{Pr}{\alpha^2}\right)\end{pmatrix}\end{pmatrix}\right)}. \quad (3.52)$$

Again, for concentration equation, in order to get the solution of the concentration equation in the form of non-dimensional nonlinear ODE, we consider a new variable t as follows:

$$t = \frac{Sc}{\alpha^2}e^{-\alpha\eta}. \quad (3.53)$$

To apply this variable in equation (3.36), we convert the differentiation w.r.t η by using chain rule for first and second order ODEs, that is

$$\frac{d}{d\eta} = \frac{d}{dt} * \frac{dt}{d\eta} \quad and \quad \frac{d^2}{dt^2}\left(\frac{dt}{d\eta}\right)^2 + \frac{d}{dt} * \frac{d^2t}{d\eta^2}. \quad (3.54)$$

After applying the above chain rule on equation (3.36), we obtain

$$t\frac{d^2\varphi}{dt^2} + \left(1 - \frac{Sc}{\alpha^2} + t\right)\frac{d\varphi}{dt} - s\varphi(t), \quad (3.55)$$

and the reduced boundary conditions are

$$\varphi\left(t = \frac{Sc}{\alpha^2}\right) = 1\ ,\ \varphi\ (t = 0) = 0\ . \quad (3.56)$$

Eq. (3.55) is similar to Kummer's D.E that's give Kummer confluent hypergeometric function $|M|$, $|M|$(KummerM) and $|U|$(KummerU).

$$\theta(\xi) = -\frac{\left(|U|\left(E,D,\frac{1}{10000000}\right)t^{\frac{Sc}{\alpha^2}}e^{-t}|M|(E,D,t)\right)}{\left(\left(\frac{Sc}{\alpha^2}\right)^{\frac{Sc}{\alpha^2}}e^{-\frac{Sc}{\alpha^2}}\left(\begin{pmatrix}|M|\left(E,D,\frac{Sc}{\alpha^2}\right)\\|U|\left(E,D,\frac{1}{10000000}\right)\end{pmatrix}-\begin{pmatrix}|U|\left(E,D,\frac{Sc}{\alpha^2}\right)\\|M|\left(E,D,\frac{1}{10000000}\right)\end{pmatrix}\right)\right)} + \frac{\left(|M|\left(E,D,\frac{1}{10000000}\right)t^{\frac{Sc}{\alpha^2}}e^{-t}|U|(E,D,t)\right)}{\left(\left(\frac{Sc}{\alpha^2}\right)^{\frac{Sc}{\alpha^2}}e^{-\frac{Sc}{\alpha^2}}\left(\begin{pmatrix}|M|\left(E,D,\frac{Sc}{\alpha^2}\right)\\|U|\left(E,D,\frac{1}{10000000}\right)\end{pmatrix}-\begin{pmatrix}|U|\left(E,D,\frac{Sc}{\alpha^2}\right)\\|M|\left(E,D,\frac{1}{10000000}\right)\end{pmatrix}\right)\right)},$$

(3.57)

Where $D = \frac{\alpha^2+Sc}{\alpha^2}$, $E = s + 1$.

The solution of Eq. (3.57) in terms of η it gives

$$\theta(\xi) = -\frac{\left(|U|\left(E,D,\frac{1}{10000000}\right)\frac{Sc}{\alpha^2}e^{-\alpha\eta}\frac{Sc}{\alpha^2}e^{-\frac{Sc}{\alpha^2}e^{-\alpha\eta}}|M|(E,D,t)\right)}{\left(\left(\frac{Sc}{\alpha^2}\right)^{\frac{Sc}{\alpha^2}}e^{-\frac{Sc}{\alpha^2}}\left(\begin{pmatrix}|M|\left(E,D,\frac{Sc}{\alpha^2}\right)\\|U|\left(E,D,\frac{1}{10000000}\right)\end{pmatrix}-\begin{pmatrix}|U|\left(E,D,\frac{Sc}{\alpha^2}\right)\\|M|\left(E,D,\frac{1}{10000000}\right)\end{pmatrix}\right)\right)} +$$

$$\frac{\left(|M|\left(E,D,\frac{1}{10000000}\right)\frac{Sc}{\alpha^2}e^{-\alpha\eta}\frac{Sc}{\alpha^2}e^{-\frac{Sc}{\alpha^2}e^{-\alpha\eta}}|U|(E,D,t)\right)}{\left(\left(\frac{Sc}{\alpha^2}\right)^{\frac{Sc}{\alpha^2}}e^{-\frac{Sc}{\alpha^2}}\left(\begin{pmatrix}|M|\left(E,D,\frac{Sc}{\alpha^2}\right)\\|U|\left(E,D,\frac{1}{10000000}\right)\end{pmatrix}-\begin{pmatrix}|U|\left(E,D,\frac{Sc}{\alpha^2}\right)\\|M|\left(E,D,\frac{1}{10000000}\right)\end{pmatrix}\right)\right)}.$$

(3.58)

3.3 Results and discussion

The subsequent conversation centers revolve about revealing the effect of parameter controls by the volumetric rate of entropy production. An amazing feature of speed profiles, in both the longitudinal and transverse segments, has two layout characters.

Fig.2 and Fig.3: demonstrate longitudinal speed profiles for real fluid ($Rc = 0$) and viscoelastic ($Rc \neq 0$) fluid when there is existence of porouse medium($K_p = 0.5$) and in the nonappearance($K_p = 100$). It should be noted that the expansion in viscoelastic and magnetic parameters decreases in speed equally. Noted that the presence of a permeable framework decreases the speed continuously. The Mn increase exerts a

stronger, Lorentz force an opposing power of electromagnetic beginning, causing velocity is decrease. Furthermore, now the event of a flexible fluid. We cannot ignore the stress. Nonetheless, it very well might be less, except aimed at the degree of stress of the viscous fluid, as it is answerable for recuperation in initial state and retrospective movement following the exclusion stress.

Fig. 4, Fig. 5: demonstrate the retardation of cross over speed due to rise in magnetic and elastic and additional diminished by the permeable medium presence. Observed the result of the relative multitude of boundaries on both the parts remains unchanged. Arranged cautious statement more discovered that within the sight of permeable substance, pressure of these profiles are defined in two of the cases noteworthy in the magnetic field occurrence.

In Fig. 6 - Fig. 8: shows whenever porous matrix is present it improves the temperature at every point which donate better field to dispersion of thermal boundary-layer. While temperature decrease when Pr increases. We can observed this temperature at all point is increase speed with magnetic parameter and elastic parameter. it appears relatively justified the recovery and opposite flow of elimination of strain as the resistance due to collaboration of magnetic field and strain energy, velocity of affecting obstruction discussed in Fig. 2 - Fig. 3: Therefore, temperature increasing at all points causes retardation of velocity increasing both are the resistive forces. Viscoelasticity increases in the temperature profile Walter's fluid B and temperature increase with Mn.

Fig. 9, Fig. 10: outline the impacts of intensity sink/source boundary. We can observe heat transfer climbs with the expansion in source strength and the converse impact exists with an expansion in r, now influence list describing the heat variety. Great concurrence by [34]. It is additionally seen that descend causes reduction in heat and permeable medium existence($K_p = 0.5$) in expands the temperature within the sight of sink.

Fig. 11: illustrates the focus conveyance for different upsides of boundaries. It is concluded from bends (i) and (ii) that if the specie is heavier then it will diminish focus without attractive field and permeable medium. Bends (i) and (iii) indicates in all focuses attractive boundary builds the fixation conveyance essentially. The existence of permeable medium builds fixation close by each point additionally displayed in Curves (iii) and (iv). Bends (iv, viii) and (iii, vii) guarantee on behalf of greater record. Fixation diminishes regardless of existence before nonappearance of permeable average. A similar perception stayed finished up before trendy regard of temperature moreover. In this way,

reasoned that thicker class and greater influence file of plate focus dissemination effect a reduction in fixation. While, affected by Lorentz power and porousness of the medium the focus level increments. Presently, unique qualities of medium i.e., volumetric entropy viewed attractive field and permeable can be examined.

Fig. 12 - Fig. 14: show the impacts of Pr, Mn and Rc on the irreversible. The higher Pr generate irreversibles and existence of force dissipation decreases. It seems that creating higher entropy is existence of permeable medium demonstrations unfavorably for greater Pr liquid stream. Flexible boundary job is amazing. This show that Ns of two-layer types inside vision of permeable medium and flexible boundary job stays similar by way of Pr and Mn .

Fig. 15 - Fig. 17: exhibition the enhancements of r, H_a and Re_d. On cautious perception it is uncovered that the characters of H_a and r are very much similar as Mn just through lesser passion on the plate and Re_d job exists additionally toward produce the higher Ns by unique differentiation causal considerably different boundaries examined, By consideration of force dispersal during time spent Ns in current review favors higher Ns level in every one of bends uncovering fluid with higher Pr. Alternative Ns is positive in every one of the sources guaranteeing the cycle is irremediable is noticeable element. Current review guarantees the irreversibility in the event of viscoelastic fluid with more elevated level Ns on the bouncing region inside the vision of permeable average causal Force dissemination.

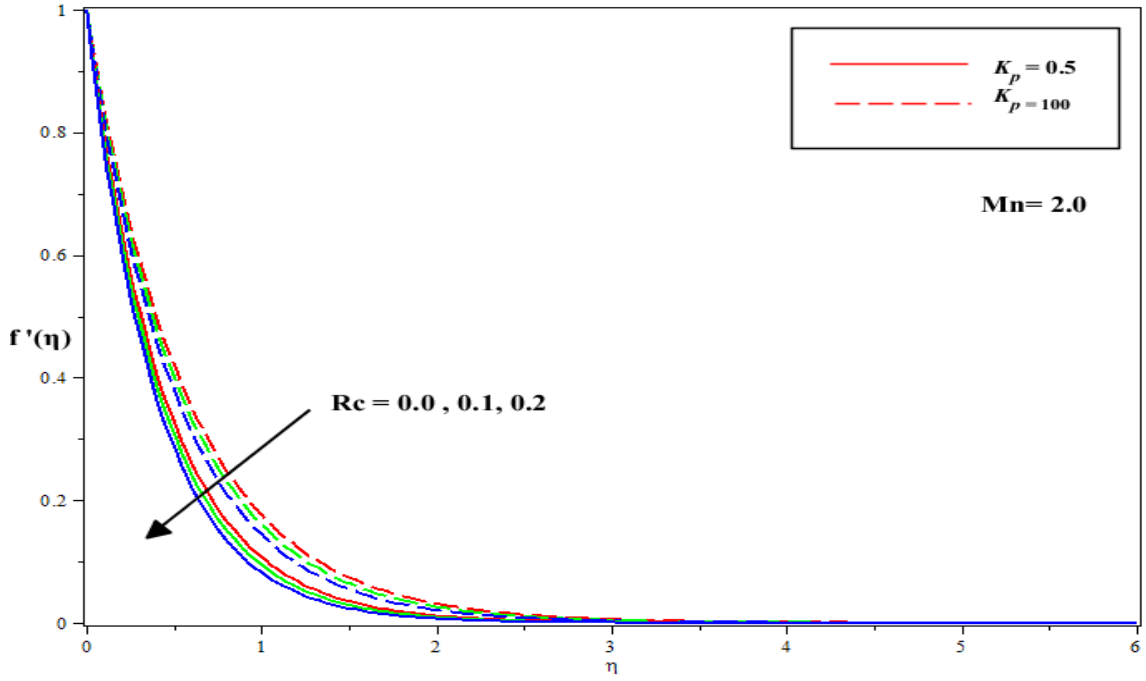

Fig. 2: Impact of Rc and Kp on longitudinal velocity for Mn

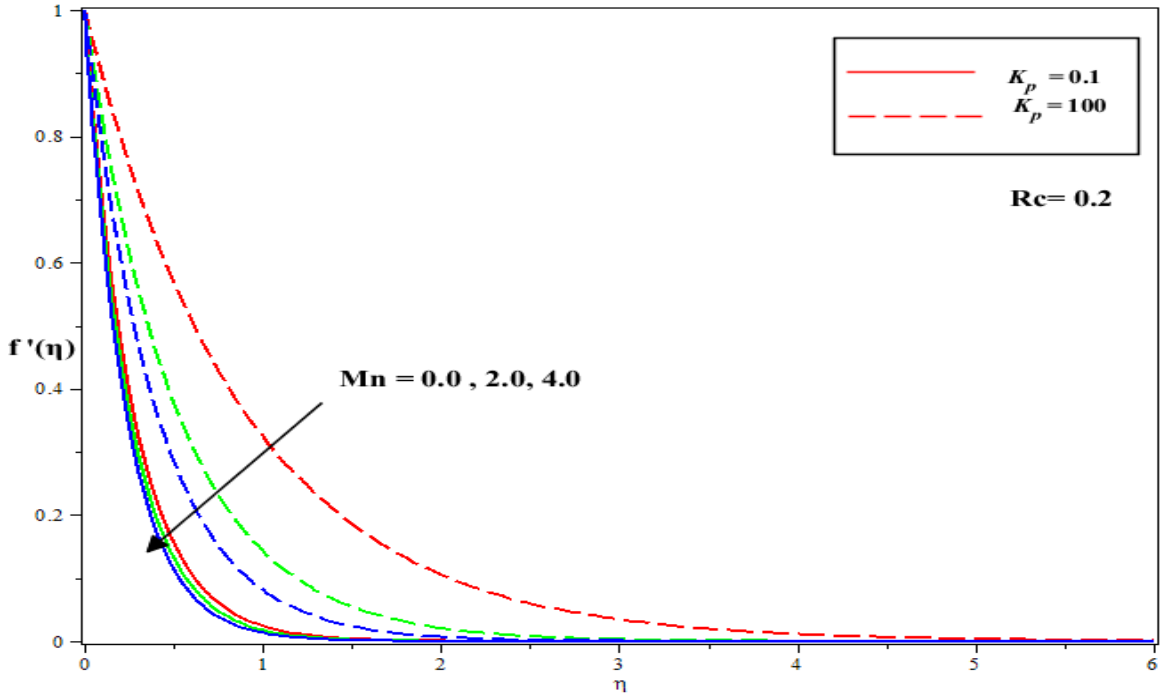

Fig. 3: Impact of Mn and Kp on transverse velocity for Rc.

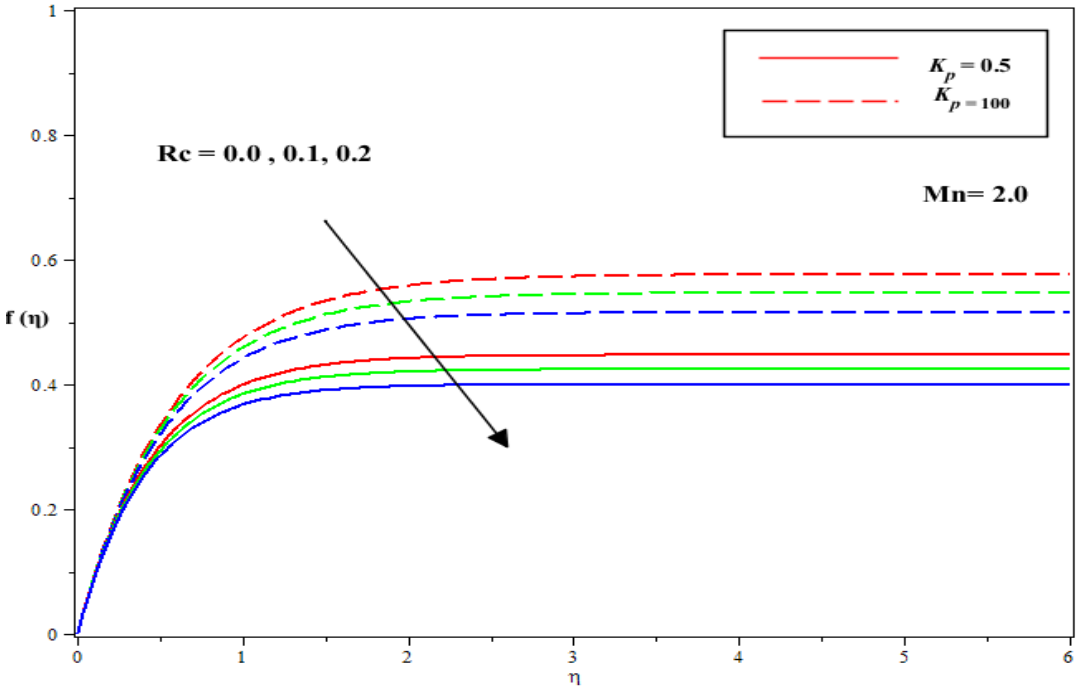

Fig. 4: Impact of Rc.And Kp on transverse velocity for Mn.

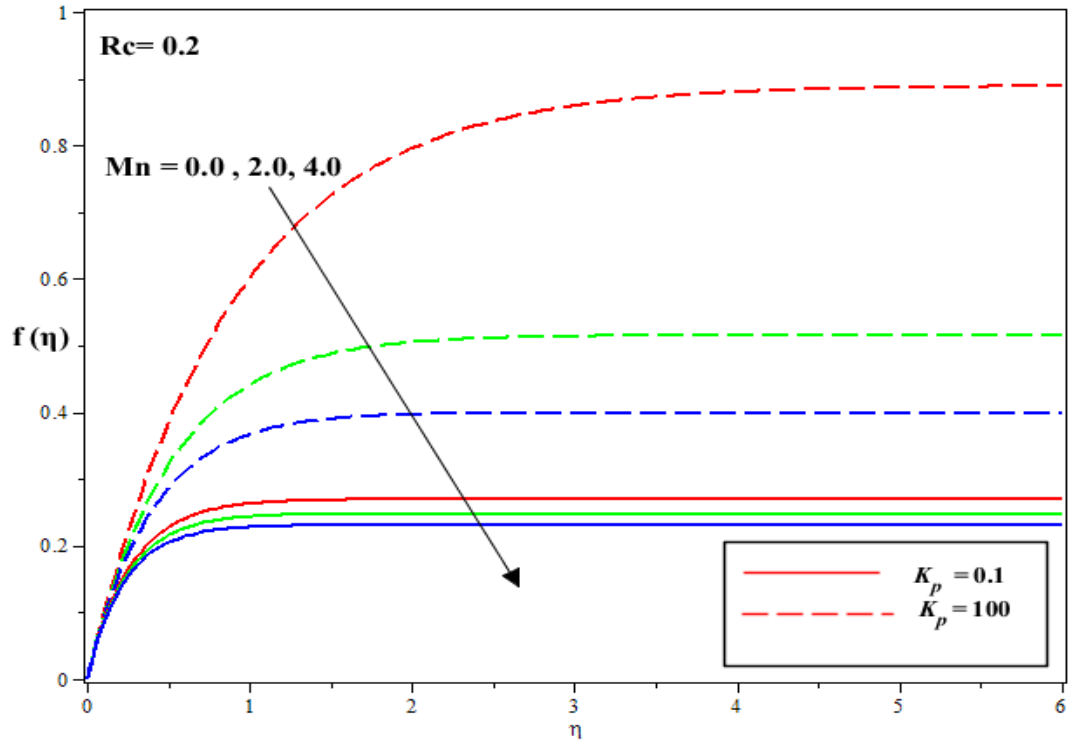

Fig. 5: Impact of Mn and Kp on longitudinal velocity for Rc

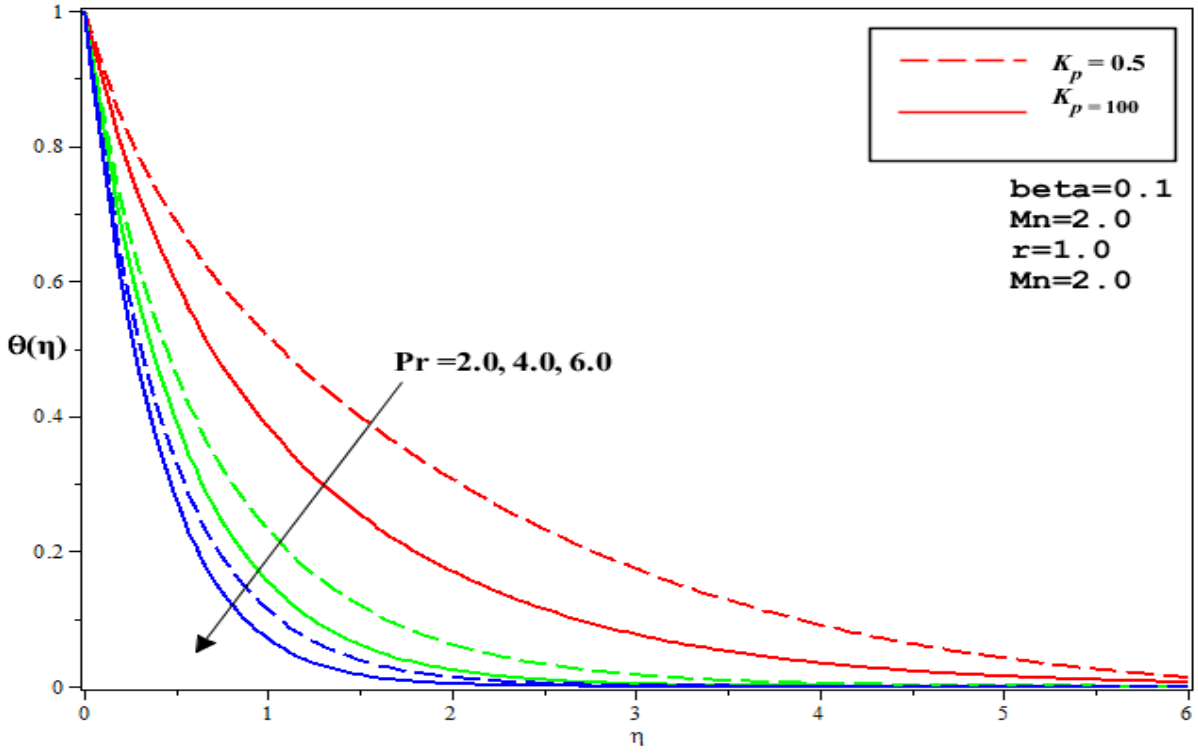

Fig. 6: Impact of Pr and Kp on $\theta\eta$ for Mn, Rc, , β, r.

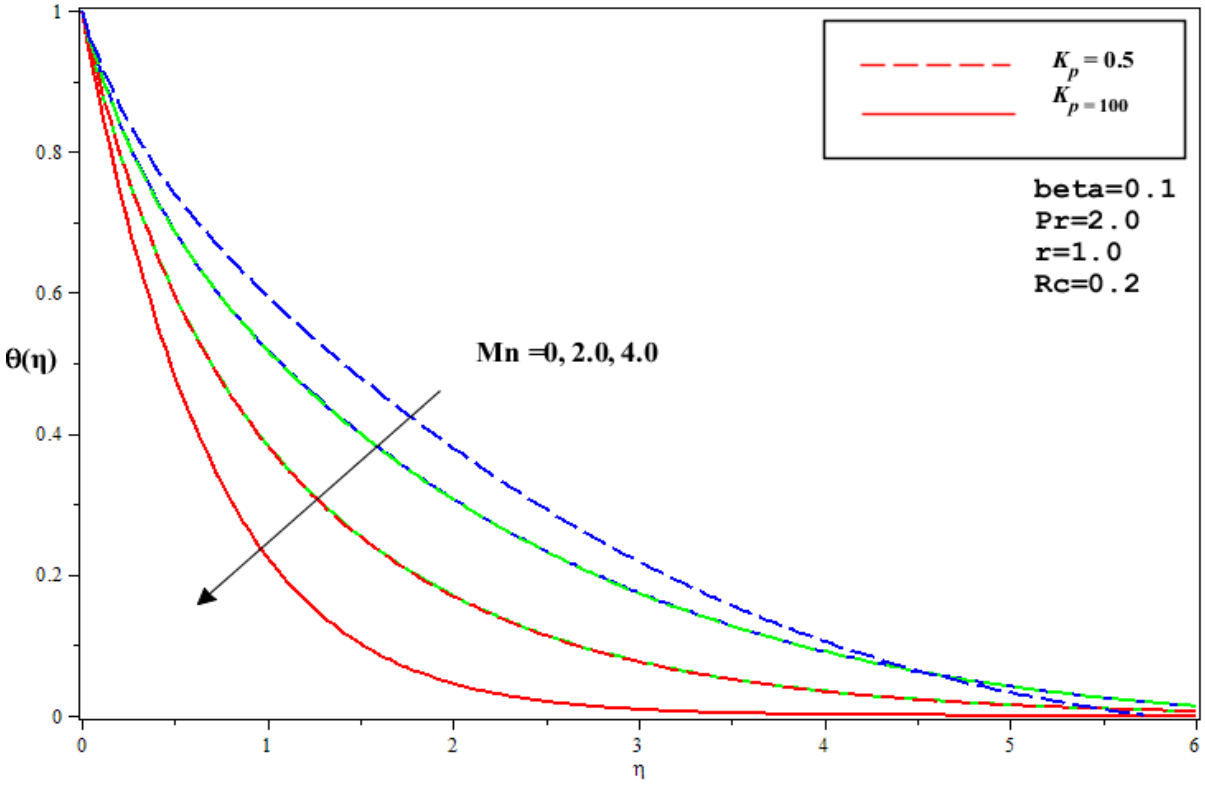

Fig. 7: Impact of Mn and Kp on $\theta(\eta)$ for Pr, Mn, β, r.

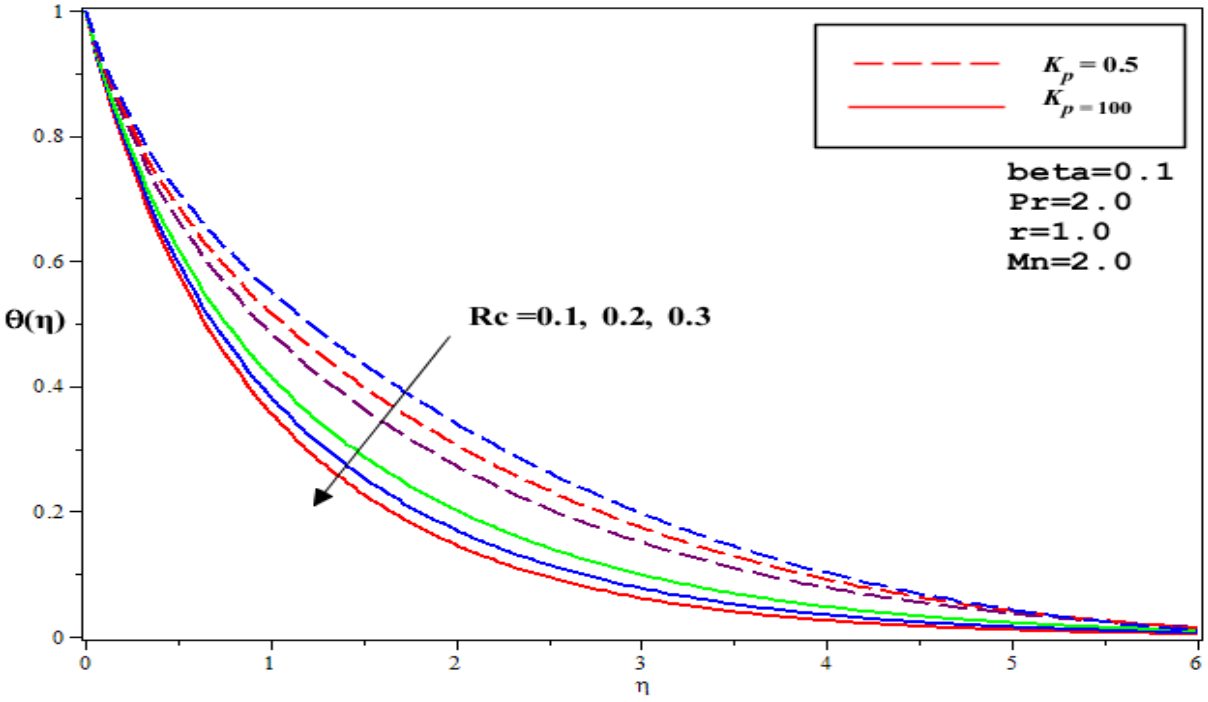

Fig. 8: Effects of Rc and Kp on $\theta(\eta)$ for Pr, Mn, β, r.

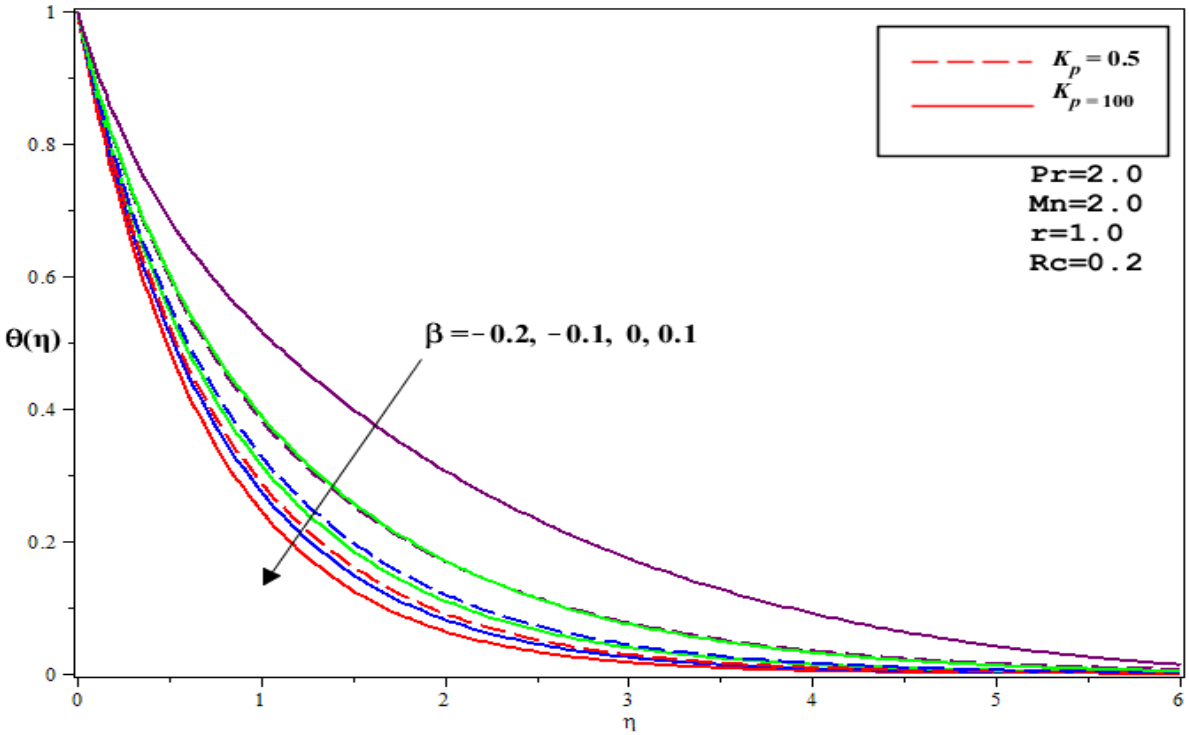

Fig. 9: Impact of β (source/sink) on $\theta(\eta)$ for Pr, Mn, Rc, r.

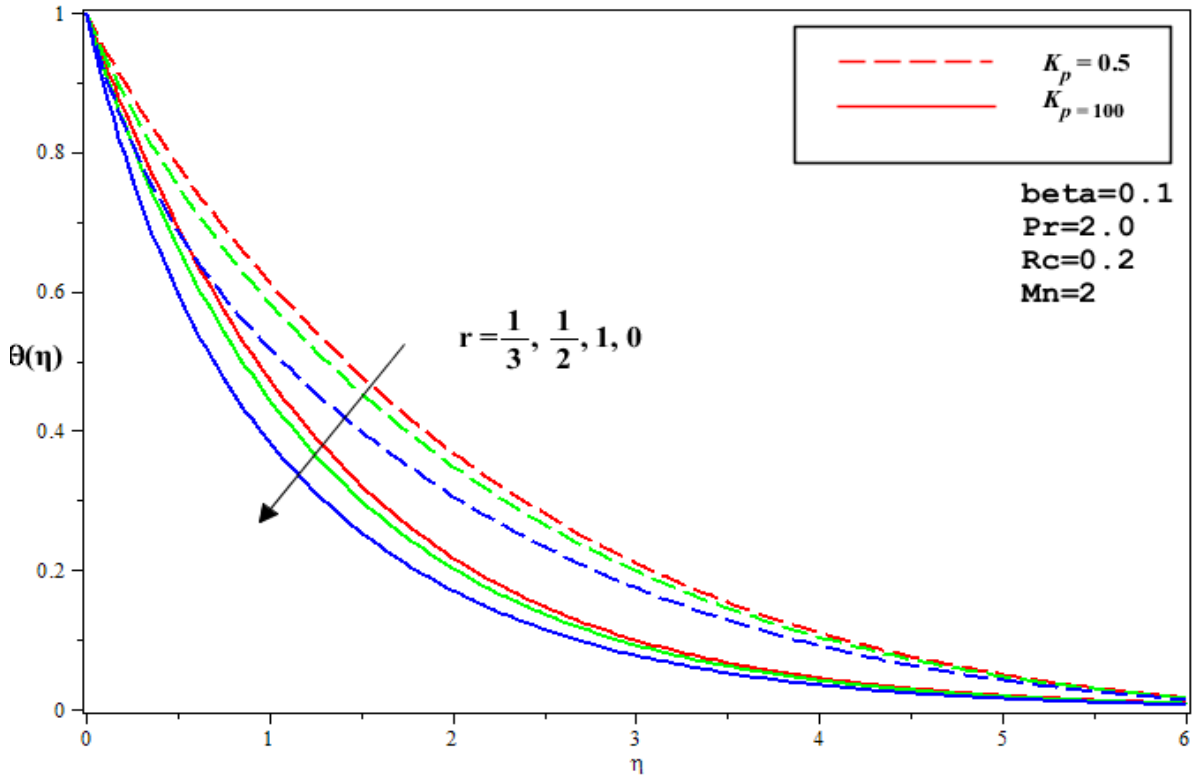

Fig. 10: Impact of r on $\theta(\eta)$ for Pr, Mn, β, Rc.

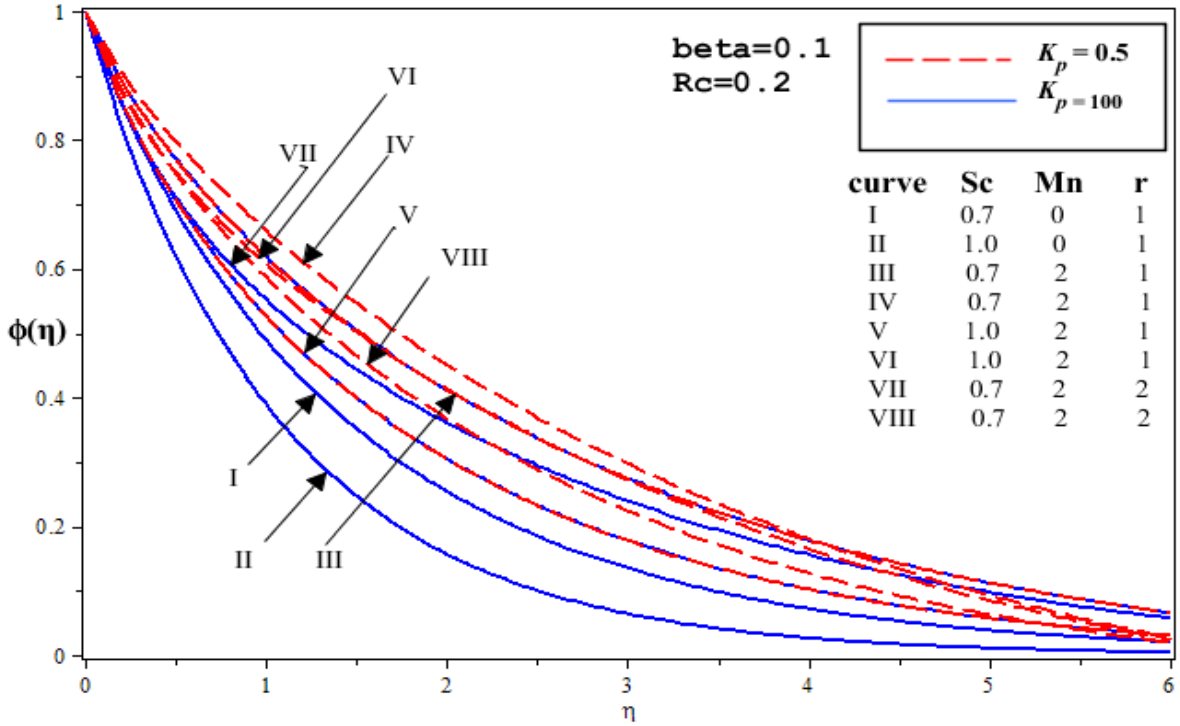

curve	Sc	Mn	r
I	0.7	0	1
II	1.0	0	1
III	0.7	2	1
IV	0.7	2	1
V	1.0	2	1
VI	1.0	2	1
VII	0.7	2	2
VIII	0.7	2	2

Fig. 11: Impact of Sc, Mn, Kp and r on $\varphi(\eta)$

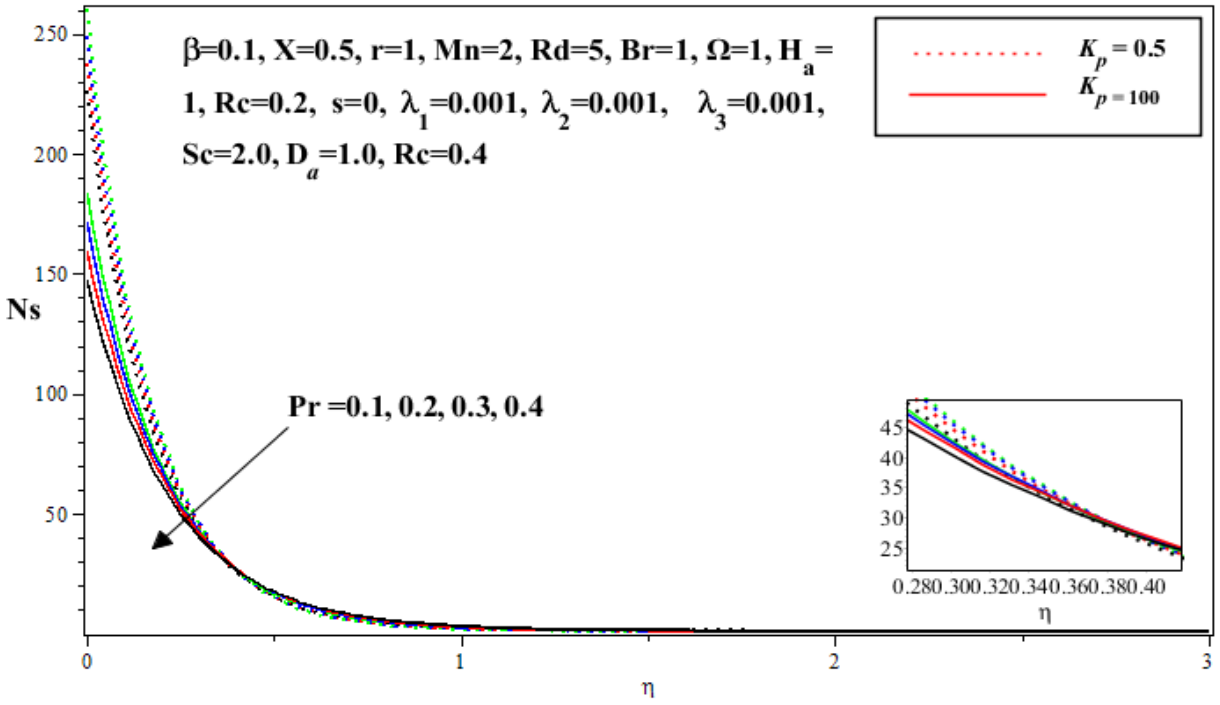

Fig. 12: Impact of Pr, and K_p on Ns for $s, \lambda_1, \lambda_2, \lambda_3$

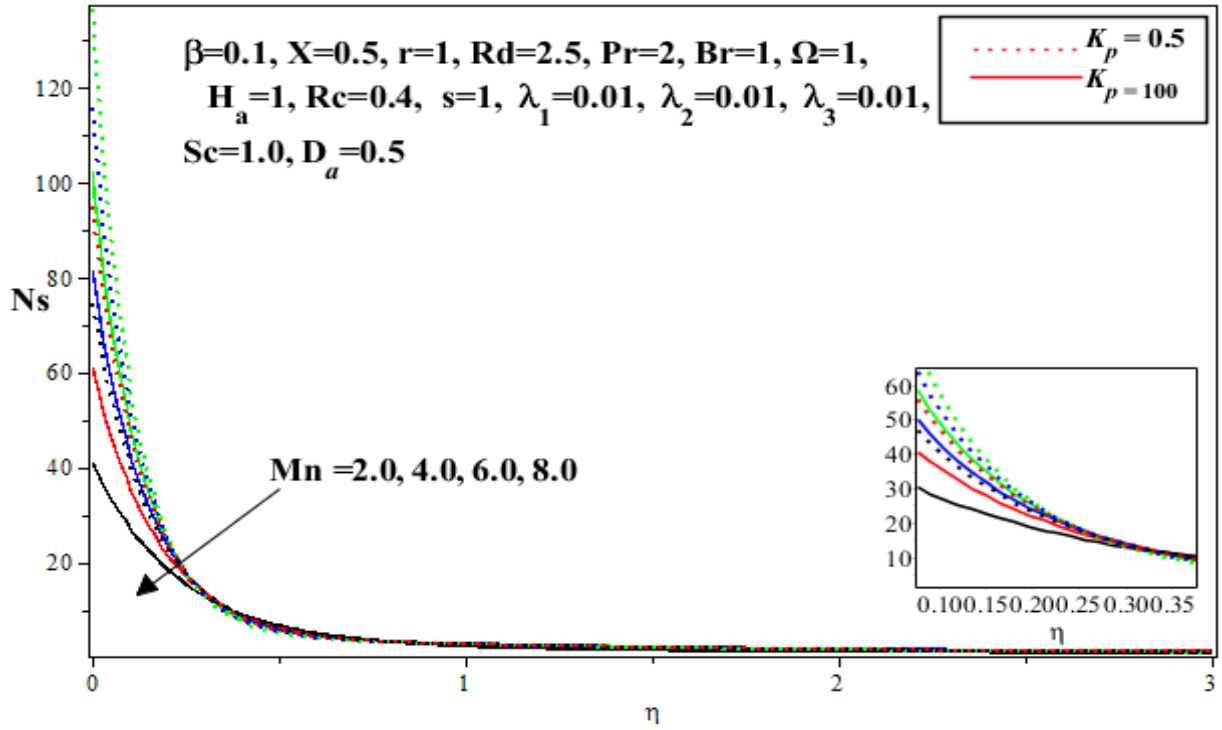

Fig. 13: Impact of Mn and K_p on Ns

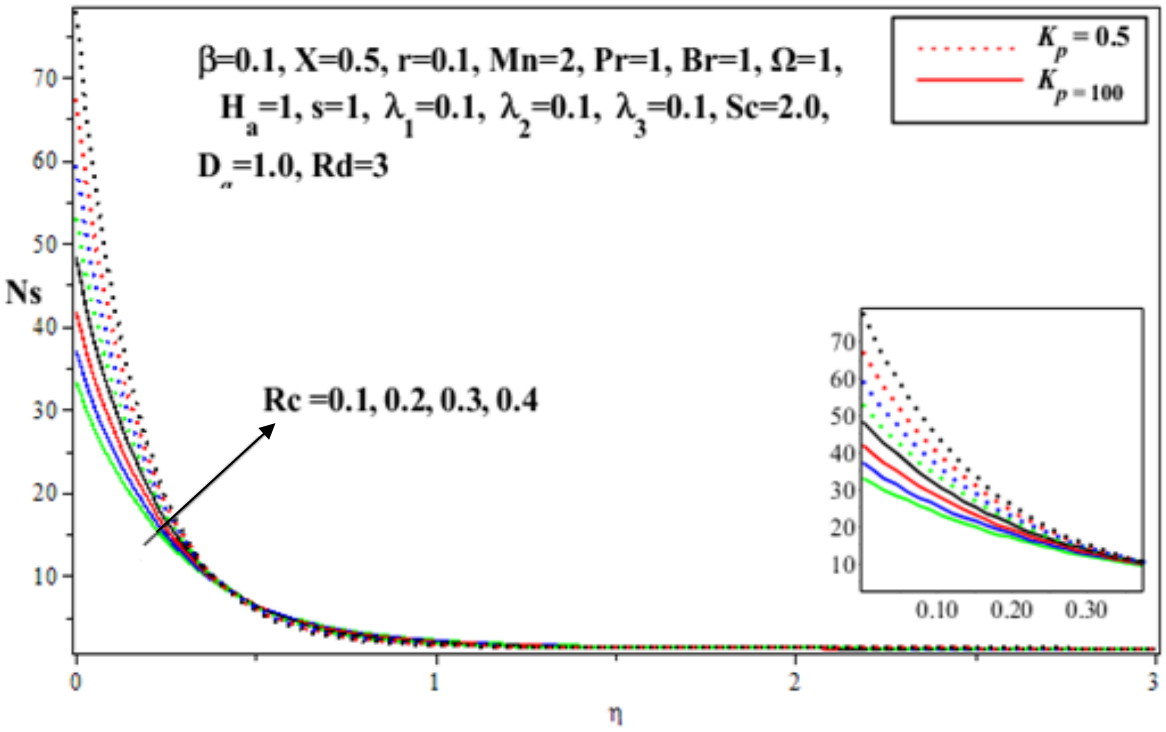

Fig. 14: Impact of Rc and K on Ns.

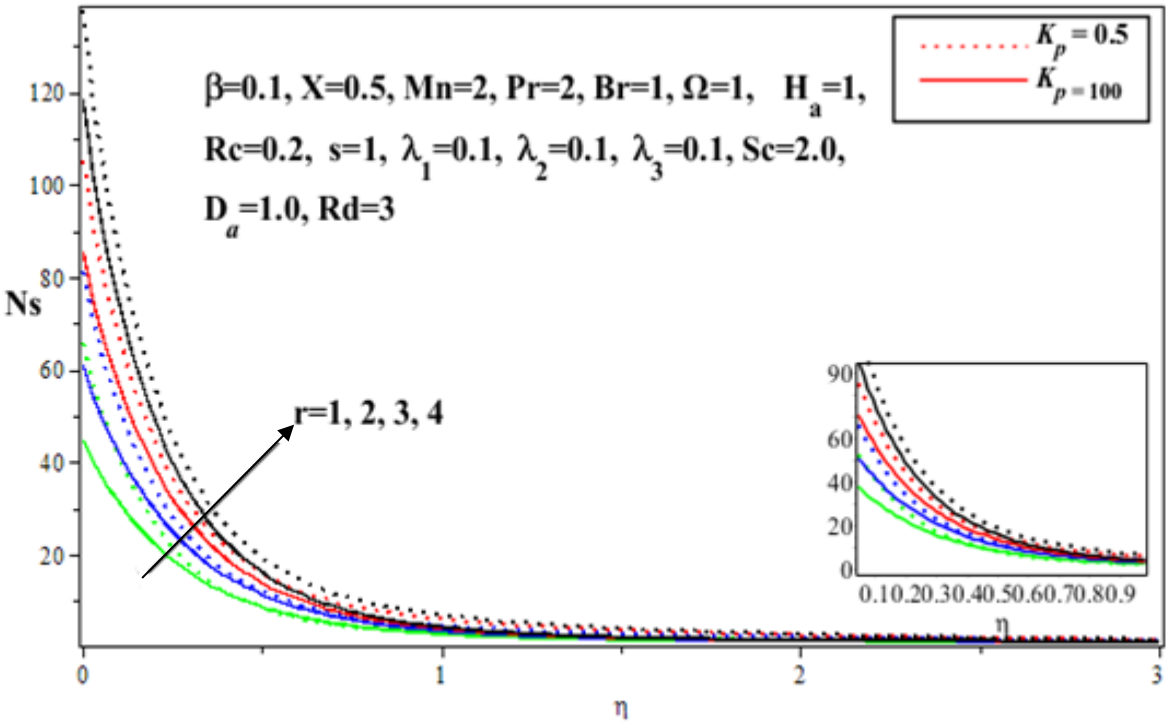

Fig. 15: Impact of r and K_p on Ns

.

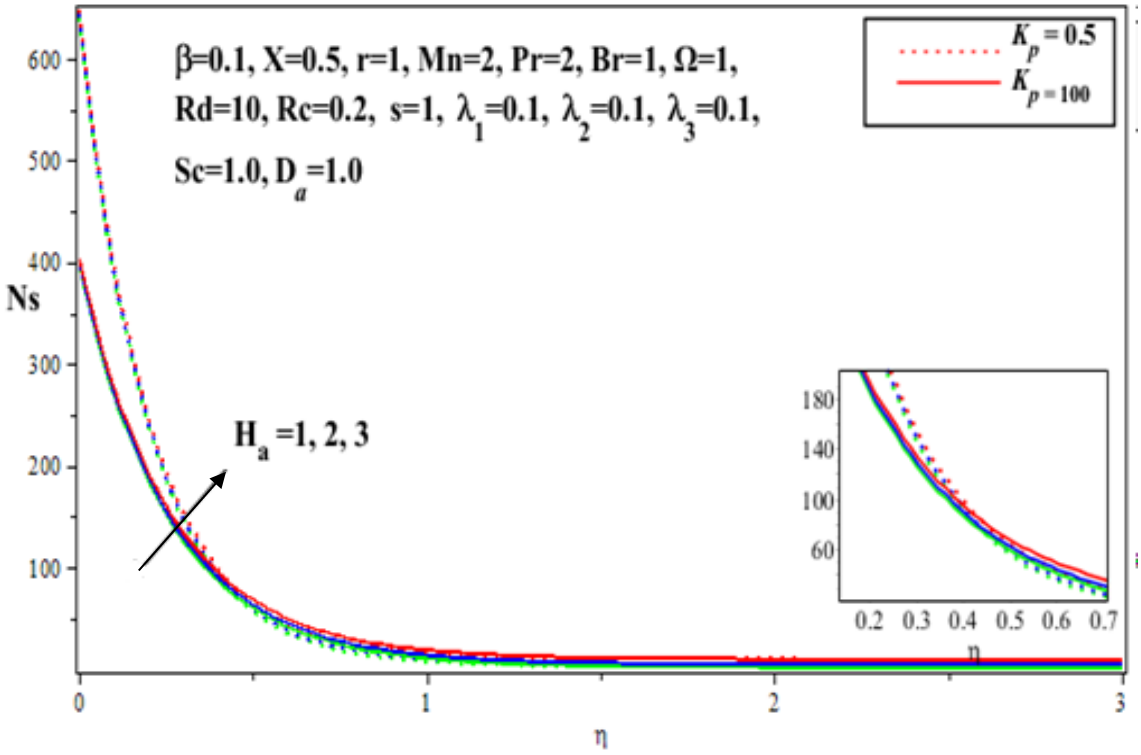

Fig. 16: Impact of H_a and K_p on Ns.

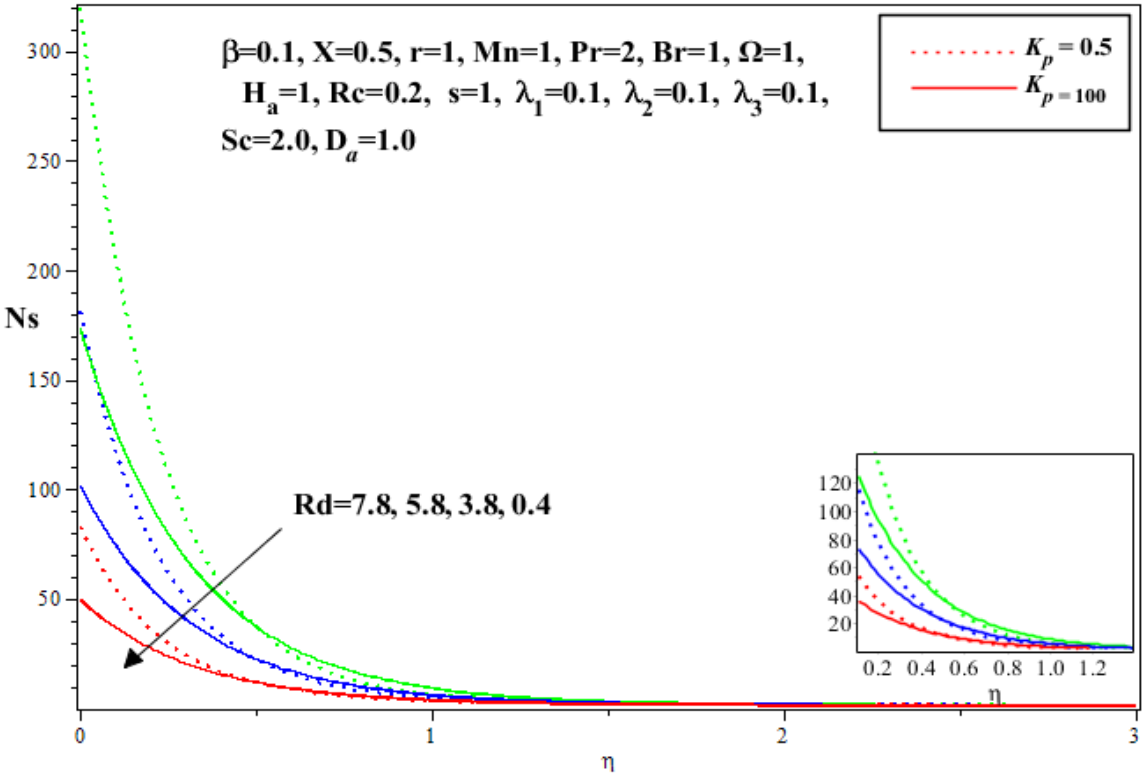

Fig. 17: Impact of Re and K_p on Ns.

.

CHAPTER 4

EXACT SOLUTION OF JEFFREY FLUID FLOW DUE TO STRETCHING/SHRINKING SURFACE

This chapter is extension work of previous chapter. In previous chapter I reviewed the exact solution of viscoelastic liquid (WaltersB'). On the other side I reviewed a paper of Jaffrey fluid model "numerical solution of non-Newtonian nanofluid flow over a stretching sheet". Based upon previous chapter 3 the mathematical model rearranged and converting Jaffrey fluid model numerical solution into exact solution by using Maple. Results are attained by analytical technique. Later, mathematical modeling was applied using boundary conditions. Using similarity variables, concentration, every PDEs of momentum and energy are transformed into nonlinear ODEs for a proper formulation.

4.1 Mathematical modeling and exact solution

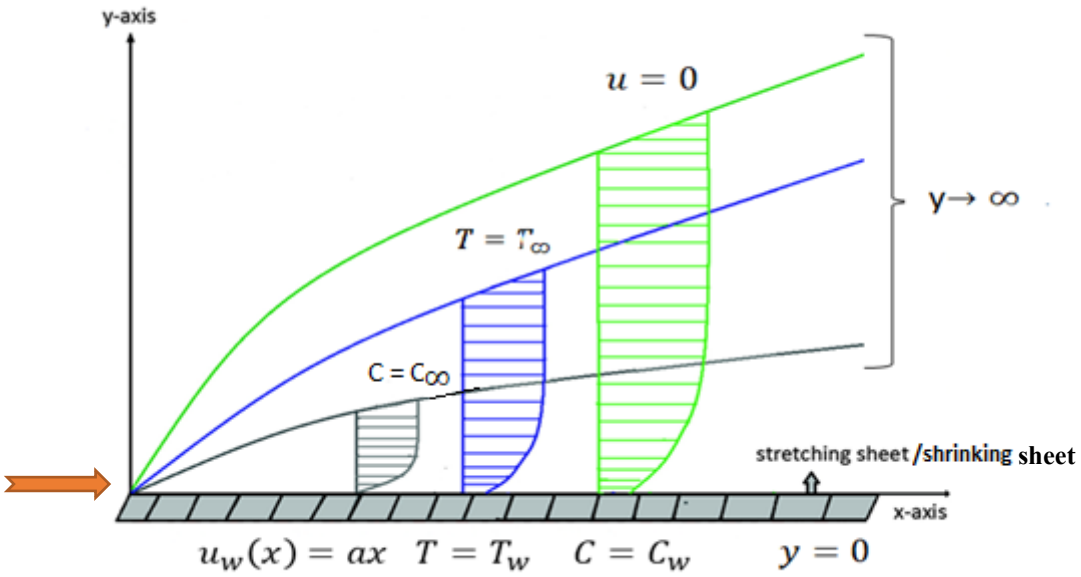

Fig. 18: Geometry of Table

Considering a steady fluid which is incompressible and flowing past a stretched sheet in two dimensions. Moreover, when the sheet is extending with the plane $y = 0$, the impacts of nanoparticles are exhausted. It is assumed that the flow is constrained to $y > 0$. The x-axis is taken along the stretching sheet, surface is stretched/shrinked with linear velocity $u_w(x) = ax$ in this example, where $a > 0$ is constant. The following are the Jeffrey fluid boundary layer equations along nanoparticles:

$$\frac{\partial u}{\partial x} + \frac{\partial v}{\partial y} = 0, \tag{4.1}$$

$$u\frac{\partial u}{\partial x} + v\frac{\partial u}{\partial y} = \frac{\nu}{1+k1}\left[\frac{\partial^2 u}{\partial y^2} + kn\left(u\frac{\partial^3 u}{\partial x \partial y^2} - \frac{\partial u}{\partial x}\frac{\partial^2 u}{\partial y^2} + \frac{\partial u}{\partial y}\frac{\partial^2 u}{\partial x \partial y} + v\frac{\partial^3 u}{\partial y^3}\right)\right], \tag{4.2}$$

$$u\frac{\partial u}{\partial x} + v\frac{\partial u}{\partial y} = \alpha\left(\frac{\partial^2 T}{\partial y^2}\right), \tag{4.3}$$

$$u\frac{\partial u}{\partial x} + v\frac{\partial u}{\partial y} = D_B\left(\frac{\partial^2 C}{\partial y^2}\right). \tag{4.4}$$

Where u velocity is along x direction and v velocity along y direction. Electrical conductivity denoted by σ. Density of the fluid and base fluid is denoted by ρ and ρ_f respectively. The. kn and $k1$ are ratio of retardation time and relaxation to retardation times. Thermal diffusivity is denoted by α .τ is the ration of $(\rho c)_p$and $(\rho c)_f$.

The associated conditions on boundary are:

$$\text{at } y = 0, \quad u = u_w(x) = ax, \quad v = 0, \quad T = T_w, \quad C = C_w, \tag{4.5a}$$

$$\text{as } y \to \infty, \; u \to 0, \quad v \to 0, \quad u_y \to 0, \quad T \to T_\infty, \quad C \to C_\infty. \tag{4.5b}$$

where $u = u_w(x) = ax$, a is the parameter of stretching/shrinking sheet.

(i) $a < 0$, for shrinking sheet.

(ii) $a > 0$, for stretching sheet.

Where, the stretching velocity is denoted by $u_w(x)$. T_w denotes wall temperature and C_w denotes concentration. T_∞ is Ambient temperature and concentration are denoted by C_∞.

To convert governing PDEs into dimensionless ODEs, have used the similarity transformation,

Using similarity variables:

$$\eta = y\sqrt{\frac{a}{\nu}},\ \varphi(\eta) = \frac{C-C_\infty}{C_w-C_\infty},\ \theta(\eta) = \frac{T-T_\infty}{T_w-T_\infty},\quad \Psi(x,y) = \sqrt{a\nu}xf(\eta). \tag{4.6}$$

The stream function ψ is expressed as

$$u = \frac{\partial}{\partial x}\psi(x,y),\ v = -\frac{\partial}{\partial y}\psi(x,y). \tag{4.7}$$

Solving above equation(4.7), we obtain

$$u = xaf'(\eta),\ v = -\sqrt{a\nu}f(\eta). \tag{4.8}$$

Making use of these transformations, identically continuity equation is satisfied and equation(4.2), (4.3)and (4.4) along with the conditions on boundary $(4.5a)$ and $(4.5b)$ takes the form

$$f''' + k2\left(f''^2 - ff'''\right) + (k1+1)\left(ff'' - f'^2\right) = 0, \tag{4.9}$$

$$\theta'' + Prf\theta' = 0, \tag{4.10}$$

$$\varphi'' + LePrf\varphi' = 0. \tag{4.11}$$

Where β is Deborah number, Lewis number and Prandtl number denoted by Le is Pr respectively,

$$Pr = \frac{\nu}{\alpha}\ ,\quad k2 = a * kn\ ,\quad Le = \frac{\alpha}{D_B}.$$

By using equation(4.8), conditions $(4.5a)$ and $(4.5b)$ takes the following form

$$\text{At}\eta = 0,\ f(0) = 0,\ f'(0) = 1,\ f'(0) = -1,\ \theta(0) = 1,\ \varphi(0) = 1, \tag{4.12a}$$

$$\text{as}\ \ \eta \to \infty,\ f''(\infty) \to 0,\ f'(\infty) \to 0,\ \theta(\infty) \to 0,\ \varphi(\infty) \to 0. \tag{4.12b}$$

(i) $f'(0) = 1$, for stretching sheet.

(ii) $f'(0) = -1$, for shrinking sheet.

Mathematically, C_f is Skin friction coefficient, Sh_x is Sherwood and Nu_x is Nusselt number defined as,

$$C_f = \frac{\tau_w}{\rho U_w^2},\quad ,\quad Sh_x = \frac{xq_m}{D_B(C_w-C_\infty)}\ ,\quad Nu_x = \frac{xq_w}{\alpha(T_w-T_\infty)}. \tag{4.13}$$

Where, τ_w represent shear stress, q_w represent heat flux, q_m represent mass flux, i.e,

$$q_w = -\alpha\left(\frac{\partial T}{\partial y}\right)_{y=0},\ \tau_w = \mu\left(\frac{\partial u}{\partial y}\right)_{y=0}, q_m = D_B\left(\frac{\partial C}{\partial y}\right)_{y=0}. \tag{4.14}$$

Using non-dimensionless similarity variables and equations (4.14) in (4.13), we obtain

$$C_f\sqrt{Re_x} = \frac{1+k2}{1+k1}f''(0)\,, \quad Nu_x\sqrt{Re_x} = -\theta'^{(0)}, \quad Sh_x\sqrt{Re_x} = -\varphi'(0). \tag{4.15}$$

In above expressions $Re_x = \frac{u_x(x)}{\nu}$, is local Reynolds number.

Generation analysis Entropy

Local entropy generation per unit volume for the Jeffrey fluid is denoted by S_G:

$$S_G = \frac{k}{T_\infty^2}\left(\frac{\partial T}{\partial y}\right)^2 + \frac{D_B}{C_\infty}\left(\frac{\partial C}{\partial y}\right)^2 + \frac{D_B}{T_\infty}\left(\frac{\partial T}{\partial y}\frac{\partial C}{\partial y}\right) + \frac{\mu}{T_\infty(1+k1)}\left(\left(\frac{\partial u}{\partial y}\right)^2 + kn\left(u\frac{\partial u}{\partial y}\frac{\partial^2 u}{\partial x\partial y} + v\frac{\partial u}{\partial y}\frac{\partial^2 u}{\partial y^2}\right)\right). \tag{4.16}$$

In Eq. (4.16) the initial term on the right-hand side of is because of intensity move, because of mass exchange the second and third term are framed, the fourth term is the entropy age because of thick dissemination and Jeffrey liquid impact. A $(S_G)_0$ is trademark entropy age rate which is characterized as:

$$(S_G)_0 = \frac{k(\Delta T)^2}{x^2T_\infty^2}, \tag{4.17}$$

The proportion of neighborhood volumetric entropy generation to the trademark entropy rate is called dimensionless entropy age number Ns:

$$Ns = \frac{S_G}{(S_G)_0}. \tag{4.18}$$

Using equations (4.16) and (4.17) in equation (4.18). then, we get the dimensionless entropy generation numbers is

$$Ns = Re\,\theta'^2(\eta) + \frac{Re\,\epsilon\Sigma^2\varphi'^2(\eta)}{\Omega^2} + \frac{Re\epsilon\Sigma\theta'(\eta)\varphi'(\eta)}{\Omega} + \frac{BrRe}{\Omega(1+k1)}\left(f''^2 + k2(f'^2f''^2 - ff''f''')\right). \tag{4.19}$$

Where Re is Reynolds number, dimensionless temperature difference is denoted by Ω, Brinkman number is Br and dimensionless concentration difference Σ, dimensionless constant parameter ϵ, which are defined as:

$$Re = \frac{u_w x}{\nu}\,,\ Br = \frac{\mu u_w^2}{k\Delta T}\,,\ \Omega = \frac{\Delta T}{T_\infty}\,,\ \epsilon = \frac{D_B C_\infty}{k},\ \Sigma = \frac{\Delta C}{C_\infty},\ u_w = ax.$$

4.2 Methodology

By assuming the solution, we get exact solution of Eq. (4.9) satisfying boundary conditions.

For stretching/shrinking sheet

$$\left.\begin{aligned} f(\eta) &= \frac{1-e^{-\gamma\eta}}{\gamma}, \\ f(\eta) &= \frac{-1+e^{-\gamma\eta}}{\gamma}. \end{aligned}\right\} \tag{4.20}$$

Using equation (4.20) in equation (4.9), it yields

$$e^{-\gamma\eta}\left(\gamma^2(1+k2)-(1+k1)\right)=0. \tag{4.21}$$

Solving the above equation for the value of γ, we get

$$\gamma = \pm\sqrt{\frac{1+k1}{1+k2}}. \tag{4.22}$$

Hence dual solution (4.22) of the proposed problem is accessible.

$f'(\eta) = -\gamma e^{-\gamma\eta}$, $f''(\eta) = e^{-\gamma\eta}$.

so, velocity components become

$$u = xae^{-\gamma\eta},\ v = -\sqrt{av}\left(\frac{1}{\gamma}-\frac{e^{-\gamma\eta}}{\gamma}\right). \tag{4.23}$$

To find the solution of Eq. (4.10), we establish a new variable ξ ,

$$\xi = \frac{Pr}{\gamma^2}e^{-\gamma\eta}. \tag{4.24}$$

To apply this variable in equation (4.10), we convert the differentiation w.r.t η by using chain rule for first and second order ODEs, that is

$$\frac{d}{d\eta} = \frac{d}{d\xi} * \frac{d\xi}{d\eta} \quad and \quad \frac{d^2}{d\xi^2}\left(\frac{d\xi}{d\eta}\right)^2 + \frac{d}{d\xi} * \frac{d^2\xi}{d\eta^2}. \tag{4.25}$$

After applying the above chain rule on equation (4.10) , we obtain

$$\xi\frac{d^2\theta}{d\xi^2} + \left(1-\frac{Pr}{\gamma^2}+\xi\right)\frac{d\theta}{d\xi} = 0, \tag{4.26}$$

and the reduced boundary conditions are

$$\theta\left(\xi=\frac{Pr}{\gamma^2}\right)=\ 1\ ,\ \theta\ (\xi=0)=0\ . \tag{4.27}$$

By solving Eq. (4.26) we obtain

$$\theta(\xi)=\frac{\left(\left(\begin{array}{c}\frac{\gamma^4\xi^H(\xi\gamma^2+\gamma^2+Pr)e^{-\frac{1}{2}\xi}|M|(F,G,\xi)}{Pr(\gamma^2+Pr)(2\gamma^2+Pr)}+\\ \frac{\gamma^2\xi^{\frac{1}{2}\frac{-3\gamma^2+Pr}{\gamma^2}}(\gamma^2+Pr)e^{-\frac{1}{2}\xi}|M|(J,G,\xi)}{Pr(2\gamma^2+Pr)}\end{array}\right)Pr(2\gamma^4+3Pr\gamma^2+Pr^2)\right)}{\left(\gamma^2\left(\frac{Pr}{\gamma^2}\right)^H(\gamma^2+Pr)e^{-\frac{1Pr}{2\gamma^2}}\left(\begin{array}{c}|M|\left(F,G,\frac{Pr}{\gamma^2}\right)\gamma^4+\\ |M|\left(J,G,\frac{Pr}{\gamma^2}\right)\gamma^4+\\ 2|M|\left(J,G,\frac{Pr}{\gamma^2}\right)Pr\gamma^2+\\ |M|\left(J,G,\frac{Pr}{\gamma^2}\right)Pr^2\end{array}\right)\right)}, \tag{4.28}$$

Where $F=\frac{1}{2}\ \frac{-\gamma^2+Pr}{\gamma^2}$, $H=\frac{1}{2}\ \frac{-3\gamma^2+Pr}{\gamma^2}$, $G=\frac{1}{2}\frac{2\gamma^2+Pr}{\gamma^2}$, $J=\frac{1}{2}\ \frac{\gamma^2+Pr}{\gamma^2}$.

By applying boundary conditions and putting the value of ξ in (4.28), the final solution is,

$$\theta(\eta)=\frac{\left(\left(\begin{array}{c}\frac{\gamma^4\left(\frac{Pr}{\gamma^2}e^{-\gamma\eta}\right)^H\left(\left(\frac{Pr}{\gamma^2}e^{-\gamma\eta}\right)\gamma^2+\gamma^2+Pr\right)e^{-\frac{1}{2}\left(\frac{Pr}{\gamma^2}e^{-\gamma\eta}\right)}|M|\left(F,G,\left(\frac{Pr}{\gamma^2}e^{-\gamma\eta}\right)\right)}{Pr(\gamma^2+Pr)(2\gamma^2+Pr)}+\\ \frac{\gamma^2\left(\frac{Pr}{\gamma^2}e^{-\gamma\eta}\right)^{\frac{1}{2}\frac{-3\gamma^2+Pr}{\gamma^2}}(\gamma^2+Pr)e^{-\frac{1}{2}\left(\frac{Pr}{\gamma^2}e^{-\gamma\eta}\right)}|M|\left(J,G,\left(\frac{Pr}{\gamma^2}e^{-\gamma\eta}\right)\right)}{Pr(2\gamma^2+Pr)}\end{array}\right)Pr(2\gamma^4+3Pr\gamma^2+Pr^2)\right)}{\left(\gamma^2\left(\frac{Pr}{\gamma^2}\right)^H(\gamma^2+Pr)e^{-\frac{1Pr}{2\gamma^2}}\left(\begin{array}{c}|M|\left(F,G,\frac{Pr}{\gamma^2}\right)\gamma^4+\\ |M|\left(J,G,\frac{Pr}{\gamma^2}\right)\gamma^4+\\ 2|M|\left(J,G,\frac{Pr}{\gamma^2}\right)Pr\gamma^2+\\ |M|\left(J,G,\frac{Pr}{\gamma^2}\right)Pr^2\end{array}\right)\right)}. \tag{4.29}$$

Again, for concentration equation, in order to get the solution of the concentration equation in the form of non-dimensional nonlinear ODE, we consider a new variable t as follows:

$$t=\frac{Le}{\gamma^2}e^{-\gamma\eta}. \tag{4.30}$$

To apply this variable in equation (4.11), we convert the differentiation w.r.t η by using chain rule for first and second order ODEs, that is

$$\frac{d}{d\eta}=\frac{d}{dt}*\frac{dt}{d\eta}\quad and\quad \frac{d^2}{dt^2}\left(\frac{dt}{d\eta}\right)^2+\frac{d}{dt}*\frac{d^2t}{d\eta^2}. \tag{4.31}$$

After applying the above chain rule on equation (4.11), we obtain

$$t\frac{d^2\varphi}{dt^2}+\left(1-\frac{LePr}{\gamma^2}+tPr\right)\frac{d\varphi}{dt}=0, \tag{4.32}$$

and the reduced boundary conditions are

$$\varphi\left(t=\frac{Le}{\gamma^2}\right)=1\ ,\ \varphi\ (t=0)=0\ . \tag{4.33}$$

By solving Eq. (4.32) . we obtain

$$\varphi(t)=\frac{\left(\left(\begin{array}{c}\frac{Le\,O\gamma^4 t\,T(tLe\gamma^2+\gamma^2+LePr)(tLe)^{-N}e^{-\frac{1}{2}Le\,t}|M|(L,M,Le\,t)}{Pr(\gamma^2+LePr)(2\gamma^2+LePr)}+\\ \frac{Le\,O\gamma^2 t\,\frac{LePr-\gamma^2}{\gamma^2}(\gamma^2+LePr)\left(\frac{Pr\,Le\,e^{-\gamma\eta}}{\gamma^2}\right)^{-N}e^{-\frac{1Pr}{2}\frac{Le\,e^{-\gamma\eta}}{\gamma^2}}|M|(N,M,Le\,t)}{Pr(2\gamma^2+LePr)}\end{array}\right)*Pr\left(2\gamma^4+3PrLe\gamma^2+Pr^2Le^2\right)\right)}{\left(Le\,O\gamma^4\left(\frac{Pr}{\gamma^2}\right)^{T}\left(\frac{LePr}{\gamma^2}\right)^{-\frac{1}{2}T}e^{-\frac{1LePr}{2\ \gamma^2}}\left(\begin{array}{c}Le^2|M|\left(L,M,\frac{LePr}{\gamma^2}\right)Pr^2+\\ 2Le\,|M|\left(N,M,\frac{LePr}{\gamma^2}\right)Pr\gamma^2+\\ 2Le\,|M|\left(L,M,\frac{LePr}{\gamma^2}\right)Pr\gamma^2+\\ |M|\left(N,M,\frac{LePr}{\gamma^2}\right)\gamma^4+\\ |M|\left(L,M,\frac{LePr}{\gamma^2}\right)\gamma^4\end{array}\right)\right)}, \tag{4.34}$$

Where $L=\frac{1}{2}\ \frac{-\gamma^2+LePr}{\gamma^2}$, $M=\frac{1}{2}\frac{2\gamma^2+LePr}{\gamma^2}$, $N=\frac{1}{2}\ \frac{\gamma^2+LePr}{\gamma^2}$, O=$\frac{LePr-2\gamma^2}{\gamma^2}$, T=$\frac{\mathrm{LePr}-\gamma^2}{\gamma^2}$.

By applying boundary conditions and putting the value of ξ in (4.28), the final solution is,

$$\varphi(\eta)=\frac{\left(\left(\begin{array}{c}\frac{Le\,O\gamma^4\left(\frac{Pr\,e^{-\gamma\eta}}{\gamma^2}\right)^{T}\left(\left(\frac{Pr\,e^{-\gamma\eta}}{\gamma^2}\right)Le\gamma^2+\gamma^2+LePr\right)\left(\left(\frac{Pr\,e^{-\gamma\eta}}{\gamma^2}\right)Le\right)^{-N}e^{-\frac{1}{2}Le\left(\frac{Pr\,e^{-\gamma\eta}}{\gamma^2}\right)}|M|\left(L,M,Le\left(\frac{Pr\,e^{-\gamma\eta}}{\gamma^2}\right)\right)}{Pr(\gamma^2+LePr)(2\gamma^2+LePr)}+\\ \frac{Le\,O\gamma^2\left(\frac{Pr\,e^{-\gamma\eta}}{\gamma^2}\right)\frac{LePr-\gamma^2}{\gamma^2}(\gamma^2+LePr)\left(\frac{Pr\,Le\,e^{-\gamma\eta}}{\gamma^2}\right)^{-N}e^{-\frac{1Pr}{2}\frac{Le\,e^{-\gamma\eta}}{\gamma^2}}|M|\left(N,M,Le\left(\frac{Pr\,e^{-\gamma\eta}}{\gamma^2}\right)\right)}{Pr(2\gamma^2+LePr)}\end{array}\right)*Pr\left(2\gamma^4+3PrLe\gamma^2+Pr^2Le^2\right)\right)}{\left(Le\,O\gamma^4\left(\frac{Pr}{\gamma^2}\right)^{T}\left(\frac{LePr}{\gamma^2}\right)^{-\frac{1}{2}T}e^{-\frac{1LePr}{2\ \gamma^2}}\left(\begin{array}{c}Le^2|M|\left(L,M,\frac{LePr}{\gamma^2}\right)Pr^2+\\ 2Le\,|M|\left(N,M,\frac{LePr}{\gamma^2}\right)Pr\gamma^2+\\ 2Le\,|M|\left(L,M,\frac{LePr}{\gamma^2}\right)Pr\gamma^2+\\ |M|\left(N,M,\frac{LePr}{\gamma^2}\right)\gamma^4+\\ |M|\left(L,M,\frac{LePr}{\gamma^2}\right)\gamma^4\end{array}\right)\right)}. \tag{4.35}$$

4.3 Results and Discussion

In the ongoing stage, the flow of the Boundary layer and the heat transfer of Jeffrey's fluid over the stretching sheet by linearly are determined. PDEs are changed over into ODEs addressed by scientifically. In order to produce exact solutions aimed at the stated problem of boundary value an algorithm developed by the Maple software. For temperature profile, velocity profile and nanoparticles fraction, Sherwood number, local Nusselt, entropy generation, skin friction coefficient the parameters discussed are Prandtl parameter P ,relaxation and redardation parameter $k1$, Deborah number $k2$, Lewis number Le, Brinkman number Br, Reynold's number Re, dimensionless concentration difference Σ, temperature difference Ω and constant parameter ϵ.

Fig. 19: designed at higher values of $k2$ as velocity escalates, although the boundary layer viscosity drops. Although, by increasing value of $k2$ both nanoparticles' fractions profile decrease and temperature. Fig. 19: illustrate the effect of $k2$ on nanoparticles fraction, temperature profile and speed profile. From Fig. 20: the impact of $k1$ on velocity, fraction and temperature of nanoparticles display opposite behavior while related through that in Fig. 19. It is assumed that increasing the elastic parameter will increase water resistance. Therefore, when there is no non-Newtonian effects the current model reduced to the Newtonian model of nanofluid, presenting a brilliant agreement [39].

In Fig. 21: we can see effects on $\theta(\eta)$ and $\varphi(\eta)$ by Prandtl number Pr. As Prandtl number is a amount of thermal distribution rate and viscous distribution rate, greater the Prandtl number is lesser will be thermal variability. Thus, the exact process can be seen in Fig. 22, when Prandtl numbers is higher, then both nanoparticles fractions and temperature will be lesser, both of them shows opposite behavior when the value of Lewis Number Le has higher values. Fig. 23: we can see impact of $k2$ on $f'(\eta)$ for shrinking case. In this shrinking case we can see that $Pr = 0.5$, $Le = 2.0$ and $k1 = 0.5$.

In Fig. 24: we can see the dimensionless Ns profiles of numerous numbers of Pr. It may be understood that the Prandtl number expands, the number of entropy generation seriously increments in the sheet locale. Yet, somewhat distant from the sheet, Prandtl number increment reasons Ns decline. Alternately, further away from the sheet district, both $\theta(\eta)$ and $\varphi(\eta)$ are diminished to Pr, which in this manner decline Ns. It is likewise

noticed that in Pr is invariant, as the changeability of comparability variable increments η.

Fig. 25: shows the Ns profiles intended for various upsides of Lewis number Le. Apparently, an increase in Le could prompt an expansion in Ns in the sheet area. In any case, extra on the sheet, the Le variety doesn't essentially influenceNs. With the ascent of Le, the gooey dissemination rate builds which can further develop entropy generation. In any case, as is notable, gooey dissemination primarily influences the fluid close to the strong (sheet). Hence, entropy is created principally on a close-by the sheet.

Fig. 26- Fig. 31: Demonstrate the effects on Ns profiles by Br , $\epsilon, k1, k2, \Sigma, R$. In Fig. 26, the Ns profiles are presented in the values of Br . The dimensionless Br concludes the relative importance of viscous effect. It is very flawless that whenever Briksman number rises Ns also increase, however we can have better understanding of this conclusion in the sheet region (i.e., $\eta < 1$). The real cause of Ns increase with Br increase is that aimed at higher Br values, Ns due to fluid friction becomes raised. According to Fig. 25 Brinkman non-dimensionless unit is direct relation of proportionality with the square of the stretchable sheet. The speed of stretching the sheets depends on liquid nearby the surface of the sheet leading towards the acceleration of the liquid and the increase of Ns.

Fig. 27: the effect of the Dimensionless ε fixed parameter in the output number of entropy is displayed. Parameter ε demonstrate the commitment of mass exchange to the production number of entropy. It can be noted that, as sheet approaches, Ns increases with ε. It is also observed that, at $\varepsilon = 0.003$, with η increase Ns initially rises and decreases gradually. However, at $\varepsilon > 0.003$ Ns gets a smooth reduction with an η increase.

In Fig. 28: illustrate the behavior of ratio of relaxation to retardation times $k1$ on Ns profile. It can be understood that irreversible Ns is a reducing function of $k1$, specifically near to the sheet region. A decrease in Ns by an increase of $k1$ near the sheet may be attributed to the reduction in velocity within the boundary layer by increase. As the temperature has a very low rise with an increase in $k1$, so the temperature effect is unable to challenge the effect of speed, and that is why Ns decreases. The effect of Deborah $k2$ number on Ns can be seen in Fig. 29. It is noted that with the greater values of Deborah's number, the entropy production number is greater in the sheet area.

Materially, when Deborah's number increase it results in more fluid movement within the boundary layer, which significantly enhances density of the speed limit and increases the fluid speed. This cannot overcome the effect of increasing speed on Ns, and thus Ns increase with $k2$ increase.

Fig. 30: presents profiles of entropy generation Ns with varying parameters for concentration difference parameter Σ. The parameter Σ defines the relation of the dimensionless concentration difference. In Fig.4.11, Σ increase in the sheet area($\eta < 0.6$) when Ns increases, which results in a mass transfer contribution to Ns. However, further on the sheet, the parameter Σ appears to have very little effect on Ns.

Fig. 31: presents the impact of various Reynolds Number Re values on the number of entropy production. It is notable that Ns are highly dependent on Re, such as the increase in the number of Reynolds significantly increases Ns. By the increase of Reynolds population, the liquid moves in very disruptive manner such that the movement of the busy fluid emerges. This movement raises the contribution of fluid friction and heat transfer to the entropy generation and, as a result, increases the number of entropy Ns. It is clear there is increase in Re, the force of inertia increases while the viscous force decreases. Therefore, in the case of the flow in the expandable sheet, with an increase of Re, the liquid near the sheet is much faster and the fluid friction.

In Fig. 32 - Fig. 38: effects on temperature profile reduce Nusstle number. Increasing values of both parameters $k1, k2$ one by one and the Nusselt number $\theta'(0)$ decreases, for variable values of Le and Pr. In such circumstances, in the parameters, we consider maximum values of Pr. The same kind of performance can be seen in the reduced Nusselt number $\theta'(0)$ with greater values of $k1, k2$.

From Fig. 39 - Fig. 49: special effects on reduce Sherwood number. Sherwood number $\varphi'(\eta)$ increases by the increasing the parameters graphs $k1, k2, Pr, Le$. Consequently, we can conclude from this context that the thermal substitution is less for the high Prandtl number.

Fig. 50: shows the distinction of the dimensionless speed angle in the sheet area $f''(0)$ with the Deborah number $k2$ for $k1$ impacts. The scramble dash line demonstrates the specific arrangement of the ongoing review. It is apparent that a fantastic arrangement between the mathematical arrangement of the ongoing review and the specific

arrangement is achieved. It can likewise be understood that $f''(0)$ increments with the Deborah number $k2$ increment. The distinction of $f''(0)$ with the proportion of unwinding to hindrance times $k1$ is laid out in Fig. 51 focused on $k2$ impacts. Presently again an extremely respectable agreement is seen between the mathematical and definite arrangements. It is likewise uncovered that the liquid dimensionless speed with the sheet district $f''(0)$diminishes with an increment of $k1$.

From Fig. 52 - Fig. 53, dual nature solution of skin friction $f''(0)$ for both shrinking and stretching case. Effects of $k1$ in $k2$ and effects of $k2$ in $k1$. Its indicates that upper case is of stretching sheet decrease and lower case is of shrinking sheet increase in both parameters effects $k1$ and $k2$.

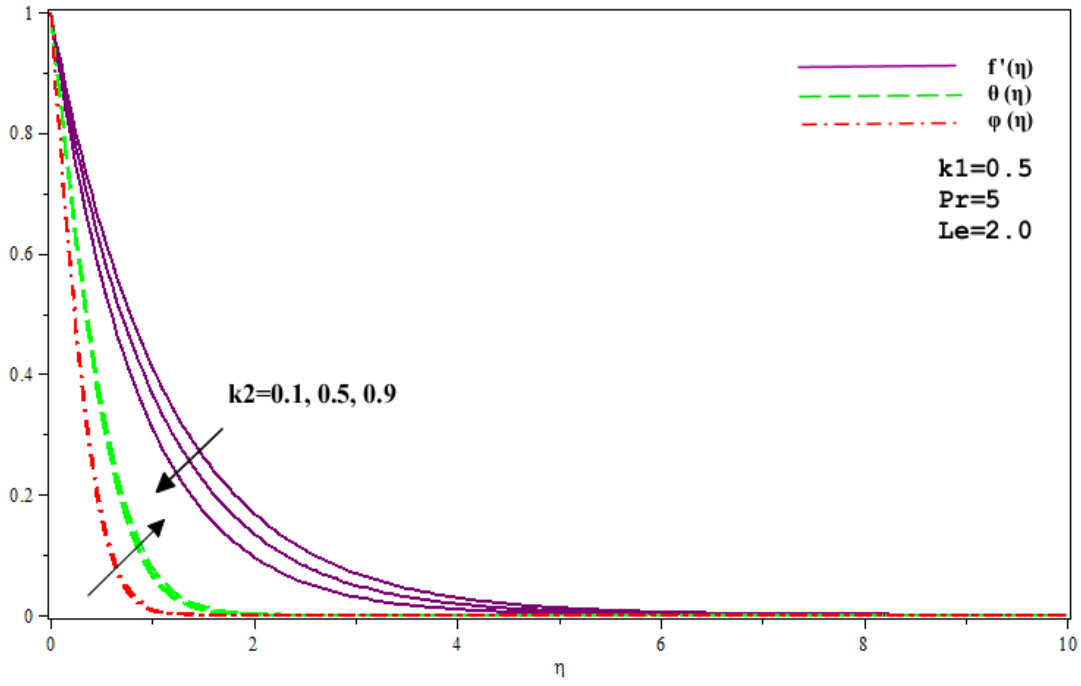

Fig. 19: Impact of $k2$ on $f'(\eta)$,, $\theta(\eta)$ and $\varphi(\eta)$.

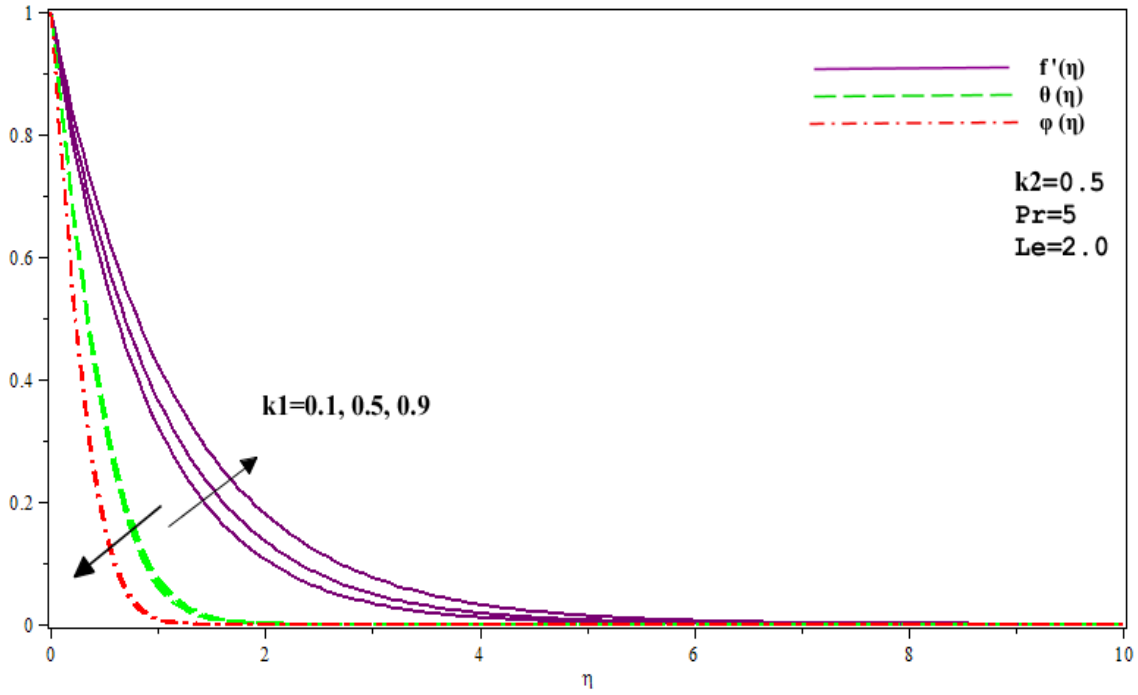

Fig. 20: Impact of $k1$ on $f'(\eta)$, $\theta(\eta)$ and $\varphi(\eta)$.

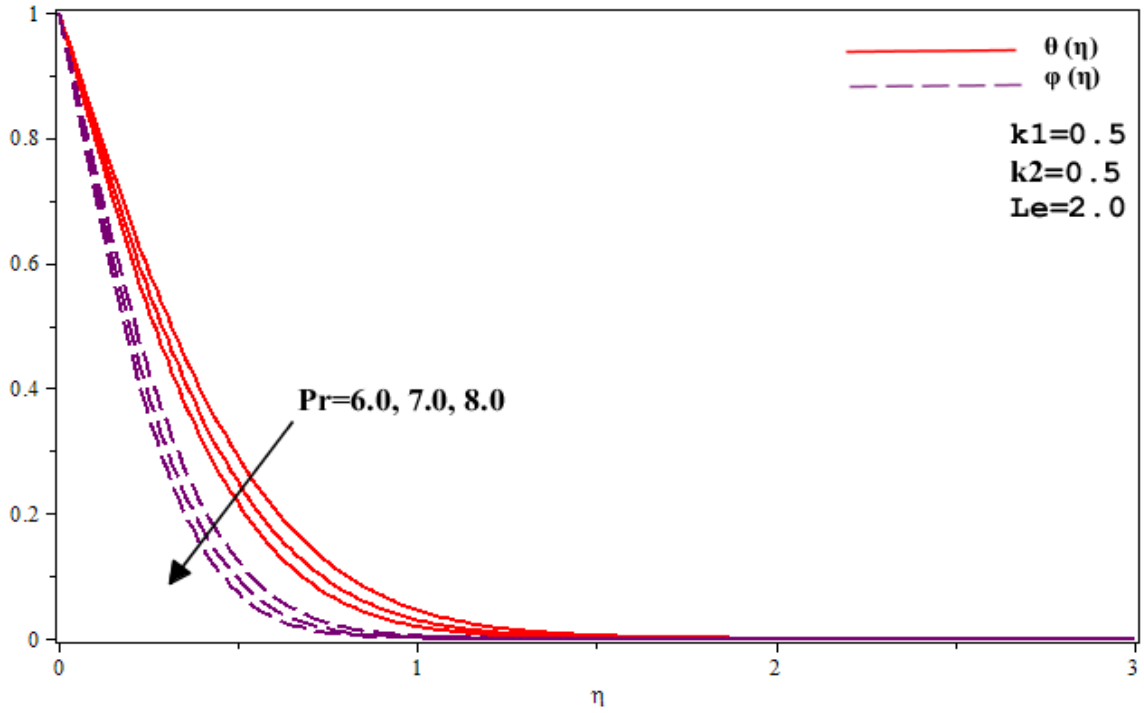

Fig. 21: Impact of Pr on $\theta(\eta)$ and $\varphi(\eta)$.

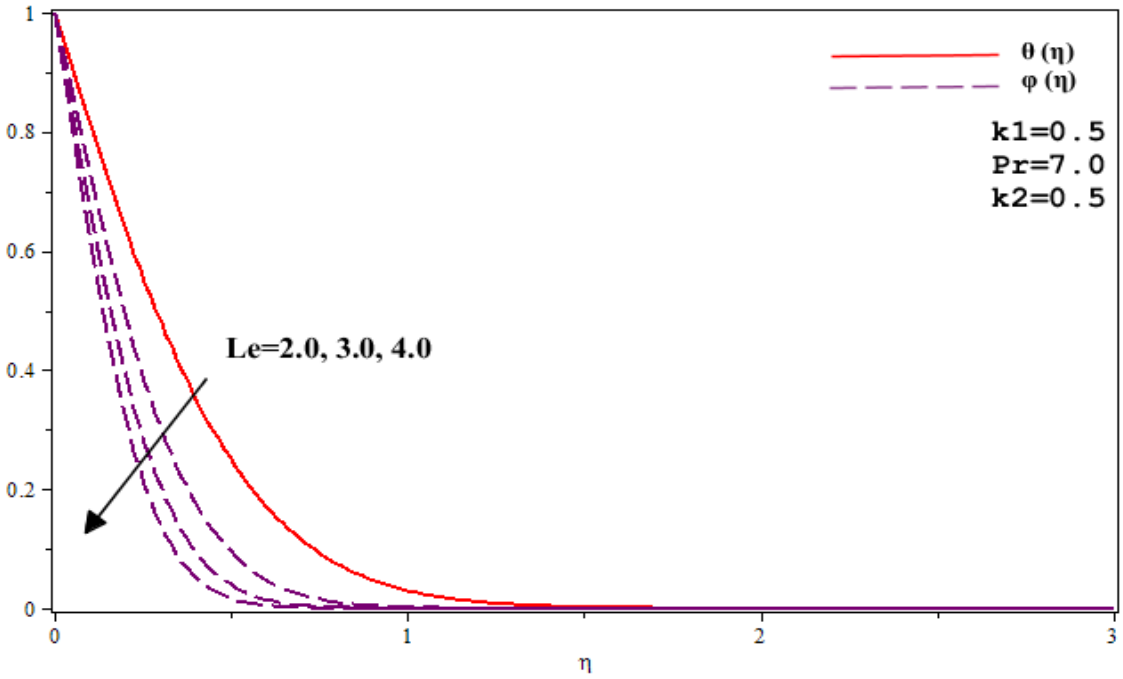

Fig. 22: Impact of Le on $\theta(\eta)$ and $\varphi(\eta)$

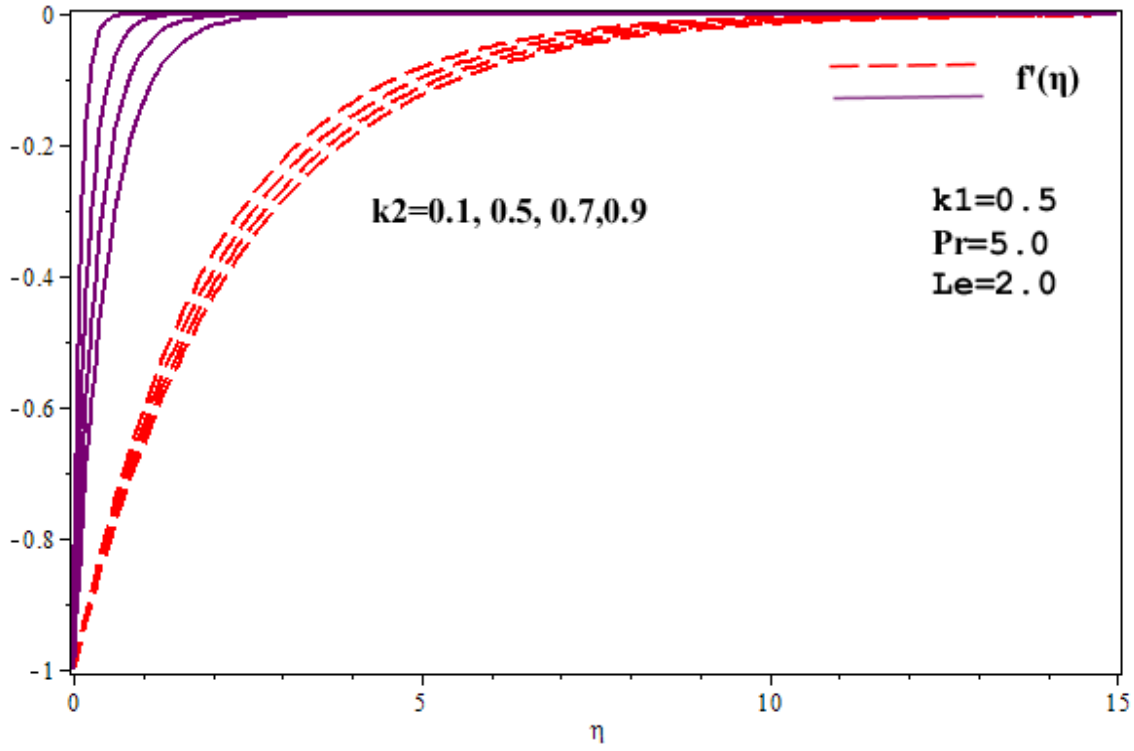

Fig. 23: Impact of $k2$ on $f'(\eta)$ for shrinking case.

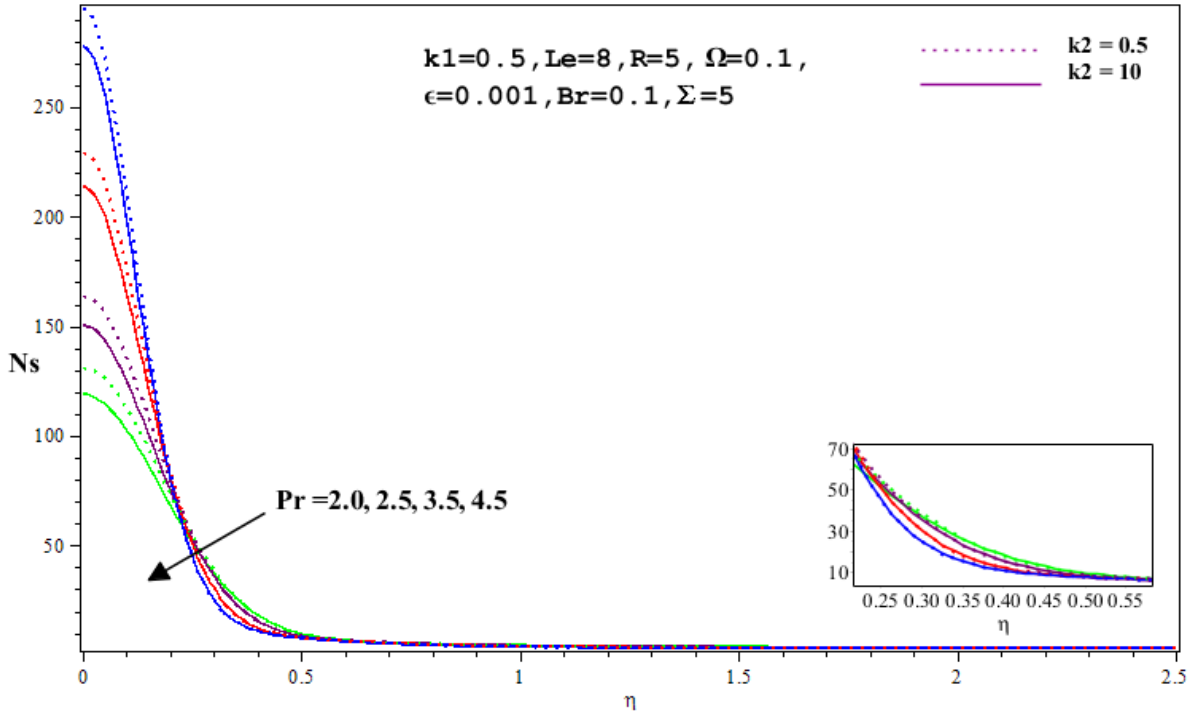

Fig. 24: Impact of Pr on $\boldsymbol{Ns}$.

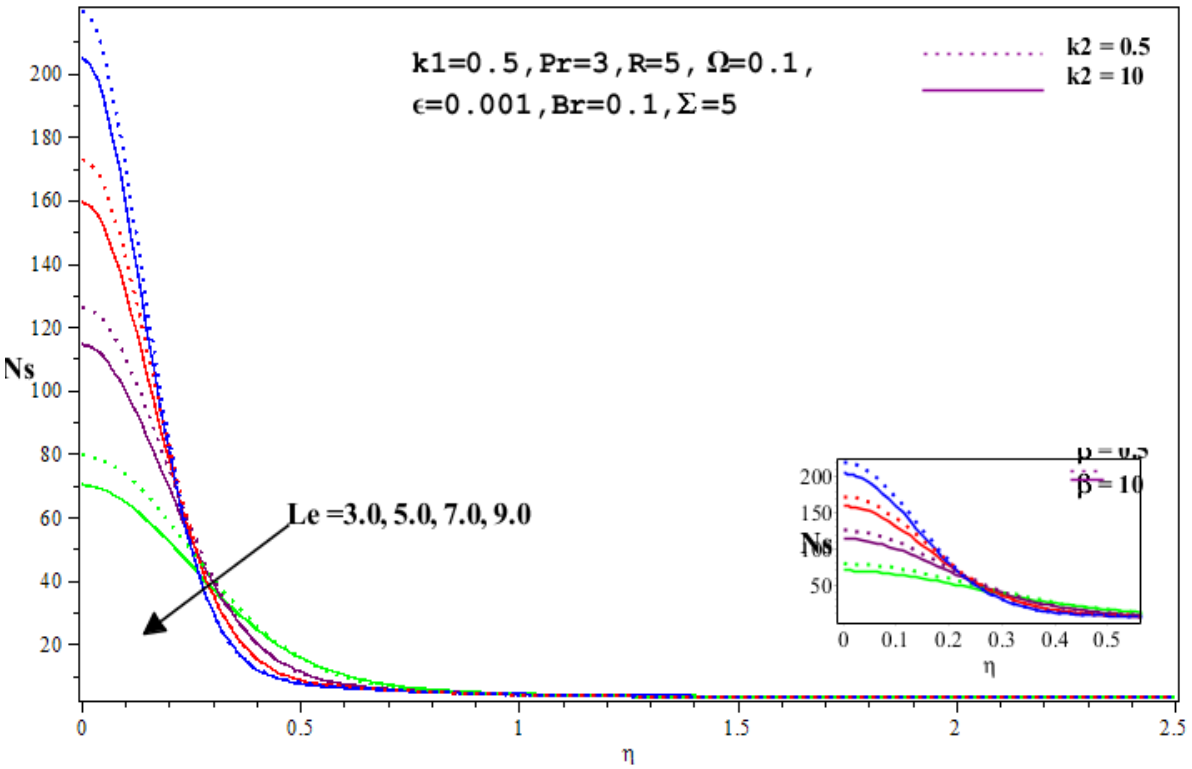

Fig. 25: Impact of Le on Ns.

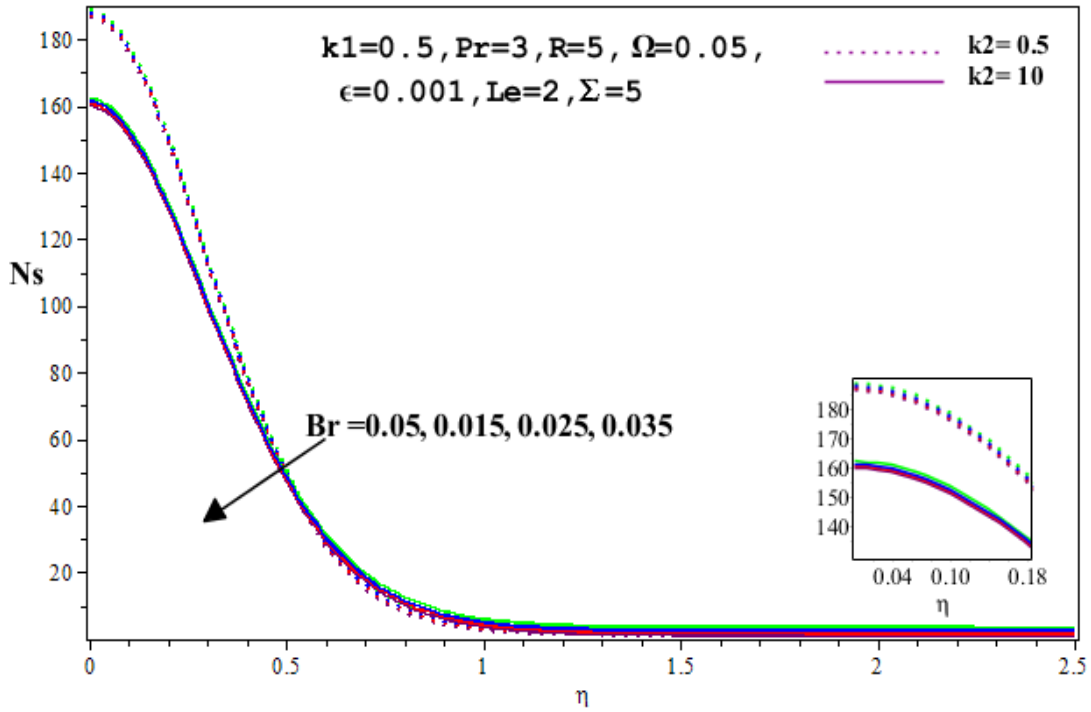

Fig. 26: Impact of Br on Ns.

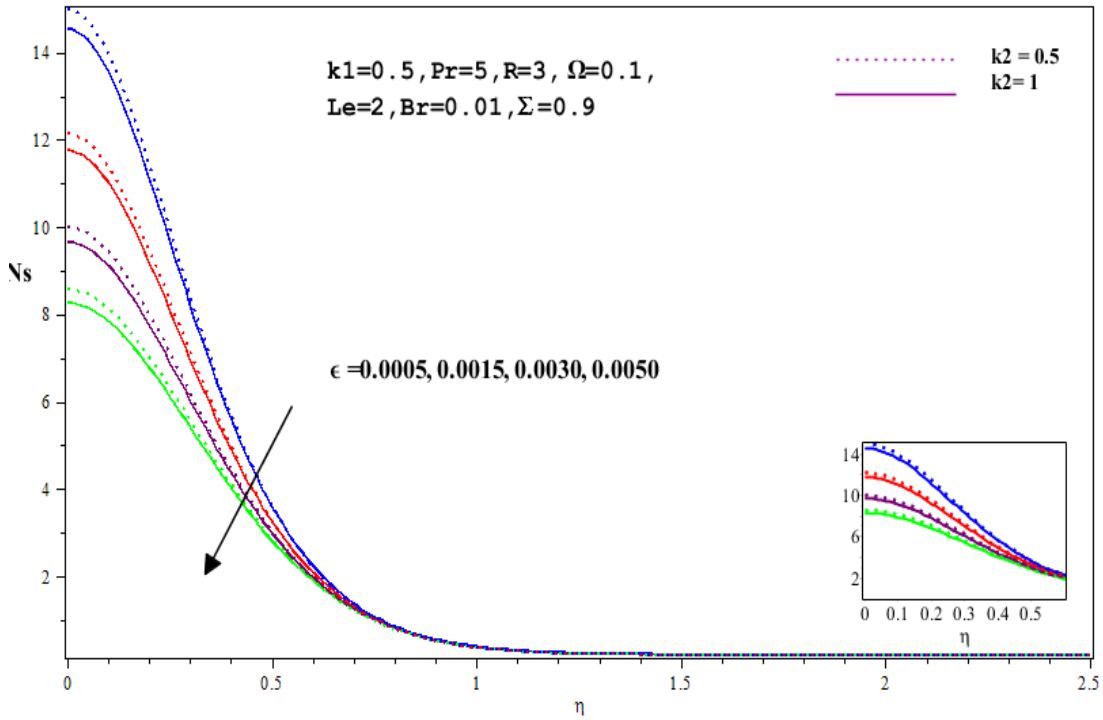

Fig. 27: Impact of ϵ on Ns.

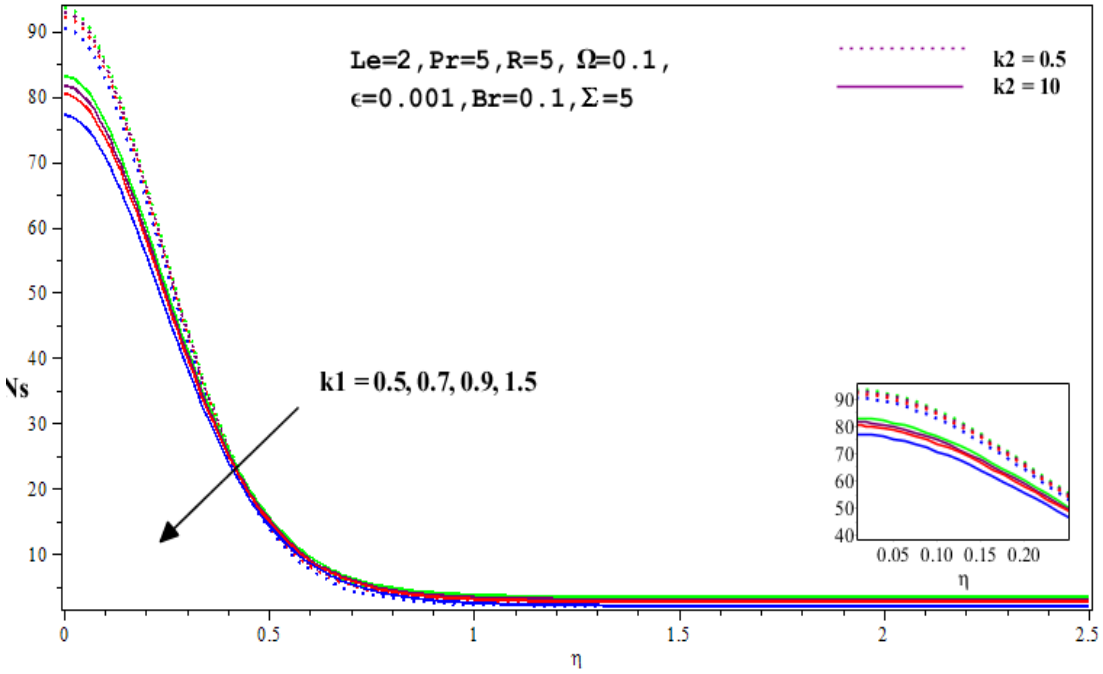

Fig. 28: Impact of $k1$ on Ns.

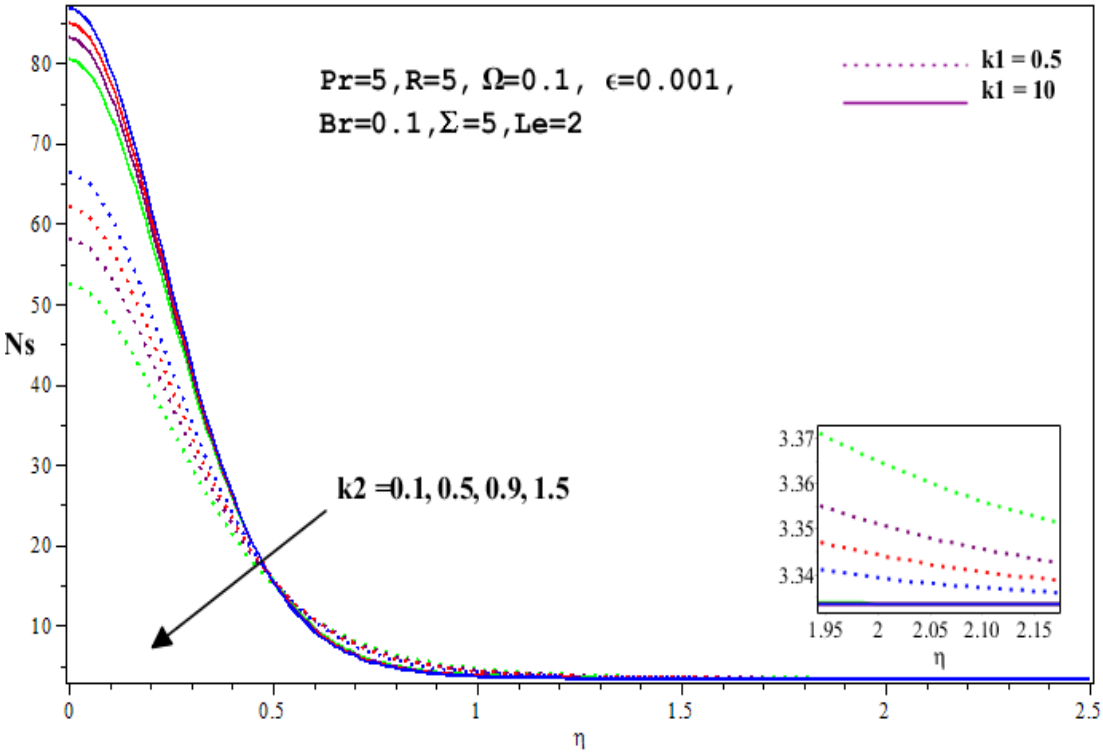

Fig. 29: Impact of $k1$ on Ns.

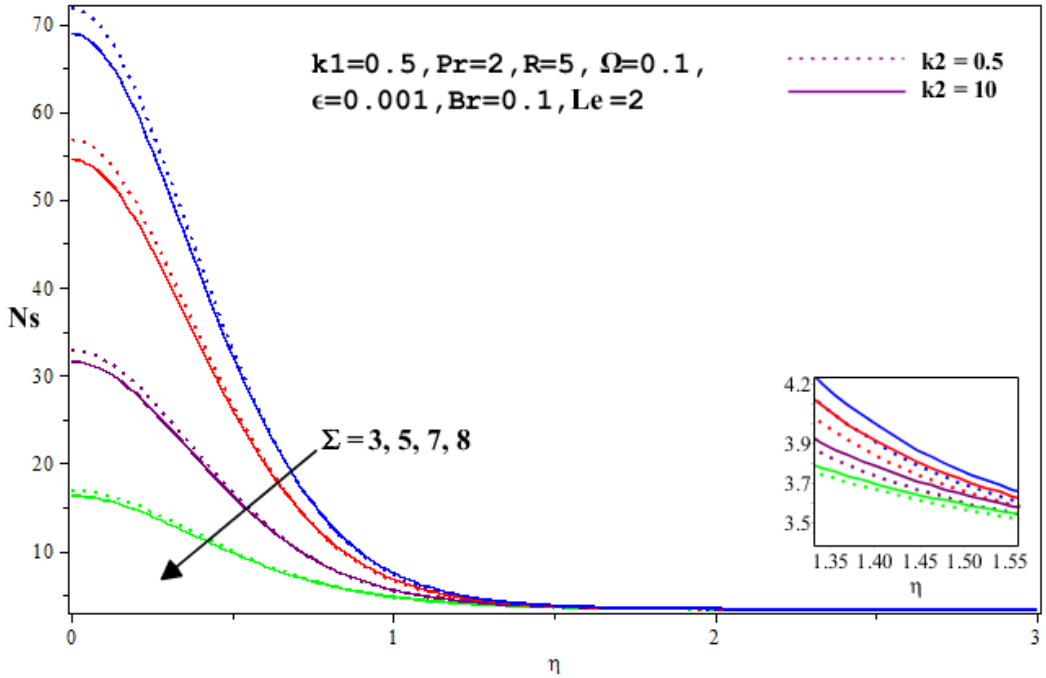

Fig. 30: Impact of Σ on Ns.

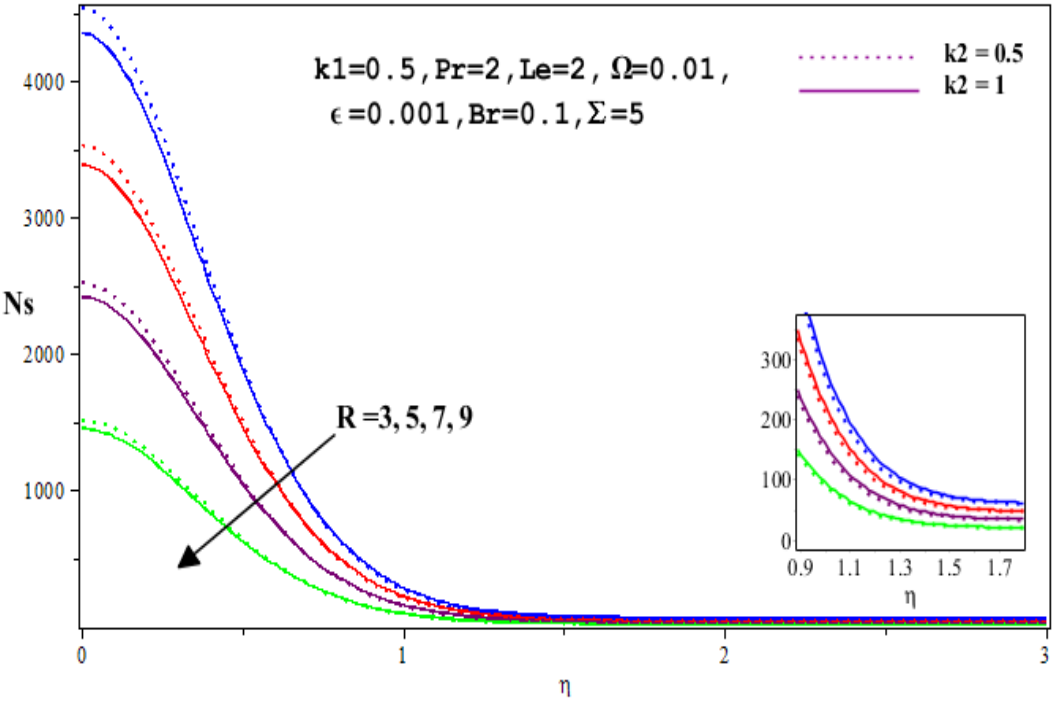

Fig. 31: Impact of Re on Ns.

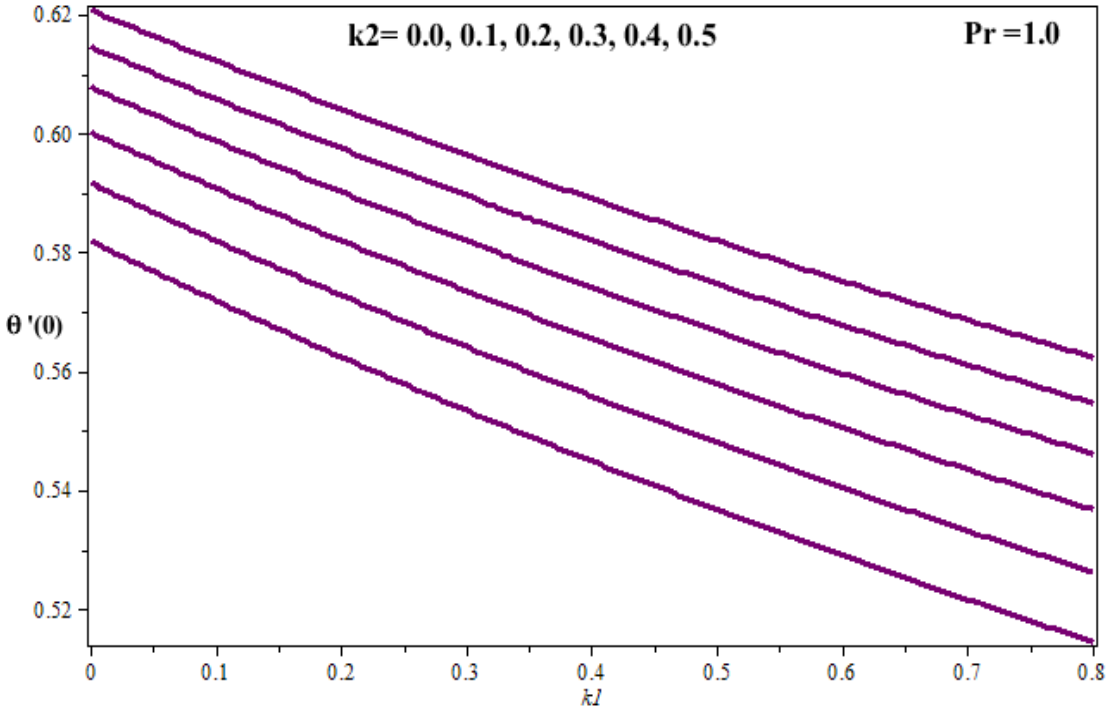

Fig. 32: Variety of $-\theta'(0)$ w.r.t $k2$ and 1. For $Pr = 1.0$.

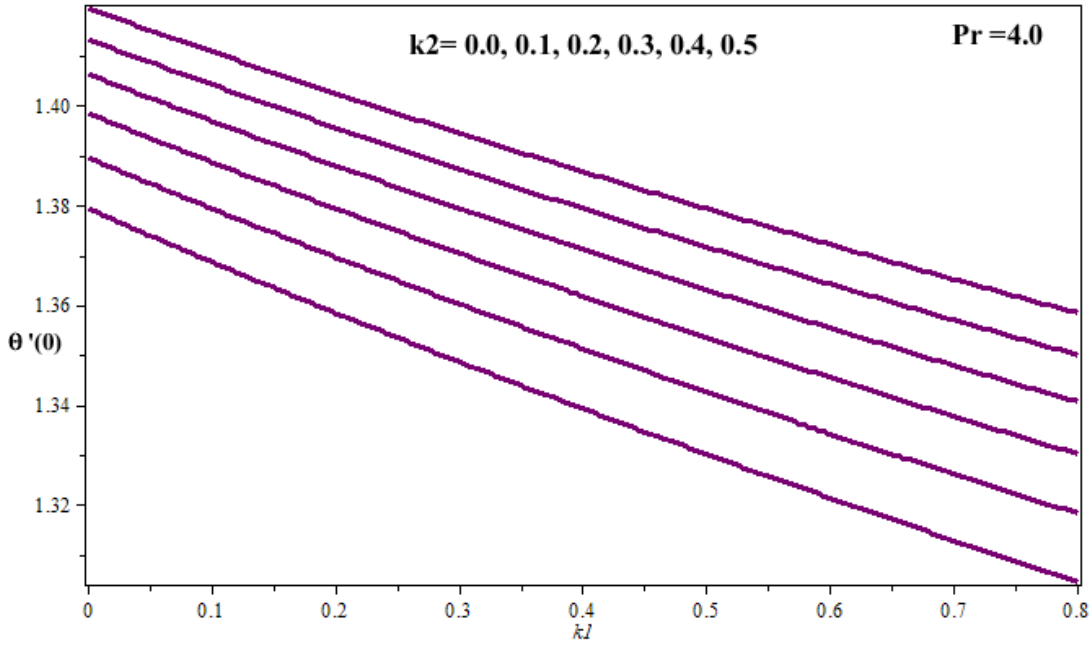

Fig. 33: Variety of $-\theta'(0)$ w.r.t $k2$ and $k1$. For $Pr = 4.0$.

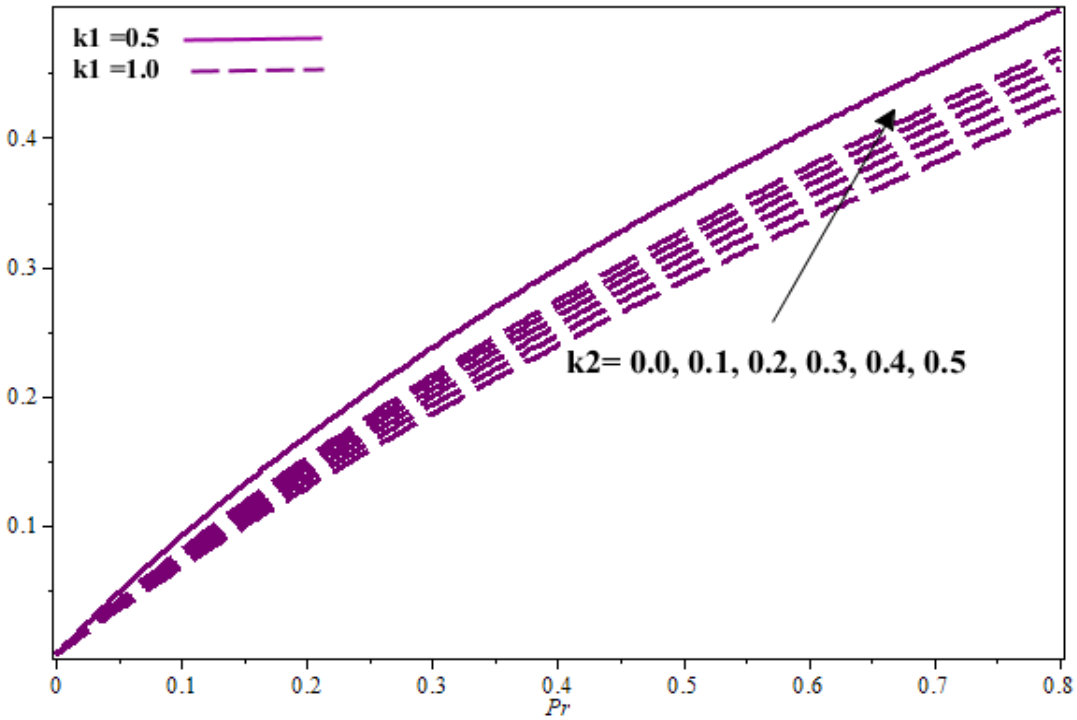

Fig. 34: Variety of $-\theta'(0)$ w.r.t $k2$ and Pr. For $k1 = 0.5,1.0$

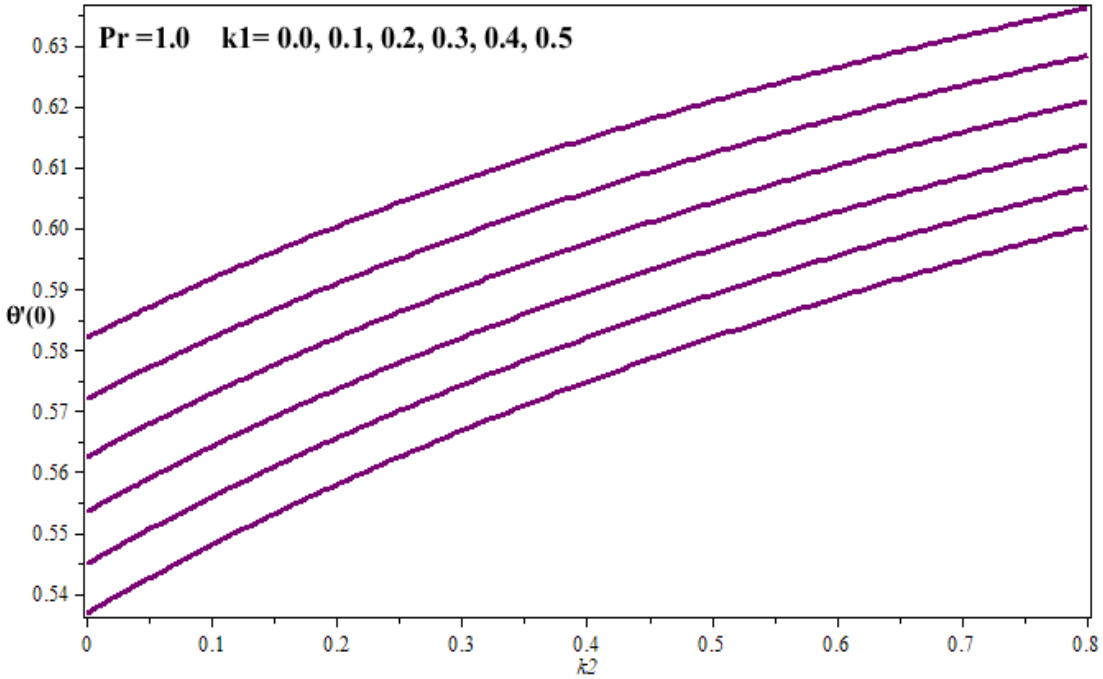

Fig. 35: Variety of $-\theta'(0)$w.r.t $k1$ and $k2$. For $Pr = 1.0$.

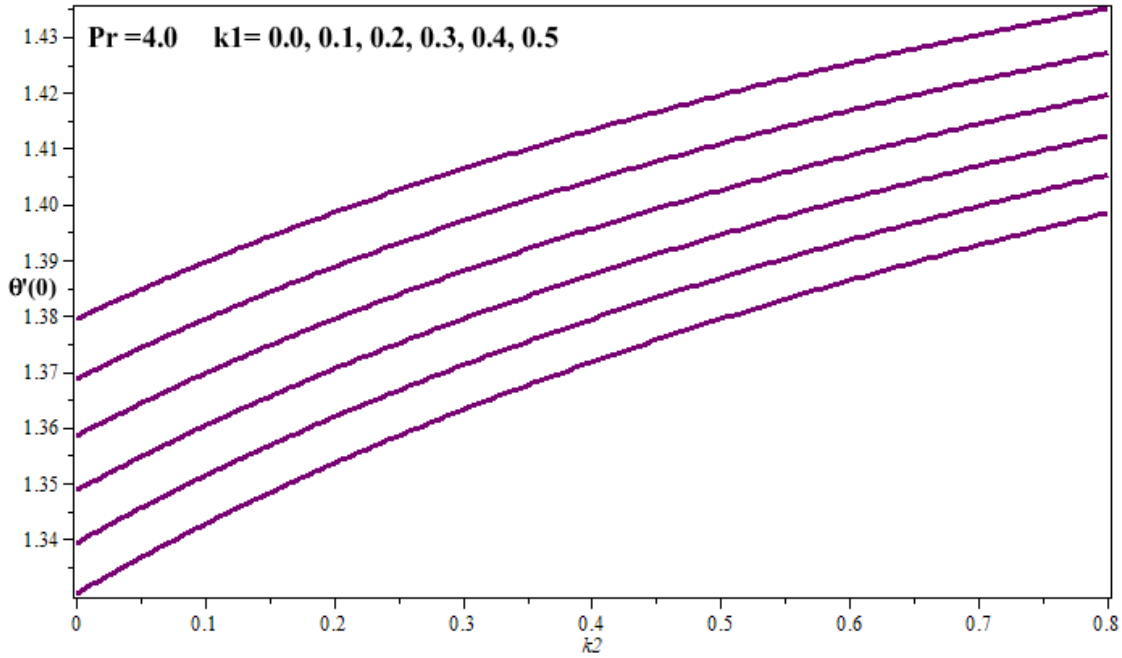

Fig. 36: Variety of $-\theta'(0)$w.r.t $k1$ and $k2$.. For $Pr = 4.0$

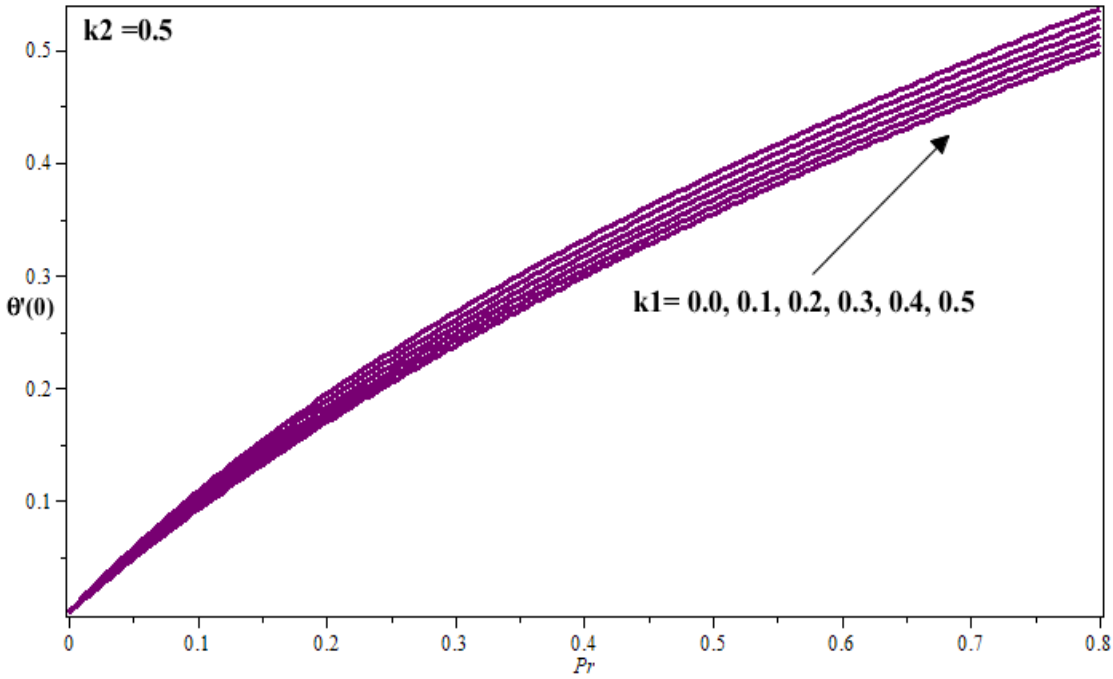

Fig. 37: Variety of $-\theta'(0)$ w.r.t $k1$ and Pr. For $k2 = 0.5$.

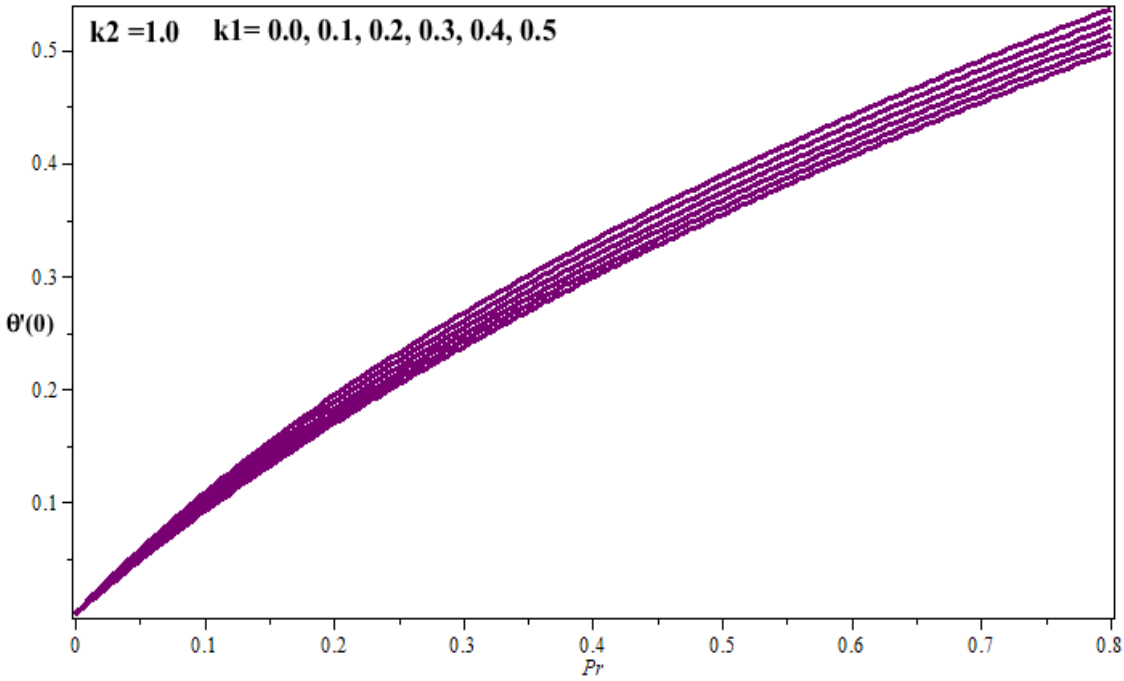

Fig. 38: Variety of $-\theta'(0)$ w.r.t $k1$ and Pr. For $k2 = 1.0$

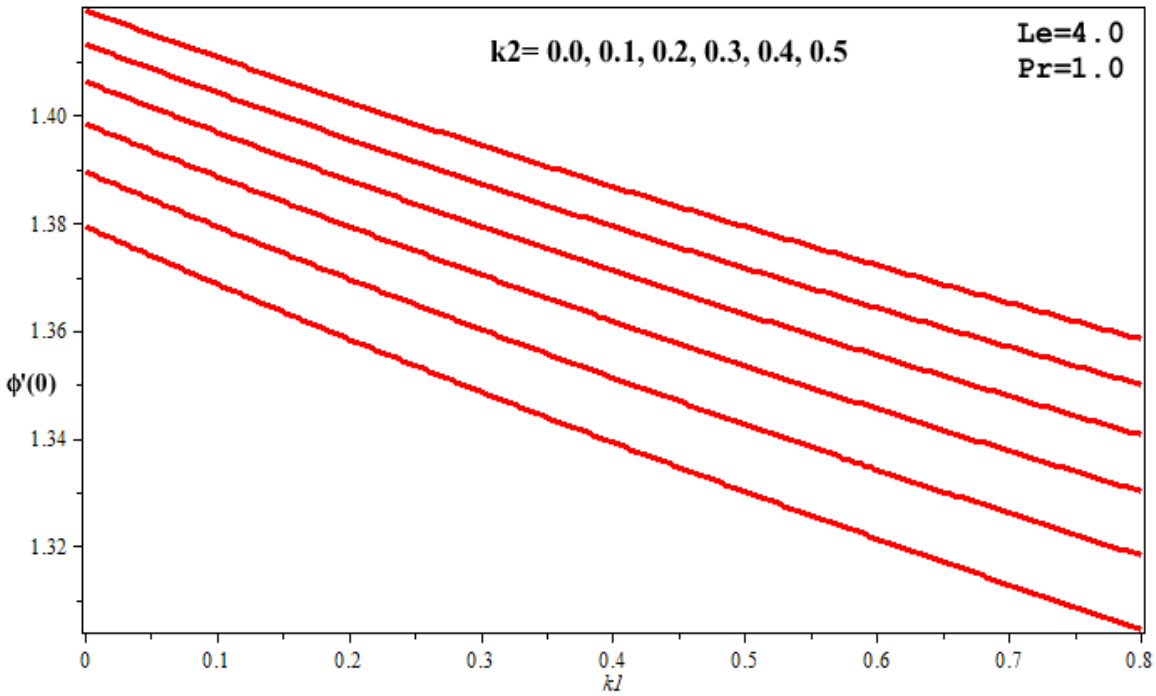

Fig. 39: Variety of $-\varphi'(0)$w.r.t $k2$ and $k1$.For $Le = 4.0\,, Pr = 1.0$.

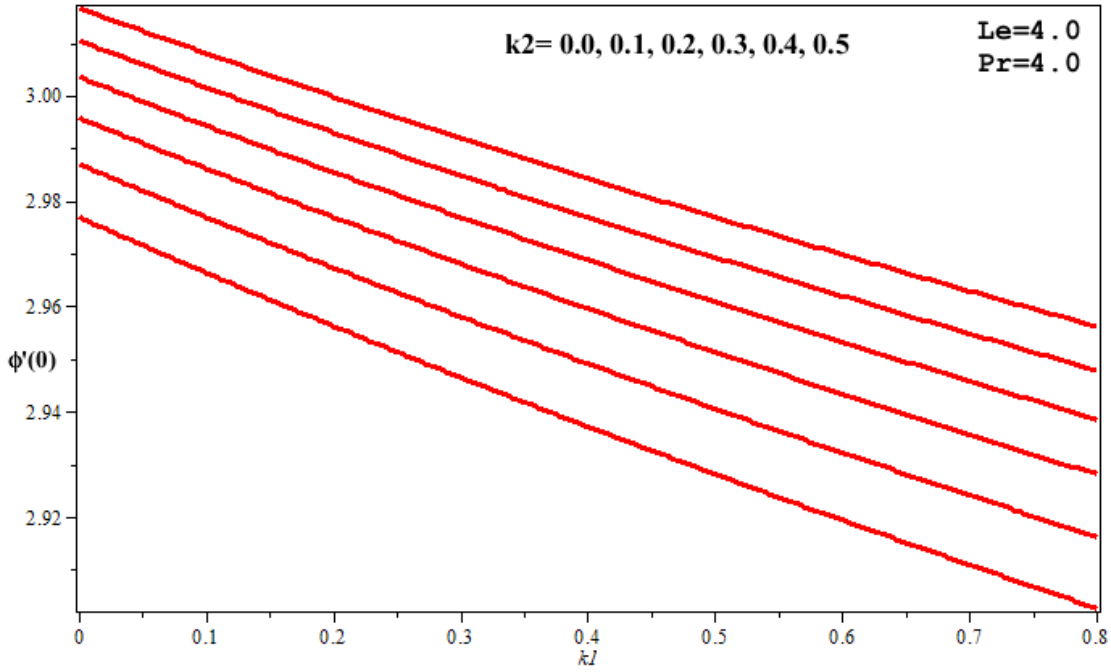

Fig. 40: Variety of -$\varphi'(0)$w.r.t $k2$ and $k1$. For $Le = 4.0\,, Pr = 4.0$

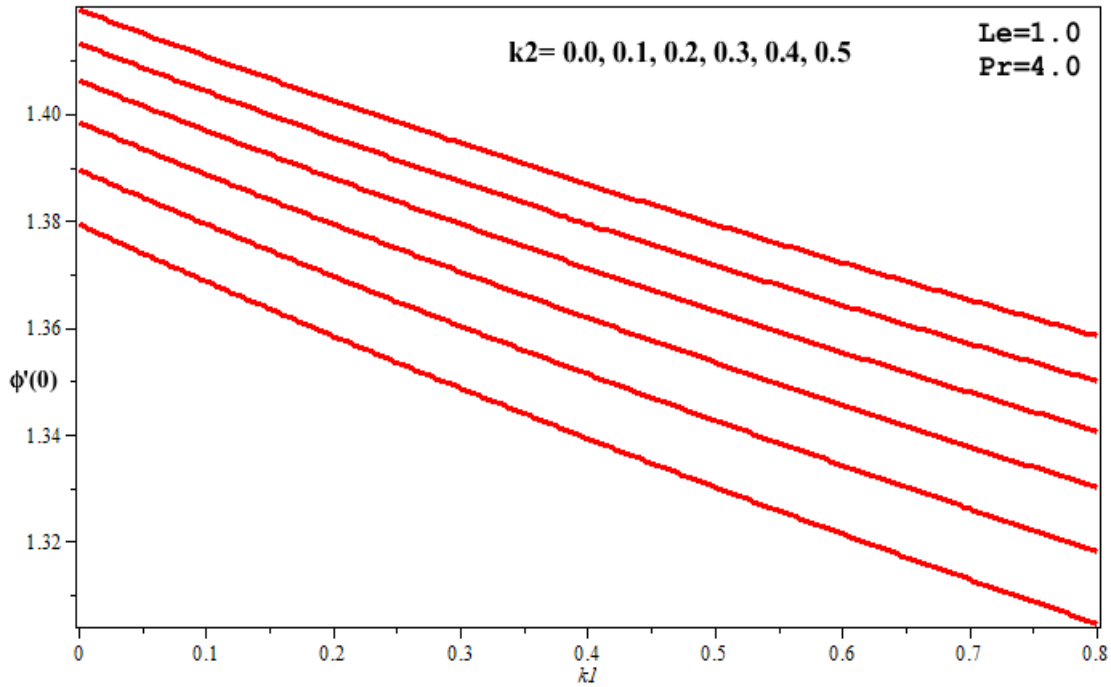

Fig. 41: Variety of $-\varphi'(0)$ w.r.t and $k1$. For $Le = 1.0\,, Pr = 4.0$

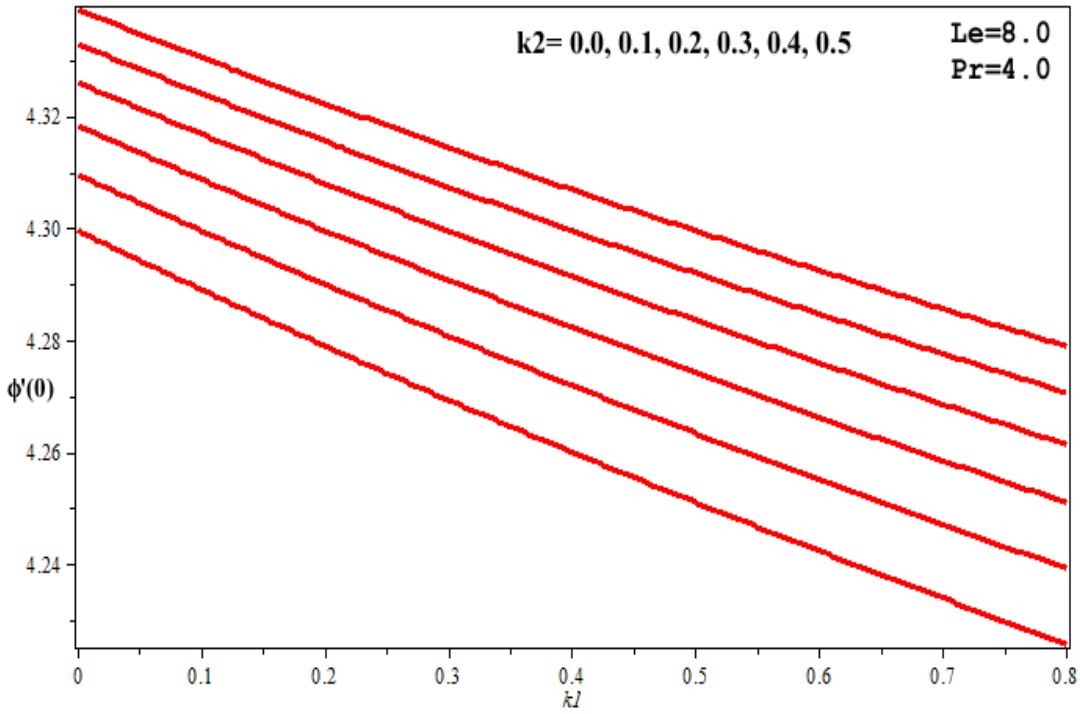

Fig. 42: Variety of $-\varphi'(0)$w.r.T $k2$ and $k1$. For $Le = 8.0$, $Pr = 4.0$

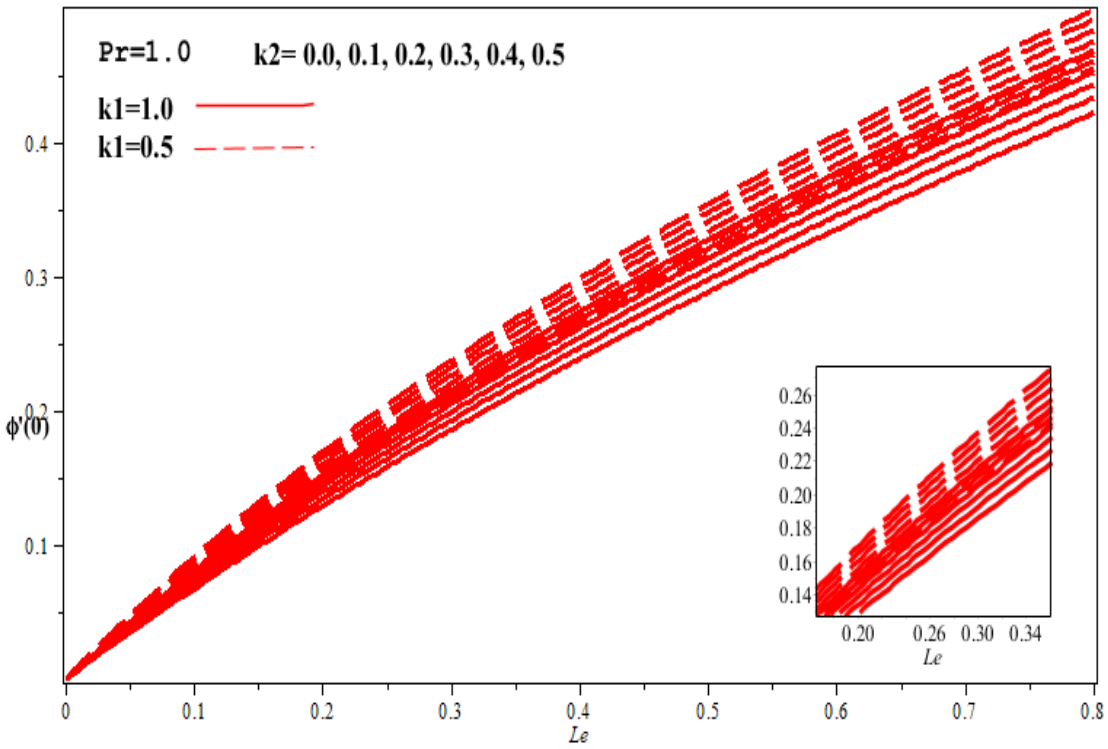

Fig. 43: Variety of $-\varphi'(0)$w.r.t $k2$ and Le For $Pr = 1.0$, $k1 = 0.5,1.0$.

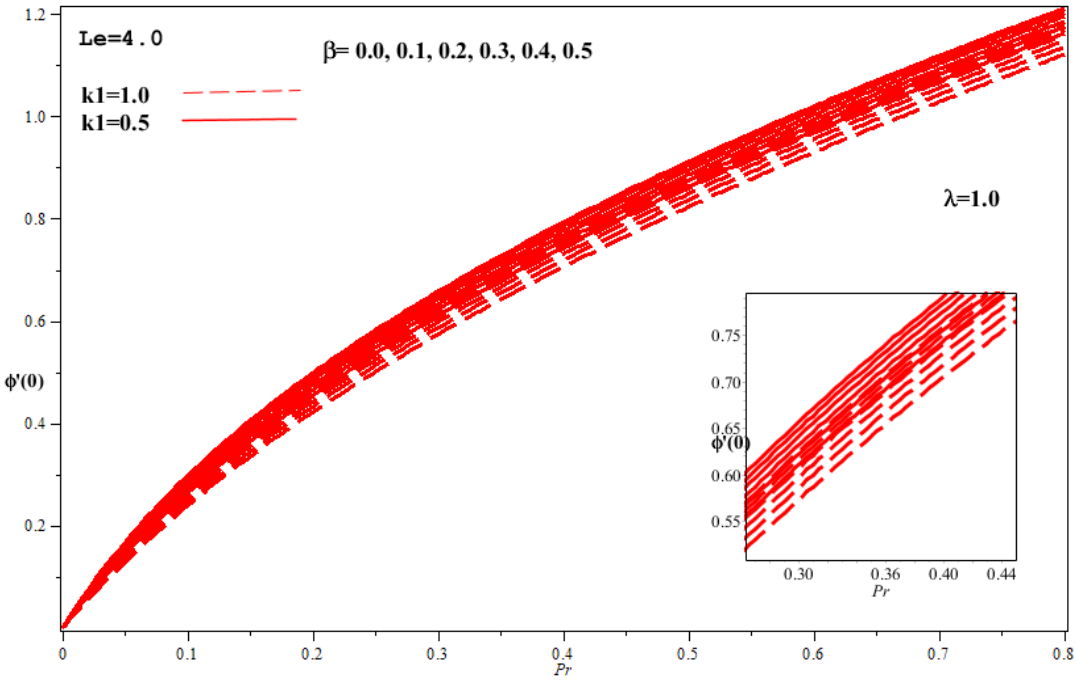

Fig. 44: Variety of --$\varphi'(0)$ w.r.t $k2$ and Pr. For $Le = 1.0\,, k1 = 0.5{,}1.0$

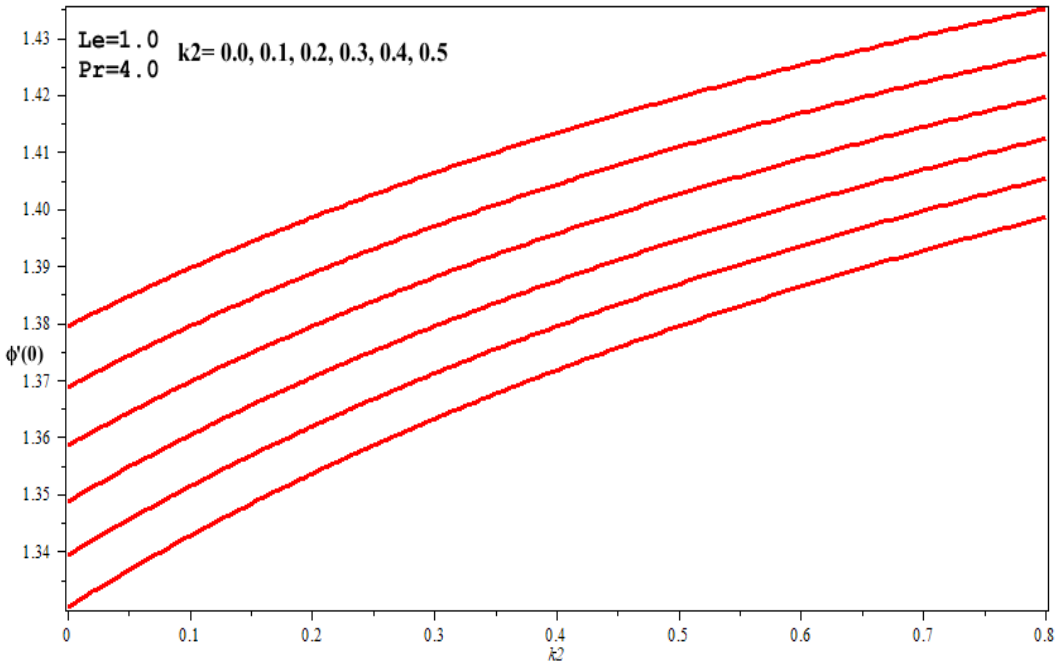

Fig. 45: Variety of $-\varphi'(0)$ w.r.t $k2$ and $k1$. For $Le = 1.0\,, Pr = 4.0$

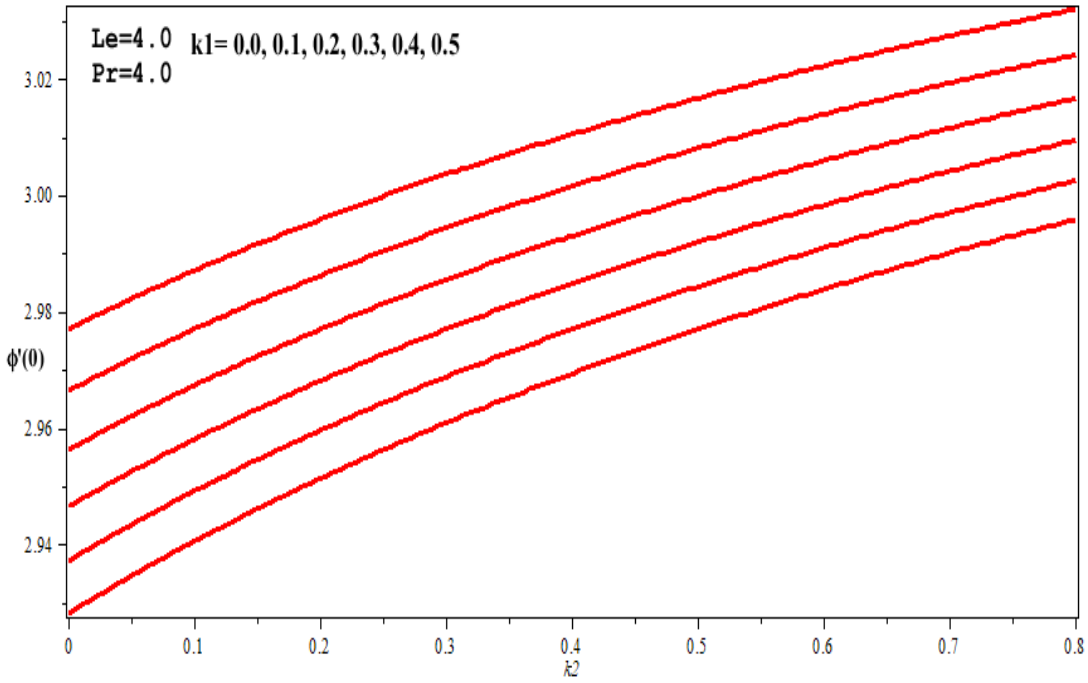

Fig. 46: Variety of -$\varphi'(0)$ w.r.t $k1$ and $k2$. For $Le = 4.0$, $Pr = 4.0$

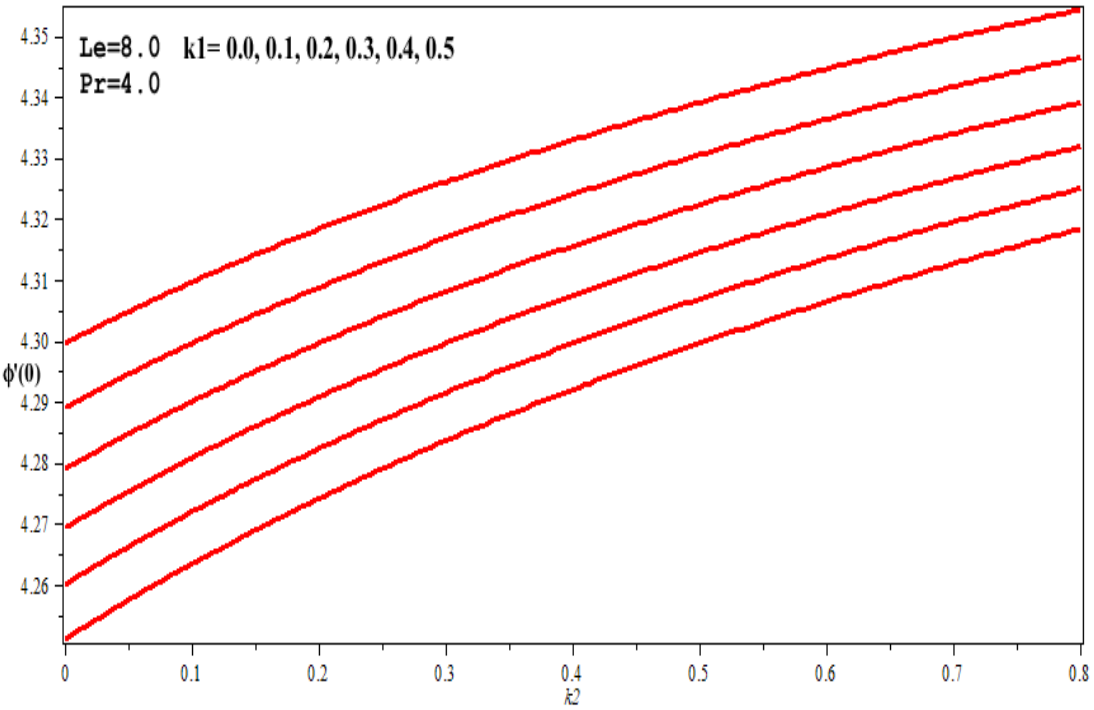

Fig. 47: Variety of $-\varphi'(0)$ w.r.t $k1$ and $k2$. For $Le = 8.0$, $Pr = 4.0$.

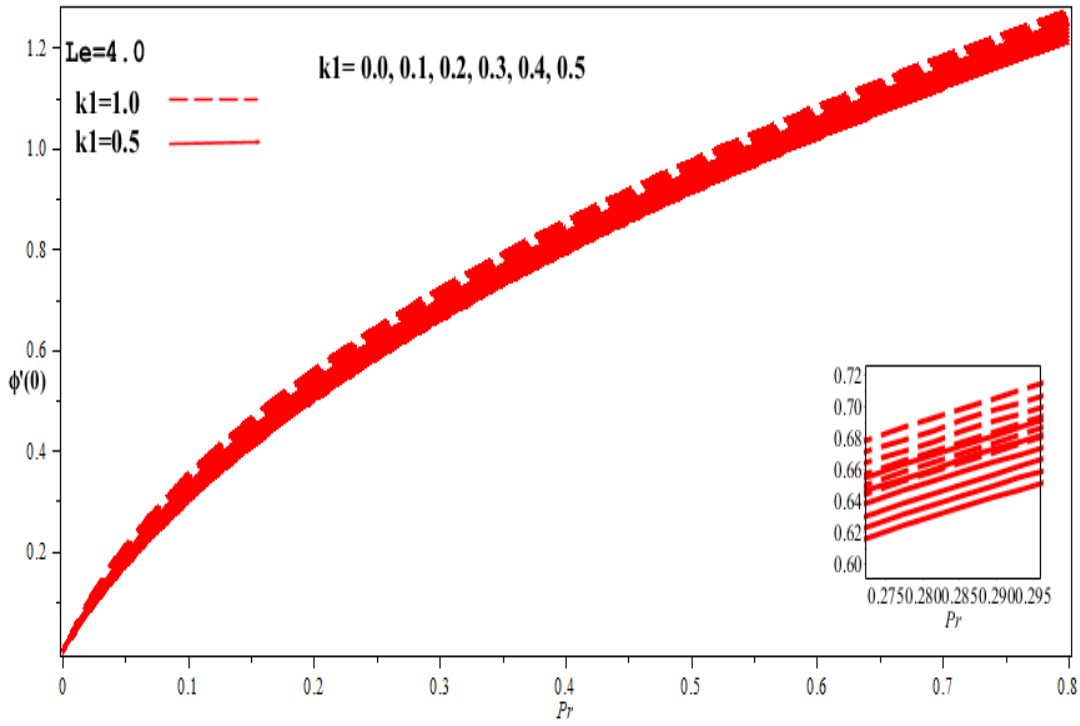

Fig. 48: Variety of $-\varphi'(0)$ w.r.t $k1$ and Pr. For $Le = 4.0$, $k2 = 0.5,1.0$.

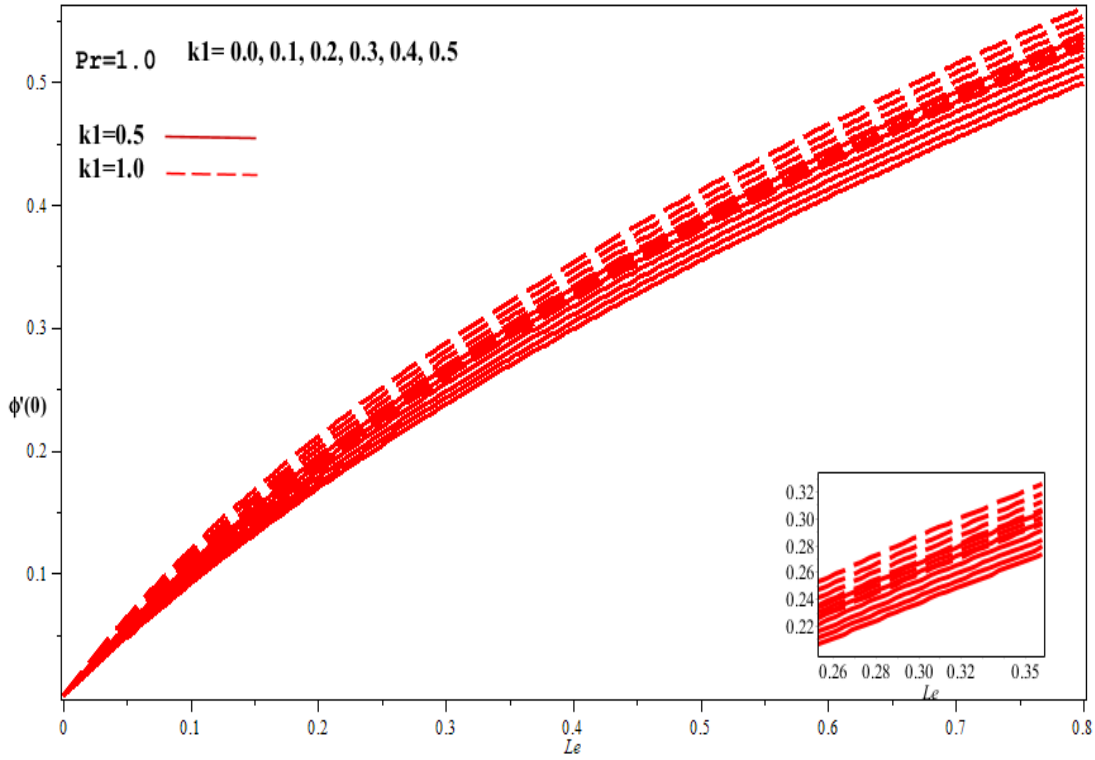

Fig. 49: Variety of $-\varphi'(0)$ w.r.t $k1$ and Le. For $Pr = 1.0$, $k2 = 0.5,1.0$.

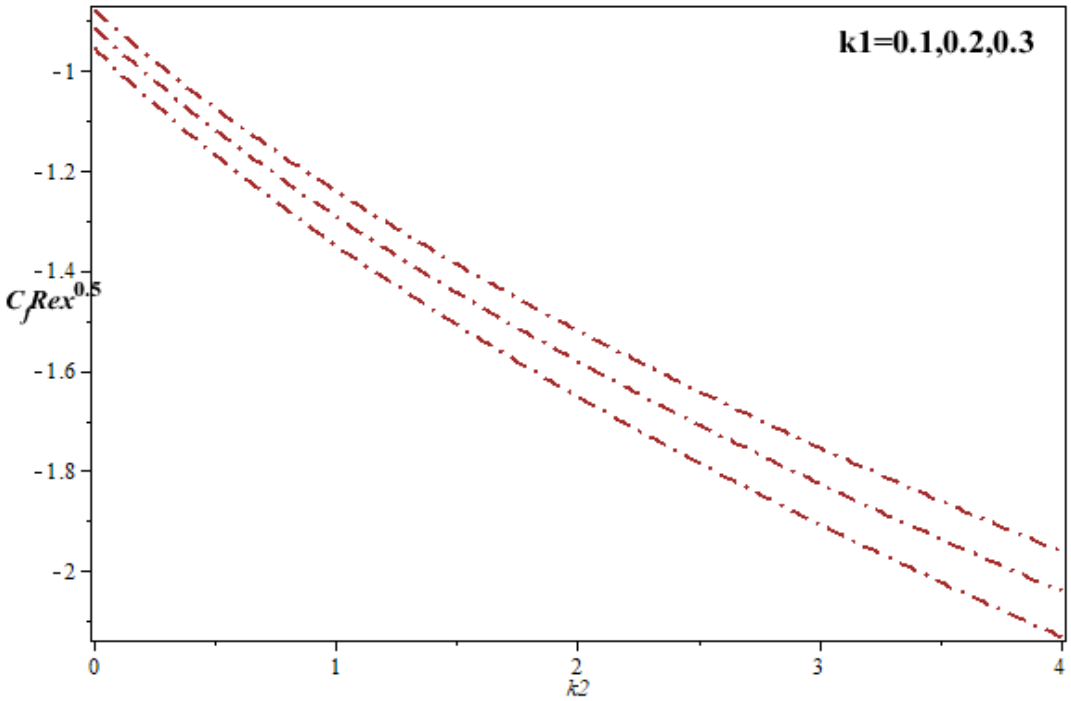

Fig. 50: Variety of $f''(0)$ w.r.t $k1$ and $k2$.

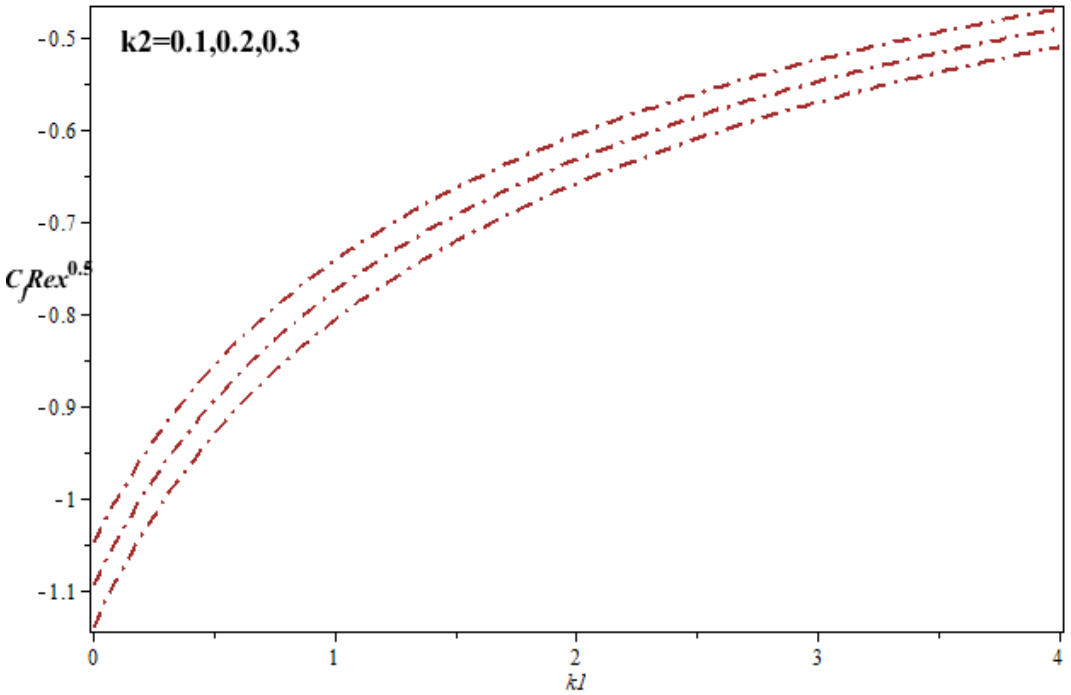

Fig. 51: Variety of $f''(0)$ w.r.t $k2$ and $k1$

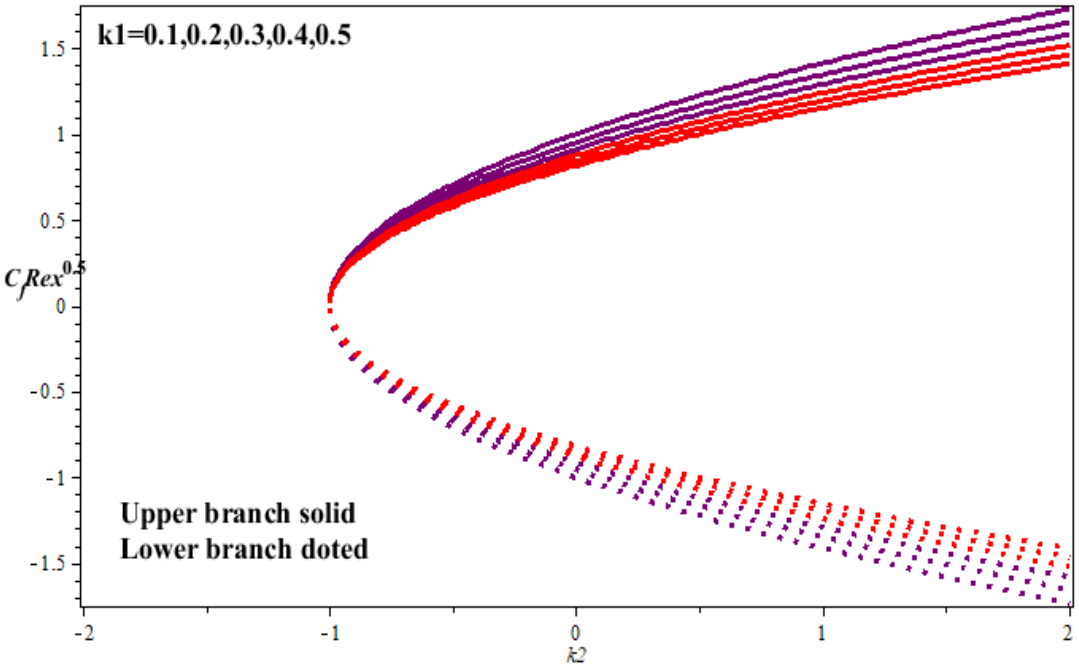

Fig. 52: Variety of dual solution skin friction $f''(0)$ both for stretching/shrinking sheet w.r.t $k1$ and $k2$.

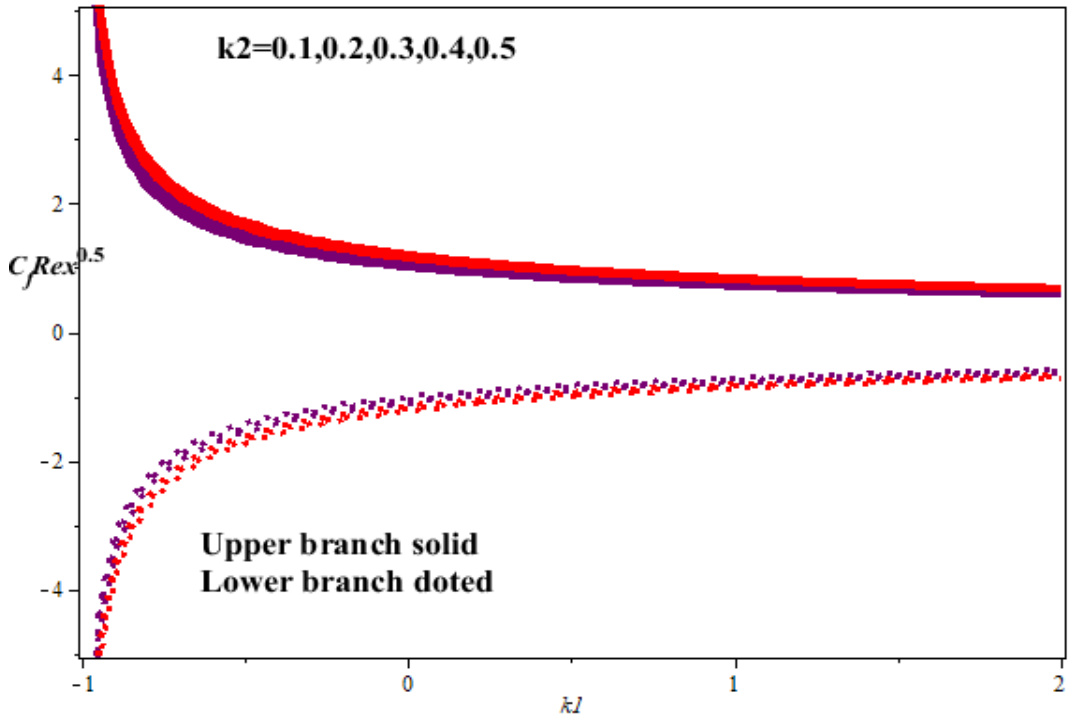

Fig. 53: Variety of dual solution friction $f''(0)$ both stretching/shrinking sheet w.r.t $k2$ and$k1$.

CHAPTER 5

CONCLUSION

This chapter summarizes the analytical and graphical findings from the review and extension work. In this chapter we have discussed all the results of both previous articles. In the current review, we introduced the nanoparticles effect of Jeffrey liquid over a sheet which was in stretched/shrinked state. The effects of various boundaries, for example, the proportion of relaxation to impediment times parameter $k1$, Deborah number $k2$, Prandtl number, Reynolds number and dimensionless Brinkman bunch on the dimensionless speed, heat move, nanoparticles, and irreversible profiles are analyzed. Careful answers for speed, temperature, entropy, and nanoparticle division are made and analyzed. The essential outcomes of the current examination can be recorded under.

- The governing PDEs are converted into ODEs which are nonlinear dimensional through a similarity transformation for an exact solution.
- To deal with the Nano fluid, the equations are resolved by using familiar software Maple.
- The velocity of dimensionless fluid within the boundary layer increments with the expansion in, although the velocity of dimensionless fluid decreases with the increase of $k1$.
- With the increment of both $k1$ and $k2$, energy dimensionless and liquid concentration within the thermal boundary layer increases marginally.
- Both Pr and Le offer similar performance for nanoparticle fraction and temperature.
- The quantity of entropy age Ns increments with the increment of Deborah number$k2$. Notwithstanding, the quantity of entropy age Ns diminishes with the increment of ratio of relaxation to retardation $k1$.
- This one concludes that the number of irreversible Ns is strongly influenced by Reynolds number(Re, Rd) variant, Prandtl number Pr, dimensionless Brinkman number Br.

- Skin friction Cf increases with increasingly both $k2$ and $k1$.
- The Nusselt numbers amount is decreases with the maximum upsides of $Pr, k1$ and $k2$ individually.
- The Sherwood numbers extent is increases with the maximum upsides of $Le, Pr, k1$ and $k2$ individually.

REFERENCES

[1] B. C. Sakiadis, Boundary-layer behavior on continuous solid surfaces: I. Boundary-layer equations for two-dimensional and axisymmetric flow AIChE Journal, 7 (1) (1961) 26-28.

[2] S. U. Choi, & J. A. Eastman, Enhancing thermal conductivity of fluids with nanoparticles (No.ANL/MSD/CP-84938; CONF-951135-29). Argonne National Lab. IL(United States) (1995).

[3] Domairry, D., Sheikholeslami, M., A shorynejad, H. R., Gorla, R. S. R., & Khani, M Natural convection flow of a non-Newtonian nanofluid between two vertical flat plates. Proceedings of the Institution of Mechanical Engineers, Part N: Journal of Nanoengineering and Nano systems, 225(3), (2011) 115-122.

[4] Hinds, W. C. Adhesion of particles. Aerosol Technology: Properties, Behavior, and Measurement of Airborne Particles (1982).

[5] Pearson, J. R. A., and P. M. J. Tardy. "Models for flow of non-Newtonian and complex fluids through porous media." Journal of Non-Newtonian Fluid Mechanics 102, no.2 (2002) 447-473.

[6] Ellahi, R., & Afzal, S. Effects of variable viscosity in a third-grade fluid with porous medium: an analytic solution. Communications in Nonlinear Science and Numerical Simulation, 14(5), (2009) 2056-2072.

[7] Ellahi, R. "Effects of the slip boundary condition on non-Newtonian flows in a channel." Communications in Nonlinear Science and Numerical Simulation 14, no.4 (2009) 1377-1384.

[8] Sakiadis, B. C Boundary-layer behavior on continuous solid surfaces:II.The boundarylayer on a continuous flat surface. AiChE journal, 7(2), (1961) 221-225.

[9] Makinde, O. D., & Aziz, A Boundary layer flow of a nanofluid past a stretching sheet with a convective boundary condition. International Journal of Thermal Sciences, 50(7), (2011) 1326-1332.

[10] Nadeem, S., & Lee, C Boundary layer flow of nanofluid over an exponentially stretchingsurface. Nanoscale Research Letters, 7(1), (2012)1-6.

[11] Dandapat, B. S., & Gupta, A. S.. Flow and heat transfer in a viscoelastic fluid over a stretching sheet. International Journal of Non-Linear Mechanics, 24(3), (1989) 215-219.

[12] Vajravelu, K., & Rollins, D.. Heat transfer in a viscoelastic fluid over a stretching sheet. Journal of Mathematical analysis and applications, 158(1), (1991) 241-255.

[13] Andersson, H. I. MHD flow of a viscoelastic fluid past a stretching surface. Act Mechanica, 95(1), (1992) 227-230.

[14] S. Bhattacharya, A. Pal, A.S. Gupta, Heat transfer in the flow of a viscoelastic fluid over a stretching surface, Heat Mass Transfer 34, (1998) 41–45.

[15] K.V. Prasad, M.S. Abel, S.K. Khan, Momentum and heat transfer in viscoelastic fluid flow in a porous medium over a non-isothermal stretching sheet, Int. J. Numer. Method Heat Flow (10) (2000) 786–801.

[16] M.S. Abel, S.K. Khan, K.V. Prasad, Study of viscoelastic fluid flow and heat transfer over stretching sheet with variable viscosity, Int. J. Non-Linear Mech. 37 (2002) 81–88.

[17] S.K. Khan, E. Sanjayanand, Viscoelastic boundary layer flow and heat transfer over an exponential stretching sheet, Int. J. Heat Mass Transfer 48 (2005) 1534–1542.

[18] R. Cortell, A note on flow and heat transfer of a viscoelastic fluid over a stretching sheet,Int. J. Non-Linear Mech. 41 (2006) 78–85.

[19] M.S. Abel, P.G. Siddheshwar, M.M. Nandeppanavar, Heat transfer in a viscoelasti boundary layer low over a stretching sheet with viscous dissipation and non-uniform heat source, Int. J. Heat Mass Transfer 50 (2007) 960–966.

[20] Kumari M, Pop I, Nath G. Transient MHD stagnation flow of a non-Newtonian fluid due to impulsive motion from rest. Int J Nonlinear Mech; 45: 463e73 (2010).

[21] Hameed M, Elahi R. Thin film flow of non-Newtonian MHD fluid on a vertically movingbelt. Int J Numer Method Fluid: 66:1409e19 (2011).

[22] Ragueb H, Mansouri K. A numerical study of viscous dissipation effect on non-Newtonian fluid flow inside elliptical duct. Energy Convers Manage:68: 124e32 (2013).

[23] Loureiro JBR, Silva Freire AP. Asymptotic analysis of turbulent boundary-layer flow of purely viscous non-Newtonian fluids. J Newt Fluid Mech 2013;199: (2008).

[24] Kefayati GHR. Simulation of magnetic field effect on natural convection of non-Newtonian power-law fluids in a sinusoidal heated cavity using FDLBM. Int Commun Heat Mass Tran 53: (2014)139e53.

[25] Kothandapani M, Srinivas S. Peristaltic transport of a Jeffrey fluid under the effect of magnetic field in an asymmetric channel. Int J Nonlinear Mech :43:915e24 (2008).

[26] Hayat, T., Ahmad, N., & Ali, N. Effects of an endoscope and magnetic field on thperistalsis involving Jeffrey fluid. Communications in Nonlinear Science and Numerical Simulation, 13(8), (2008) 1581-1591.

[27] Hayat, T., & Mustafa, M. Influence of thermal radiation on the unsteady mixed convection flow of a Jeffrey fluid over a stretching sheet. Zeitschrift für Naturforschung A, 65(8-9), (2010) 711-719.

[28] Das, K. Influence of slip and heat transfer on MHD peristaltic flow of a Jeffrey fluid in an inclined asymmetric porous channel. Indian Journal of Mathematics, 54(1), (2012) 19-45.

[29] Qasim, M Heat and mass transfer in a Jeffrey fluid over a stretching sheet with heat source/sink. Alexandria Engineering Journal, 52(4), (2013) 571-575.

[30] Nadeem, S., Haq, R. U., & Khan, Z. H Numerical solution of non-Newtonian nanofluid Flow over a stretching sheet. Applied Nanoscience, 4(5), (2014), 625-631.

[31] S. Aiboud, S. Saouli, Entropy analysis for viscoelastic magnetohydrodynamic flow over a stretching surface, Int. J. Nonlinear Mech. 45 , (2010) 482–489.

[32] O.D. Makinde, Second law analysis for variable viscosity hydromagnetic boundary layer flow with thermal radiation and Newtonian heating, Entropy 13 (2011) 1446–1464.

[33] M. Dehsara, M. Habibi-Matin, N. Dalir, Entropy analysis for MHD flow over a non-linear stretching inclined transparent plate embedded in a porous medium due to solar radiation, Mechanika 18 (5) (2012) 524–533.

[34] A.S. Butt, S.M. Unawar, A. Mehmood, A. Ali, Effect of viscoelasticity on entropygeneration in a porous medium over a stretching plate, World Appl. Sci. J. 17 (4) (2012) 516–523.

[35] Dalir, N. Numerical study of entropy generation for forced convection flow and heat transfer of a Jeffrey fluid over a stretching sheet. Alexandria Engineering Journal, 53(4), (2014) 769-778.

[36] Dalir, N., Dehsara, M., & Nourazar, S. S. Entropy analysis for magnetohydrodynamic flow and heat transfer of a Jeffrey nanofluid over a stretching sheet. Energy, 79, (2015) 351-362.

[37] Baag, S., Mishra, S. R., Dash, G. C., & Acharya, M. R.. Entropy generation analysis for viscoelastic MHD flow over a stretching sheet embedded in a porous medium. Ain Shams Engineering Journal, 8(4), (2017) 623-632.

[38] Baag, S., Mishra, S. R., Dash, G. C., & Acharya, M. R.. Entropy generation analysis for viscoelastic MHD flow over a stretching sheet embedded in a porous medium. Ain Shams Engineering Journal, 8(4), (2017) 623-632.

[39] Khan WA, Pop I, Boundary-layer flow of a nanofluid past a stretching sheet. Int J Heat Mass Transf 53: (2010) 2477–2483.

Exact solution of Jeffrey fluid flow due to stretching/shrinking surface

ORIGINALITY REPORT

10%	6%	7%	3%
SIMILARITY INDEX	INTERNET SOURCES	PUBLICATIONS	STUDENT PAPERS

PRIMARY SOURCES

1	cyberleninka.org Internet Source	1%
2	Nemat Dalir, Mohammad Dehsara, S. Salman Nourazar. "Entropy analysis for magnetohydrodynamic flow and heat transfer of a Jeffrey nanofluid over a stretching sheet", Energy, 2015 Publication	1%
3	Submitted to Higher Education Commission Pakistan Student Paper	1%
4	researchspace.ukzn.ac.za Internet Source	1%
5	Chun Li. "Processing Mutual Nearest Neighbor Queries for Moving Object Trajectories", The Ninth International Conference on Mobile Data Management (mdm 2008), 04/2008 Publication	<1%
	nssdcftp.gsfc.nasa.gov	